U.S. DEPARTMENT OF COMMERCE
National Technical Information Service

PB-280 712

Simulation of Nitrogen Movement, Transformation, and Uptake in Plant Root Zone

Florida Univ, Gainesville

Prepared for

Environmental Research Lab, Athens, Ga

Mar 78

United States
Environmental Protection
Agency

Environmental
Research Laboratory
Athens GA 30601

EPA-600/3-78-029
March 1978

PB 280 712

Research and Development

Simulation of Nitrogen Movement, Transformation, and Uptake in Plant Root Zone

Ecological Research Series

REPRODUCED BY
NATIONAL TECHNICAL
INFORMATION SERVICE
U. S. DEPARTMENT OF COMMERCE
SPRINGFIELD, VA. 22161

RESEARCH REPORTING SERIES

Research reports of the Office of Research and Development, U.S. Environmental Protection Agency, have been grouped into nine series. These nine broad categories were established to facilitate further development and application of environmental technology. Elimination of traditional grouping was consciously planned to foster technology transfer and a maximum interface in related fields. The nine series are:

1. Environmental Health Effects Research
2. Environmental Protection Technology
3. Ecological Research
4. Environmental Monitoring
5. Socioeconomic Environmental Studies
6. Scientific and Technical Assessment Reports (STAR)
7. Interagency Energy-Environment Research and Development
8. "Special" Reports
9. Miscellaneous Reports

This report has been assigned to the ECOLOGICAL RESEARCH series. This series describes research on the effects of pollution on humans, plant and animal species, and materials. Problems are assessed for their long- and short-term influences. Investigations include formation, transport, and pathway studies to determine the fate of pollutants and their effects. This work provides the technical basis for setting standards to minimize undesirable changes in living organisms in the aquatic, terrestrial, and atmospheric environments.

This document is available to the public through the National Technical Information Service, Springfield, Virginia 22161.

TECHNICAL REPORT DATA

(Please read Instructions on the reverse before completing)

1. REPORT NO.
EPA-600/3-78-029

2.

3. RECIPIENT'S ACCESSION NO.
PB280712

4. TITLE AND SUBTITLE
Simulation of Nitrogen Movement, Transformation, and Uptake in Plant Root Zone

5. REPORT DATE
March 1978 issuing date

6. PERFORMING ORGANIZATION CODE

7. AUTHOR(S)
James M. Davidson, Donald A. Graetz, P. Suresh C. Rao, and H. Magdi Selim

8. PERFORMING ORGANIZATION REPORT NO.

9. PERFORMING ORGANIZATION NAME AND ADDRESS
University of Florida
Gainesville, FL 32611

10. PROGRAM ELEMENT NO.
1BB770

11. CONTRACT/GRANT NO.
R803607

12. SPONSORING AGENCY NAME AND ADDRESS
Environmental Research Laboratory--Athens, GA
Office of Research and Development
U.S. Environmental Protection Agency
Athens, GA 30605

13. TYPE OF REPORT AND PERIOD COVERED
Final, 3/10/75-3/9/77

14. SPONSORING AGENCY CODE
EPA/600/01

15. SUPPLEMENTARY NOTES

16. ABSTRACT

A detailed research model and a conceptual management model were developed to describe the fate of nitrogen in the plant root zone. Processes considered in both models were one-dimensional transport of water and water-soluble N-species as a result of irrigation/rainfall events, equilibrium absorption-desorption, microbiological N-transformations, and uptake of water and nitrogen species by a growing crop.

The research model was based on finite-difference approximations (explicit-implicit) of the partial differential equations describing one-dimensional water flow and convective-dispersive NH_4^+ and NO_3^- transport along with simultaneous plant uptake and microbiological N-transformations. Ion-exchange (absorption-desorption) of NH_4^+ was also considered. The micro-biological transformations incorporated into the model describe nitrification, denitrification, mineralization and immobilization. All transformations were assumed to be first-order kinetic processes.

The management model consists of several simplifying assumptions requiring minimal input data. The model provides an integrated description of the behavior of various nitrogen species in the plant root zone.

17. KEY WORDS AND DOCUMENT ANALYSIS

a. DESCRIPTORS	b. IDENTIFIERS/OPEN ENDED TERMS	c. COSATI Field/Group
Simulation Fertilizers Nitrogen Mathematical models Plant nutrition	Agricultural chemicals Modeling Nitrogen compounds	68D 72E 98A

18. DISTRIBUTION STATEMENT
RELEASE TO PUBLIC

19. SECURITY CLASS (This Report)
UNCLASSIFIED

20. SECURITY CLASS (This page)
UNCLASSIFIED

21. NO. OF PAGES
118

22. PRICE
A06- A01

U.S. GOVERNMENT PRINTING OFFICE: 1978— 260-880/45

EPA-600/3-78-029
March 1978

SIMULATION OF NITROGEN MOVEMENT, TRANSFORMATION, AND UPTAKE IN PLANT ROOT ZONE

by

James M. Davidson
Donald A. Graetz
P. Suresh C. Rao
H. Magdi Selim
University of Florida
Gainesville, Florida 32611

Grant No. R-803607

Project Officer

Charles N. Smith
Technology Development and Applications Branch
Environmental Research Laboratory
Athens, Georgia 30605

Technical Advisor

Arthur G. Hornsby
Source Management Branch
Robert S. Kerr Environmental Research Laboratory
Ada, Oklahoma 74820

ENVIRONMENTAL RESEARCH LABORATORY
OFFICE OF RESEARCH AND DEVELOPMENT
U.S. ENVIRONMENTAL PROTECTION AGENCY
ATHENS, GEORGIA 30605

DISCLAIMER

This report has been reviewed by the Environmental Research Laboratory, U. S. Environmental Protection Agency, Athens, GA, and approved for publication. Approval does not signify that the contents necessarily reflect the views and policies of the U. S. Environmental Protection Agency, nor does mention of trade names or commercial products constitute endorsement or recommendation for use.

FOREWORD

Environmental protection efforts are increasingly directed towards preventing adverse health and ecological effects associated with specific compounds of natural or human origin. As part of the Athens Environmental Research Laboratory's research on the occurrence, movement, transformation, impact, and control of environmental contaminants, the Technology Development and Applications Branch develops management and engineering tools for assessing and controlling adverse environmental effects of nonirrigated agriculture and of silviculture.

Surface and ground waters may, under certain conditions, be adversely affected by the accumulation of nitrate resulting from the application of nitrogen fertilizer to agricultural lands to increase crop production. Because of its water pollution potential, it is important to understand the fate of nitrogen in the plant root zone. This report presents a detailed research model that describes the movement, transformation, and plant uptake of nitrogen in soils. Because of the complexity of the research model, a simpler, user-oriented management model that requires minimal input data was also developed. Both simulation models are useful management tools for predicting the behavior of nitrogen and for assessing nonpoint sources of pollution.

David W. Duttweiler
Director
Environmental Research Laboratory
Athens, Georgia

ABSTRACT

Two simulation models, a detailed research-type and a conceptual management-type, for describing the fate of nitrogen in the plant root zone are discussed. Processes considered in both models were: one-dimensional transport of water and water-soluble N-species as a result of irrigation/rainfall events, equilibrium adsorption-desorption of NH_4, microbiological N-transformations, and uptake of water and nitrogen species by a growing crop.

The research-type model was based on finite-difference approximations (explicit-implicit) of the partial differential equations describing one-dimensional, transient water flow and convective-dispersive NH_4 and NO_3 transport along with simultaneous plant uptake and microbiological N-transformations. Ion-exchange (adsorption-desorption) of NH_4 was also considered. The microbiological transformations incorporated into the model describe nitrification, denitrification, mineralization and immobilization. All transformations were assumed to follow first-order kinetics. The numerical solution was flexible in its soil surface boundary conditions as well as initial conditions for soil-water content and nitrogen concentration distributions in the soil profile. The numerical solution can be used for non-homogeneous or multilayered soil systems.

The research-type model contains a detailed description of the individual processes and requires a large number of input parameters, most of which are frequently unavailable. Because of this, a less detailed management-type model employing several simplifying assumptions was developed. The management-type model requires a minimal number of input parameters, and provides an integrated description of the behavior of various nitrogen species in the plant root zone.

This report was submitted in fulfillment of Grant No. R-803607 by J. M. Davidson, D. A. Graetz, P. S. C. Rao, and H. M. Selim, University of Florida, Gainesville under the partial sponsorship of the U. S. Environmental Protection Agency. This report covers the period March 10, 1975 to March 9, 1977, and work was completed as of March 9, 1977.

CONTENTS

Foreword. iii
Abstract. iv
Figures vi
Tables. ix
Acknowledgments x

1. Introduction 1
2. Conclusions. 5
3. Recommendations. 7
4. Research Model 9
    Equations for Water Flow. 9
    Nitrogen Transformations. 11
    Nitrogen Transport and Transformations. 14
    Solute Transport in Multi-Layered Soils 18
5. Models for Plant Uptake. 21
    Plant Uptake of Water 21
    Plant Uptake of Nitrogen. 25
    Root Growth Models. 30
6. Management Model 34
    Transport of Water and Nitrogen 34
    Nitrogen Transformations. 40
    Nitrogen Uptake 44
7. Research Model Simulations 46
    Transport and Transformations 46
    Transport, Transformations, and Uptake. 52
    Summary 60
8. Management Model Simulations 61
    Model Verification. 61
    Model Simulations 63

References. 67

Appendices

A. Description of the Computer Program for the Research Model. 77
B. Flow Chart of the Computer Program 82
C. FORTRAN IV Program Listing 83
D. Kinetic Rate Coefficients for Nitrogen Transformations 99
E. List of Publications Resulting from this Project 104

FIGURES

Number Page

1 Soil nitrogen transformations considered in the research model. The subscripted symbol k is a first order rate coefficient, while the subscripts e, s, i, and g refer to exchangeable, solution, immobilized, and gaseous phases, respectively. K_D is the Freundlich distribution coefficient. 11

2 Soil-water content (θ) and soil-water suction (h) versus depth in a clay-sand soil profile. For A the water table is at x = 100 cm, and for B it is at a great depth ($x \to \infty$). 18

3 Adsorbed and nonadsorbed solute relative effluent solute concentration (C/Co) distributions from unsaturated clay-sand soil profiles. Open circles were calculated based on average soil-water content within each soil layer, while the solid and dashed lines were calculated using the soil-water content shown in Figure 2A and 2B 19

4 Evapotranspiration (ET) as a fraction of potential evapotranspiration (PET) with time as simulated by the Molz-Remson (M-R) and the Nimah-Hanks (N-H) models. 27

5 Root length density distributions for corn (Zea mays L.) at selected times during the growth season as calculated by the empirical model 33

6 Distribution of soil-water (solid line) and nonadsorbed solute (dashed line) after 5 and 10 cm of water had infiltrated into an initially dry (θ_i=0) soil profile 35

7 Distribution of soil-water (solid line) and nonadsorbed solute (dashed line) after 5 and 10 cm of water had infiltrated into a soil profile at a uniform initial water content (θ_i, shown as vertical dashed line) of 0.1 cm^3/cm^3 36

Number Page

8 Agreement between d_{sf}/d_{wf} and θ_i/θ_f as calculated by Equation (50) and experimental data from various sources 37

9 Comparison between measured (solid circles) and predicted (solid lines) position of a nonadsorbed solute front in a sandy soil at various times. The soil was planted to millet [Pennisetum americanum (L.) K. Schum] 41

10 Simulated soil-water content distributions in a deep uniform loam soil profile during infiltration and redistribution of soil-water. 47

11 Simulated solution-phase concentration distributions of NO_3-N and NH_4-N in a deep uniform loam soil profile during infiltration and redistribution of soil-water. The rate coefficient for nitrification (k_1) was 0.01 hr.$^{-1}$ 48

12 Simulated solution-phase concentration distributions of NO_3-N and NH_4-N in a deep uniform loam soil profile during infiltration and redistribution of soil-water. The rate coefficient for nitrification (k_1) was 0.1 hr.$^{-1}$ 49

13 Total amounts of NH_4-N and NO_3-N in a deep uniform loam soil profile during infiltration and redistribution of soil-water. The nitrification rate (k_1) was 0.01 or 0.1 hr^{-1}. These plots were derived from the simulated data presented in Figures 11 and 12. 50

14 Simulated soil-water content distributions during infiltration and redistribution of soil-water in a loam soil profile with an impermeable barrier at a depth of 40 cm 51

15 Simulated solution-phase concentration distributions of NH_4-N and NO_3-N during infiltration and redistribution of soil-water in a loam soil profile with an impermeable barrier at 40 cm depth. The kinetic rate coefficient for denitrification (k_1) was 0.01 hr^{-1}. 52

Number | Page

16 Total amounts of NO_3-N remaining and total amount of N released by denitrification during infiltration and redistribution of soil-water in a loam soil profile with an impermeable barrier at a depth of 40 cm. The denitrification rate coefficient (k_1) was 0.001 or 0.01 hr^{-1} 53

17 Simulated soil-water content distribution in a deep uniform loam soil profile during infiltration and redistribution following three irrigation events. 55

18 Simulated NO_3-N solution concentrations in the soil profile at selected times following three irrigation events (Figure 17) 55

19 Simulated NH_4-N solution concentrations in the soil profile at selected times following three irrigation events (Figure 17) 56

20 Soil-water content (θ) distributions with time during plant-water uptake and evaporation in a uniform soil profile of Lakeland soil (from Selim et al.[89]) 57

21 Percent of applied nitrogen remaining within the plant root zone during the simulated growth season. The curves were based on data presented in Figures 18 and 19. 58

22 Comparison between simulated cumulative nitrogen uptake and that when maximum uptake demand is satisfied at all times during the growth season . . 59

23 Fraction of applied nitrogen remaining in the plant root zone of Maury soil, simulated by the management model, during the corn growing season. 62

24 The predicted depth of nitrate front under three water application schemes during the growing season in a sandy soil profile. Increase in the maximum root zone depth (L) with time is also shown. 64

25 Cumulative nitrogen uptake by corn grown in a sandy soil under three water application schemes, as simulated by the management model . . . 66

TABLES

Number Page

1 Comparison between soil-water content (θ) profiles during an 8-day period in a sandy soil as simulated using the Molz-Remson (M-R) and the Nimah-Hanks (N-H) models for plant uptake of soil water. 26

2 Comparison between measured nitrogen uptake by corn (Zea mays L.) grown under field conditions and that predicted by three simulation models 63

3 Kinetic transformation rate coefficients for various nitrogen species in selected soils. 101

ACKNOWLEDGMENTS

The assistance of Dr. Luther C. Hammond (University of Florida), Dr. Ron E. Phillips (University of Kentucky), and Mr. Ron E. Jessup, and Mr. William G. Volk (all of University of Florida) is gratefully acknowledged. Also, the cooperation and overall project coordination by Mr. Charles N. Smith (EPA Environmental Research Lab., Athens, GA) as the Project Officer and by Dr. Arthur G. Hornsby (Robert S. Kerr Environmental Research Lab., Ada, OK) as Technical Advisor is appreciated.

The project investigators wish to express their appreciation to the Center for Environmental Programs in the Institute of Food and Agricultural Sciences at the University of Florida for financial support during the project period. The project investigators are also indebted to their colleagues in the Department of Soil Science at the University of Florida for their assistance and suggestions during the development of the simulation models presented in this report.

SECTION 1

INTRODUCTION

Nitrogen is an essential element for all biological processes. In an undisturbed environment the cycle of synthesis, consumption, and decay of nitrogenous compounds takes place without increasing or decreasing the total nitrogen content in the system. This delicate balance is disturbed when man separates the areas of nitrogen assimilation (plant and animal growth and development) from areas of consumption and waste accumulation (large metropolitan areas). Because of this separation, most agricultural soils now require supplementary applications of nitrogen fertilizer to maintain high yields and profits. These commercial nitrogen applications may, under certain conditions, adversely affect water quality through significant accumulations of nitrate in surface and ground water. Therefore, the fate of nitrogen in the plant root zone is of interest not only because of its use in biological systems, but also because of its water contamination potential and quantity and petroleum energy required for its commercial production.

The fate of nitrogen at and below the soil surface is governed by a variety of interrelated and complex processes. Various inorganic (NH_4, NO_3, NO_2, N_2O and N_2) and organic nitrogen forms exist simultaneously in the soil. These and other nitrogen substrates undergo reversible and/or irreversible transformations owing to chemical and microbiological processes. The water-soluble nitrogen species (NH_4, NO_3, and NO_2) may also be transported through the soil in response to soil-water movement. The NH_4 and NO_3 distribution is complexed further by absorption by plant roots. The extent of water and nitrogen uptake by plants is determined, in part, by the transpiration demand, which in turn is dependent upon plant species, growth stage, and meteorological conditions. Soil microhydrologic properties also influence the rate at which water and nutrients are transported through the soil to the root surfaces.

The complexity of the soil-water-plant system is further enhanced by the fact that all of the above processes are transient in nature and occur simultaneously. The relative importance of these processes in determining nitrogen behavior is dependent not only on several physical, chemical and biological soil properties, but also on the plant species and the growth stage of the crop. Therefore, a prerequisite to modeling the fate of nitrogen in soil-water-plant systems is a complete understanding of the nitrogen transformation processes. A considerable amount of qualitative information is available regarding nitrogen and its agronomic aspects and individual processes in soils.[1] However, due to the nature and conditions under which much of this research was conducted, it is difficult to integrate this information into a form that can be used to develop accurate relationships which are required for simulation and/or prediction purposes.

The degree of sophistication and detail in any simulation model is determined by (i) the understanding of the system to be modeled, (ii) the modeler's conceptualization of system processes, (iii) the modeling approach and error bounds in the approximations required to solve the problem, (iv) the data base available for input into the model and verification of the model, and (v) the intended application of the model. When the system processes are initially unknown and the model is designed on the basis of inductive reasoning, the approach is referred to as "black box" modeling. On the other hand, when a complete quantitative description of the system to be modeled is available and the model is deduced from established laws, a "white box" approach is said to be utilized. Thus, depending on the completeness of the knowledge of the system, mathematical models may be considered as having various "shades of gray"--the darker the shade of gray, the less is known about the system.[2]

Mathematical models to describe physical, chemical, and biological processes are generally of three distinct types. A stochastic model assumes the processes to be modeled obey the laws of probability. Empirical models are designed on the basis of experience and observation and the use of regression equations which correlate input with output parameters. Mechanistic models are based on well established physical, chemical and biological laws that describe individual processes. Mechanistic models are versatile in that extensive historical records are not required for their development. However, these models require a complete understanding of the process or system being described. A frequent limitation of mechanistic models, therefore, is an inadequate understanding of the system. Empirical models are of assistance in such situations since they identify parameters which influence the system being described.

OBJECTIVES AND SCOPE OF THIS STUDY

Intensive research efforts by several researchers during the past decade have yielded a multitude of models for simulation of nitrogen behavior in soil-water-plant systems. However, due to the limited understanding of major processes and the interrelationships among them, considerable divergence exists among the modeling approaches undertaken. A state-of-the-art review[3] of nitrogen simulation models indicated that these models range from totally empirical to those that are mechanistic in nature. The major objective of the work presented in this report was to evaluate and design comprehensive models for describing the behavior of nitrogen in the plant root zone.

A systems analysis concept, i.e., an examination and mathematical description of important processes that function in the system, was employed in developing a mechanistic model describing the fate of nitrogen in the plant root zone. Empirical models were also used when necessary because of the vast complexity of the problem and the lack of a thorough understanding of the system.

The modeling efforts in this study were conducted on the basis that two distinct groups of individuals are interested in predicting the behavior of nitrogen in the plant root zone. The research model is mechanistic and requires a detailed description of the individual processes and a precise knowledge of the input parameters. The research model was useful in understanding the complex interactions among various processes and in identifying major contributing parameters. The research model described in this report is flexible and can incorporate other transformation and transport processes in addition to those presented. The computer time required to simulate an entire crop growing season is quite large for the research model (see Appendix A for details). Furthermore, the values of several parameters and coefficients required in the research model are generally unavailable for most sites. For this reason, an alternate model for management purposes was developed from the research model. Several simplifying assumptions were made in order to save computer time. The management model was developed so that a minimum amount of input information was necessary to provide an integrated description of nitrogen behavior in the plant root zone during a growing season. The loss of accuracy resulting from the simplification and assumptions made in developing the management model was estimated with the research model. Both models are modular in nature and allow changes to be made in individual process descriptions without altering the basic structure of the total model.

REPORT FORMAT

A mechanistic research model is presented in Section 4 for simulating nitrogen transport and transformation during transient unsaturated water flow in soils. Mathematical relationships used to describe water and nitrogen uptake by plants are described in Section 5. The management model and its assumptions are discussed in Section 6. Simulations obtained from the research model are presented in Section 7. Simulations obtained from the management model are discussed in Section 8. A description and FORTRAN IV computer program listing for the research model and a list of publications resulting from this project are given in the appendices. A table of transformation rate coefficients for various nitrogen species in selected soils, compiled from a literature search, is also included in the appendices.

SECTION 2

CONCLUSIONS

A thorough literature search was conducted to identify the mathematical relationships being used to describe the fate of nitrogen species in the plant root zone. The results of this initial effort provided the direction and emphasis for the project. In so far as possible, mathematical relationships that had been verified and used with some degree of success were incorporated into our modeling effort. Several conclusions can be made based upon this study.

(1) Current experimental data base is inadequate to verify mathematical models for describing the behavior of nitrogen species in the plant root zone with time. Soil fertility experiments to establish optimum yields generally include very few, if any, soil-water and nitrogen content distributions and plant-nitrogen uptake measurements with time. Also absent in these studies are soil-water characteristic measurements for the soils on which the experiments were conducted. Cooperative experiments involving various disciplines need to be initiated and measurements must be made during the crop growing season.

(2) Soil-water plant root uptake models of Nimah and Hanks and Molz and Remson were evaluated and shown to predict similar soil-water content distributions with time in the absence of plant-water stress. Due to differences in conceptualization of plant response to water stress in these two models, predicted soil-water content distributions differed in the presence of water stress. The two models could be made to predict identical soil water uptake patterns if plant water stress was defined similarly in both models.

(3) The management model was in general agreement with the research model when simulating the total quantity of a given nitrogen species in the plant-root zone. Because of the number of coefficients and computer time required to simulate a growing season, the management model has considerable appeal. Also, because of soil spatial variability it is difficult to obtain coefficients which represent the soil profile.

(4) Increasing the first-order transformation rate coefficients by 100% increased the amount of nitrate produced in a given time period by a maximum of only 17%. A similar

difference was observed when all rate coefficients were assumed constant with soil depth rather than a function of organic matter and water content with depth.

(5) The research model is a valuable tool for evaluating conceptual nitrogen transformation processes in the soil profile. The model is flexible and designed for maximum research use.

(6) The level of knowledge on water and nitrogen uptake by plant roots is inadequate at the present time for modeling these processes at the microscopic level. Root growth and distribution characteristics are also too inadequately understood to formulate mechanistic models at this time. Therefore, in this study it was necessary to use a macroscopic model to describe the uptake of water and nitrogen by a relative root distribution. This approach agreed with experimental data.

(7) Temperature was not included in our models, not because of a lack of understanding of how temperature influences nitrogen transformations but because of the difficulty in modeling temperature fluctuations at the soil surface during the growing season. As the plant canopy increases, the insulation to the soil surface changes making it difficult to model with any degree of accuracy the temperature at the soil surface with time.

SECTION 3

RECOMMENDATIONS

This project has identified some major difficulties in describing the fate of selected nitrogen species in a biologically active soil. Based upon these observations, research areas requiring immediate attention before quantitative mathematical relationships can be applied with confidence are pointed out. The following recommendations and/or suggestions were developed by the project investigators.

(1) Careful laboratory experiments involving the uptake of water and nitrogen by plants should be conducted with special attention given to measurement of root growth and root distribution and location of the water and nitrogen uptake by the root during the growing season.

(2) Careful field and laboratory experiments need to be conducted to develop a data base to provide input parameters for mathematical models describing the fate of nitrogen in the soil profile. Measurements should include soil-water content, nitrogen species, root distribution, and cumulative nitrogen uptake with time and soil-water characteristics of the soil used in the study. Water and nitrogen inputs as well as climatic environmental conditions should be well-defined during the growing season. It would be best if these studies were conducted using research personnel from several disciplines.

(3) The output from various available simulation models need to be compared. Due to significant differences in the conceptualization of the soil-water-plant system and initial and boundary conditions assumed in each model, it is frequently difficult to compare the output from simulation models.

(4) The importance of spatial variability should be considered with regard to the sophistication needed in our current mathematical modeling efforts for nitrogen. Current research on spatial variability suggests that differences in nitrogen distribution with depth in the field may be as great as an order of magnitude.

(5) The models developed in this study need to be expanded to include mineralization of plant residue and organic waste. This would require a more detailed description of

microbial populations and biomass with time. Some procedures have been developed but none have been verified and shown to be accurate for different environmental conditions.

(6) The management model needs to be improved in order to consider nonhomogeneous or multilayered soil profiles as well as to allow for prediction of concentration distributions of nitrogen species within the root zone.

SECTION 4

RESEARCH MODEL

In this section, a mechanistic research model is presented for describing simultaneous transport and transformations of nitrogen species during transient unsaturated water flow through soils. A model for simulation of transformations during steady-state water flow was also devised under the auspicies of this grant; a detailed description of the latter model is available elsewhere.[4] It should be emphasized that the research model presented in this report is flexible and can be adapted to incorporate other processes which influence water and nitrogen transport and nitrogen transformations in soils. Processes such as partial displacement of soil-water due to water channelling (Quisenberry and Phillips[5]) or due to the presence of mobile and immobile water (van Genuchten and Wierenga[6]) are not included in this study.

EQUATIONS FOR WATER FLOW

The nonlinear partial differential equation governing one-dimensional flow of water in unsaturated soils may be written as (see Kirkham and Powers[7], Selim et al.[8]):

$$\mathrm{Cap}(h)\frac{\partial h}{\partial t} = \frac{\partial}{\partial z}\, K(h)\frac{\partial h}{\partial z} - \frac{\partial K(h)}{\partial z} \qquad (1)$$

where,

θ = soil-water content (cm^3/cm^3),
h = soil-water head or suction (cm),
K(h) = soil hydraulic conductivity (cm/day)
z = distance in soil, positive downward (cm),
t = time (days),
Cap(h) = soil water capacity (cm^{-1}).

In equation (1) the soil-water capacity, Cap(h), is a measure of the change of soil-water content with water head (Cap(h) = $\partial\theta/\partial h$) which is determined using soil water characteristic relationships (θ versus h).

The initial condition of nonuniform soil-water content in a semi-infinite soil column is stated as:

$$h = h\ (z,0) \qquad 0 < z < \infty \qquad (2)$$

The boundary condition at the soil surface (z=0) is a constant (or variable) water head H:

$$h = H \qquad z = 0 \qquad t \leq t_1 \qquad (3)$$

which describes continuous water infiltration for a time t_1. Following the cessation of water infiltration, i.e. for times greater than t_1, the boundary condition is:

$$q_{z=0} = -K(h)\ \frac{\partial h}{\partial z} + K(h)\ , \qquad z=0 \qquad t > t_1 \qquad (4)$$

which describes water redistribution under a constant (or variable) evaporative water flux $q_{z=0}$ at the soil surface.

In order to obtain a numerical solution for equation (1) subject to conditions (2) to (4), we express these equations in finite-difference approximation form. In this study, the explicit-implicit finite difference scheme (Carnahan et al.[9]; Salvadori and Baron[10]) was used. We refer to a discrete set of points in the (z,t) plane given by a grid with spacings Δz and Δt, respectively. Grid or mesh points are denoted by (i,n) where:

$z = i\ \ \Delta z,$ $\qquad$ $i = i,\ 2,\ 3,\ \ldots$

$t = n\ \ \Delta t,$ $\qquad$ $n = 1,\ 2,\ 3,\ \ldots$

The finite difference approximation for the water flow equation (1) is:

$$\begin{aligned}
\mathrm{Cap}(h_i^{n+1/2})\ [h_i^{n+1} - h_i^n] = {} & \gamma\ K(h_{i+1/2}^{n+1/2})\,[h_{i+1}^{n+1} - h_i^{n+1}] \\
& - \gamma\ K(h_{i-1/2}^{n+1/2})\,[h_i^{n+1} - h_{i-1}^{n+1}] \\
& + \gamma\ K(h_{i+1/2}^{n+1/2})\,[h_{i+1}^{n} - h_i^{n}] \qquad (5) \\
& - \gamma\ K(h_{i-1/2}^{n+1/2})\,[h_i^{n} - h_{i-1}^{n}] \\
& - \beta\ [K\ (h_{i+1/2}^{n}) + K(h_{i-1/2}^{n})]
\end{aligned}$$

where $\gamma = \Delta t/2(\Delta z)^2$ and $\beta = \Delta t/\Delta z$.

Numerical solutions to the water flow equation are presented by Davidson et al.[11] and Selim et al.[8] for similar finite-difference explicit-implicit approximations.

NITROGEN TRANSFORMATIONS

The microbiological nitrogen transformations considered in this model were: (i) nitrification of NH_4 to NO_3, (ii) mineralization of organic-N to NH_4, (iii) immobilization of both NH_4 and NO_3 to organic-N, and (iv) denitrification of NO_3 to gaseous forms. In addition, ion-exchange of NH_4 was also considered. These processes are summarized in Figure 1. The ion-exchange process was considered to be instantaneous, whereas all other processes were of first order kinetic type. The rate coefficients associated with these first-order reactions were k_1, k_2, k_3, k_4 and k_5, respectively, for NH_4 nitrification, NO_3 immobilization, NH_4 mineralization, NH_4 immobilization and NO_3 denitrification (day^{-1}).

Although nitrification follows the sequential oxidation pathway of $NH_4 \rightarrow NO_2 \rightarrow NO_3$, the NO_2 ions are rapidly oxidized to NO_3 in most soils. Hence, nitrification may be considered as a single-step process with the $NH_4 \rightarrow NO_2$ step controlling the rate of NO_3 production.

Mehran and Tanji[12], Hagin and Amberger[13], Beek and Frissell[14], and Misra et al.[15] have all used first-order rate equations to describe transformations of nitrogen. Environmental

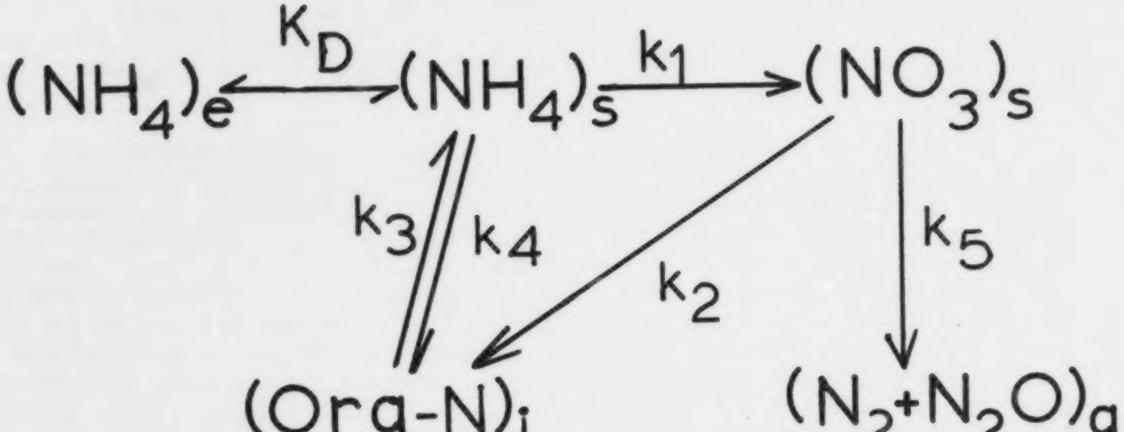

Figure 1. Soil nitrogen transformations considered in the research model. The subscripted symbol k is a first-order rate coefficient, while the subscripts e, s, i, and g refer to exchangeable, solution, immobilized, and gaseous phases, respectively. K_D is the Freundlich distribution coefficient.

factors such as soil-water content, temperature, pH, and aeration have significant effects on nitrogen transformations. In this study optimum conditions with regard to pH and temperature were assumed. However, submodels may be added as necessary to take into account the influence of these parameters on the rate coefficients. Optimum temperature for most transformations is between 30° to 35°C. Neutral pH is optimal for a majority of the transformations. It was assumed in this study that agricultural soils will have pH values between 5.5 and 7.0.

The major limitation in selection of a rate coefficient for nitrification appears to center around the selection of a value that represents the activity of the microbial population responsible for nitrification. However, because of the relative speed of conversion of NH_4 to NO_3, it is believed that the error introduced by not using the correct rate coefficient for this process may introduce only a small error when simulating long time periods for known NH_4 inputs.

Based on the nitrogen mineralization potentials of a large number of soils, Stanford and Smith[16] concluded that the cumulative amount of nitrogen mineralized followed a first order rate equation. Moreover, Stanford et al.[17] showed that the mineralization rate coefficient (k_3) varied with temperature in an exponential fashion. In this study, the transformation rate coefficients were chosen to represent an average temperature during a period of 2-3 weeks. The model can be adapted to incorporate changes in the rate coefficients owing to soil temperature. However, temperature distributions in the soil profile and in the crop canopy with time would be the required input parameters.

First-order rate processes have been used by Mehran and Tanji[12] and Hagin and Amberger[13] to describe denitrification in soils. Hagin and Amberger[13] included the effect of pH, temperature, oxygen and organic carbon content in their simulation of denitrification. In this project, oxygen diffusion as a controlling mechanism for denitrification was not included since it required additional parameters describing oxygen exchange in the root zone (respiration) as well as oxygen diffusion properties in the unsaturated soil profile. It should be pointed out that several investigators have reported denitrification rates which were independent of nitrate concentration (zero order kinetic) over a fairly wide range.[18,19,20] Bowman and Focht[21] have observed that many of these studies, however, were conducted at relatively high nitrate concentrations where zero-order reactions would be expected.

The kinetic rate coefficients for nitrogen transformations are frequently assumed to be constant[12,15], although their magnitude depends upon several soil environmental factors.

McLaren[22] suggested that these rate coefficients are dependent upon the size of the microbial population responsible for the transformation. The population and/or activity of any group of microbes is determined, in part, by the energy source available at any given depth in the soil profile. Based upon this, Rao et al.[4] assumed that the magnitude of k decreased exponentially with depth in a similar fashion to the organic matter content distribution in the soil profile.

The transformation rate coefficients are also dependent upon the soil-water content (θ) or soil-water suction (h). Selim et al.[23] have developed the following empirical relationships, similar to those used by Hagin and Amberger[13], using published data (Miller and Johnson[24], Stanford and Epstein[25], and Myers[26])

$$k_1 = \overline{k}_1 \; f_1(h) \tag{6a}$$

where,

$$f_1(h) = \begin{cases} 0 \; ; & h > -10 \text{ cm} \\ 0.005(-h-10); & h > -50 \text{ cm} \\ 0.2+0.006(-h-50); & h > -100 \text{ cm} \\ 0.5+0.0015(-h-100); & h > -433 \text{ cm} \\ 1.0-0.002(-h-433); & h < -433 \text{ cm} \end{cases} \tag{6b}$$

$$k_2 = \overline{k}_2 \tag{7}$$

$$k_3 = \overline{k}_3 \; f_3(h) \tag{8a}$$

where,

$$f_3(h) = \begin{cases} 0.25 + 0.0064(50+h) \; ; & h > -50 \text{ cm} \\ 0.25 + 0.005(-50-h) \; ; & h < -50 \text{ cm} \\ 1.0 \; ; & h < -200 \text{ cm} \end{cases} \tag{8b}$$

$$k_4 = \overline{k}_4 \tag{9}$$

and,

$$k_5 = \overline{k}_5 \; f_5(\text{OM},h,\,\theta) \tag{10a}$$

where,

$$f_5(\text{OM},h,\theta) = \begin{cases} 0 & ; \; (\theta/\theta_{sat}) < 0.8 \\ \left(\dfrac{\text{OM}(z)}{\text{OM}_{max}}\right) \left(\dfrac{\theta - 0.8\,\theta_{sat}}{0.1\,\theta_{sat}}\right) & ; \; 0.8 \le (\theta/\theta_{sat}) \le 0.9 \\ \text{OM}(z)/\text{OM}_{max}) & ; \; (\theta/\theta_{sat}) \ge 0.9 \end{cases} \tag{10b}$$

Note that in equations (6a) through (10b), $\bar{K}_i$ for i = 1 to 5 are constants, θ_{sat} is saturated water constant, and OM_{max} is the maximum mineralizable organic-N content in the soil profile. The functions f_i (i = 1 to 5) are empirical representations which describe the dependence of the transformation processes on θ, h, and/or OM.

NITROGEN TRANSPORT AND TRANSFORMATIONS

The movement of water-soluble nitrogen species through soil occurs as a result of molecular diffusion and mass transport in the soil-water phase. Because of the general acceptance of chromatography theory and its applicability to soil-water system, this approach was used to describe the vertical movement and distribution of water-soluble nitrogen species in a soil profile. The partial differential equation for transient one-dimensional solute transport and simultaneous transformations is (Selim et al.[23]):

$$\frac{\partial(\theta C_i)}{\partial t} = \frac{\partial}{\partial z} D(\theta,v)\frac{\partial C_i}{\partial z} - \frac{\partial(qC_i)}{\partial z} - \rho \frac{\partial S_i}{\partial t} \pm \Phi_i \qquad (11)$$

where C_i is the solution concentrations of the i^{th} nitrogen species (μg/cm^3), $D(\theta,v)$ is the dispersion coefficient (cm^2/day), q is the Darcy flux (cm/day), v is average pore-water velocity (cm/day) and obtained from q/θ, ρ is soil bulk density (g/cm^3), S_i is adsorbed solute phase of the i^{th} nitrogen species (μg/g), and Φ_i describes the biological transformations influencing the i^{th} nitrogen species.

The mobility of the ammonium (NH_4^+) ion in a soil-water system is directly influenced by the adsorption-desorption of NH_4^+ within the soil matrix. Numerous equations have been used to describe adsorption-desorption, but the most common are the Freundlich, first-order kinetic, and Langmuir equations (Davidson et al.[27]). Other types of cation exchange equations that could be used to describe the adsorption-desorption of NH_4^+ are described by Dutt et al.[28] Thermodynamically based adsorption-desorption equations require more information about the composition of the soil solution than is generally available. It is believed that simpler adsorption models can be used as reasonable approximations for the adsorption-desorption of NH_4^+ in many soil-water systems.

Assuming a linear Freundlich adsorption for NH_4^+ and first-order rate processes for the nitrogen transformations shown in Figure 1, equation (11) can be rewritten in the following form for NH_4^+ and NO_3^- in the soil solution (Selim et al.[23]):

$$R\frac{\partial A}{\partial t} = D\frac{\partial^2 A}{\partial z^2} - \frac{V}{\theta}\frac{\partial A}{\partial z} - k_1 A - k_4 A + \frac{\rho}{\theta} k_3 (OM) \qquad (12)$$

$$\frac{\partial B}{\partial t} = D\frac{\partial^2 B}{\partial z^2} - \frac{V}{\theta}\frac{\partial B}{\partial z} + k_1 A - k_2 B - k_5 B \qquad (13)$$

where, A = concentration of NH_4^+ in soil solution ($\mu g/cm^3$),
B = concentration of NO_3^- in soil solution ($\mu g/cm^3$),
OM = amount of mineralizable N in organic phase ($\mu g/g$),
k_1, k_2, k_3, k_4, k_5 = kinetic rate coefficients, respectively, for NH_4^+ nitrification, NO_3^- immobilization, NH_4^+ mineralization, immobilization of organic-N, and NO_3^- denitrification (day^{-1})

$V = q(z) - \theta\frac{\partial D}{\partial z} - D\frac{\partial \theta}{\partial z}$, where q(z) is the Darcy water flux (cm/day),

$R = 1 + \rho K_D/\theta$, retardation factor[23] for NH_4^+ exchange,

K_D = distribution coefficient for ion-exchange (cm^3/g), such that $E = K_D A$ where E is amount of NH_4 in exchangeable phase ($\mu g/g$).

The transformation processes for organic N are described by:

$$\rho\frac{\partial (OM)}{\partial t} = k_2 \theta B + k_4 \theta A - k_3 \rho (OM) \qquad (14)$$

and the gaseous loss of N due to denitrification is calculated from:

$$\rho\frac{\partial G}{\partial t} = k_5 \theta B \qquad (15)$$

where, G is the sum total of N_2O, NO, and/or N_2 gas ($\mu g/g$).

Finite difference approximations for the nonlinear partial differential equation governing transport and transformations of NO_3 and NH_4, respectively, may be expressed as follows[23]:

$$\begin{aligned} B_i^{n+1} - B_i^n = {} & \gamma D_i^{n+1/2} [B_{i+1}^{n+1/2} - 2B_i^{n+1} + B_{i+1}^{n+1}] \\ & - \gamma D_i^{n+1/2} [B_{i+1}^n - 2B_i^n + B_{i-1}^n] \\ & - (V/\theta)_i^{n+1} \beta [B_{i+1}^{n+1} - B_i^n] + k_1 \Delta t A_i^{n+1} \qquad (16) \\ & - (k_2 + k_5) \Delta t B_i^n \end{aligned}$$

and,

$$\begin{aligned}R_i^{n+1}\ [A_i^{n+1} - A_i^n] = {} & \gamma D_i^{n+1/2}\ [A_{i+1}^{n+1} - 2A_i^{n+1} + A_{i-1}^{n+1}] \\ & + \gamma D_i^{n+1/2}\ [A_{i+1}^n - 2A_i^n + A_{i-1}^n] \\ & - (V/\theta)_i^{n+1}\ \beta\ [A_{i+1}^{n+1} - A_i^{n+1}] \\ & - (k_1 + k_4)\ \Delta t\ A_i^n + k_3(\rho/\theta)\Delta t\ OM_i^n\end{aligned} \tag{17}$$

The initial condition of a nonuniform nitrogen concentration distribution in a semi-infinite soil column may be stated as:

$$\begin{aligned}A &= A\ (z,0) & 0 < Z < \infty \\ B &= B\ (z,0) & 0 < Z < \infty \\ OM &= OM(z,0) & 0 < Z < \infty\end{aligned} \tag{18}$$

For nitrogen transport and transformation, equations (12) and (13), the boundary condition considered was that of a continuous solute (NH_4 or NO_3) flux where:

$$qA - \theta D\frac{\partial A}{\partial z} = q\ CI \qquad z = 0 \qquad t \leq t_2 \tag{19a}$$

$$qB - D\frac{\partial B}{\partial z} = q\ CII \qquad z = 0 \qquad t \leq t_2 \tag{19b}$$

where, CI and CII are the applied solution concentrations of NH_4 and NO_3, respectively. When application of these solute solutions is terminated (i.e. $t>t_2$), equations (19a) and (19b) are also used with CI and CII equal to zero (provided that $t_2 \leq t_1$).

The finite difference approximations for water, NO_3, and NH_4 transport (equations (5), (16), and (17), respectively) are nonlinear since the values of $Cap(h_i^{n+1/2})$, $K(h_i^{n+1/2})$, and $D_i^{n+1/2}$ are dependent on h_i^{n+1} for which solutions are being sought. The iteration method described by Remson et al.[29] is frequently used to predict $h^{n+1/2}$ using h^n. Selim and Kirkham[30] showed that the solution of the water flow equation could be approximated satisfactorily using h^n, and a smaller Δt than required for a stable solution. This simplifies the computation considerably since the system of equations becomes linear. Accordingly, the following approximations were made:

$$Cap(h_i^{n+1/2}) = Cap(h_i^n)$$

$$K(h_i^{n+1/2}) = K(h_i^n)$$

$$D_i^{n+1/2} = D_i^n$$

Incorporation of the appropriate initial and boundary conditions in their respective finite difference forms and rearrangement of equations (5), (16), and (17) yield three linear systems of equations. In matrix-vector form, each system of equations yield a tridiagonal real matrix associated with a real column vector. The absolute value of each main diagonal coefficient is greater than the raw sum of the off-diagonal coefficients in the matrix. Hence, the matrix for each system of equations is diagonally dominant (Varga[31]). Therefore, each matrix is nonsingular and a unique solution exists.

To satisfy the convergence criteria in solving equations (5), (16), and (17), the increments Δz and Δt were chosen such that

$$\Delta z \leq D_{max}/V_{max}$$

$$\Delta t \leq \Delta z/2V_{max}$$

$$(\frac{\Delta t}{z})^2 (\frac{K}{Cap_{max}}) \leq 1/2$$

where D_{max}, V_{max}, K_{max}, Cap_{max} are the maximum values of D, V, K, and Cap at any time step.

Thus far we have presented numerical solutions for water flow (equation [1]), and the NH_4 and NO_3 transport and transformations (equations [12] and [13]). In order to complete the nitrogen transformation processes, it is necessary to solve for exchangeable NH_4(E), organic-N (OM), and gaseous-N (G) at every time step and incremental distance in the soil profile. This was achieved as follows:

$$E_i^{n+1} = K_D C_i^{n+1}, \tag{20}$$

$$OM_i^{n+1} = OM_i^n + (\Delta t/\rho)\ [k_2\ \theta\ B_i^{n+1} + k_4\ \theta\ A_i^{n+1} - k_3\ \rho\ OM_i^n] \tag{21}$$

$$G_i^{n+1} = G_i^n + (\Delta t/\rho)\ k_5\ \theta\ B_i^{n+1} \tag{22}$$

SOLUTE TRANSPORT IN MULTI-LAYERED SOILS

For the research model discussed thus far, represented by equations (1), (12), and (13), the soil profile has been assumed homogeneous with respect to soil physical properties and solute adsorption characteristics. Most soil profiles, however, are multi-layered or nonhomogeneous in nature. Therefore, a separate study was initiated to develop a simulation model for describing solute transport through a saturated and unsaturated multilayered soil profile. The model was based on finite-difference approximations of the convective-dispersive equation for solute transport (see eq. 11). Details of model development are reported by Selim et al.[32]. The major features of the model and conclusions reached are presented in the following discussion.

Figure 2 shows the soil water content (θ) and soil water suction (h) distributions in a soil profile consisting of two distinct layers, clay and sand, each having equal lengths ($L_1 = L_2 = 50$ cm). The case where the water table was at a finite depth L = 100 cm is illustrated in Figure 2A. The case where the water table was at depth $x \to \infty$, i.e. the bottom layer having a great length, is shown in Figure 2B. The steady state soil-water content (θ) and water suction (h) distributions for the clay-sand soil profiles shown in Figure 2 resulted from a constant flux (q) of 0.072 cm/day at the soil surface. The saturated water content (θ_{sat}) of the sand and the clay layer were 0.40 and 0.55 cm^3/cm^3, respectively.

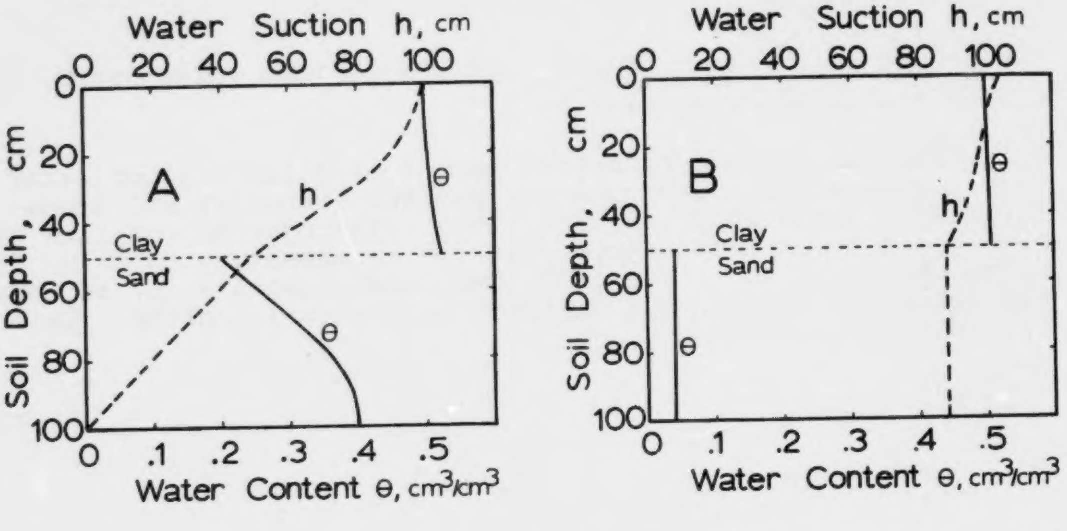

Figure 2. Soil-water content (θ) and soil-water suction (h) versus depth in a clay-sand soil profile. For A the water table is at x = 100 cm, and for B it is at a great depth ($X \to \infty$).

Effluent concentration distributions (relative solute concentration, C/Co, versus effluent pore volume, V/V_o) for a nonadsorbed and adsorbed solute exiting the soil profiles in Figure 2 at x = 100 cm are shown in Figure 3. For the nonadsorbed solute, the concentration distributions were similar regardless of the position of the water table. In contrast, concentration distributions for the adsorbed (first order kinetic adsorption) solute were distinctly different. A lower average regardation factor exists for the soil profile having a water table at x = 100 cm (Figure 3). The average soil-water content in the soil profile with a water table at x = 100 results in a lower retardation factor in comparison with the case where the water table was at $x \to \infty$. Note that because of the marked differences in soil-water content distributions, the pore volumes V_o were significantly different among all cases considered.

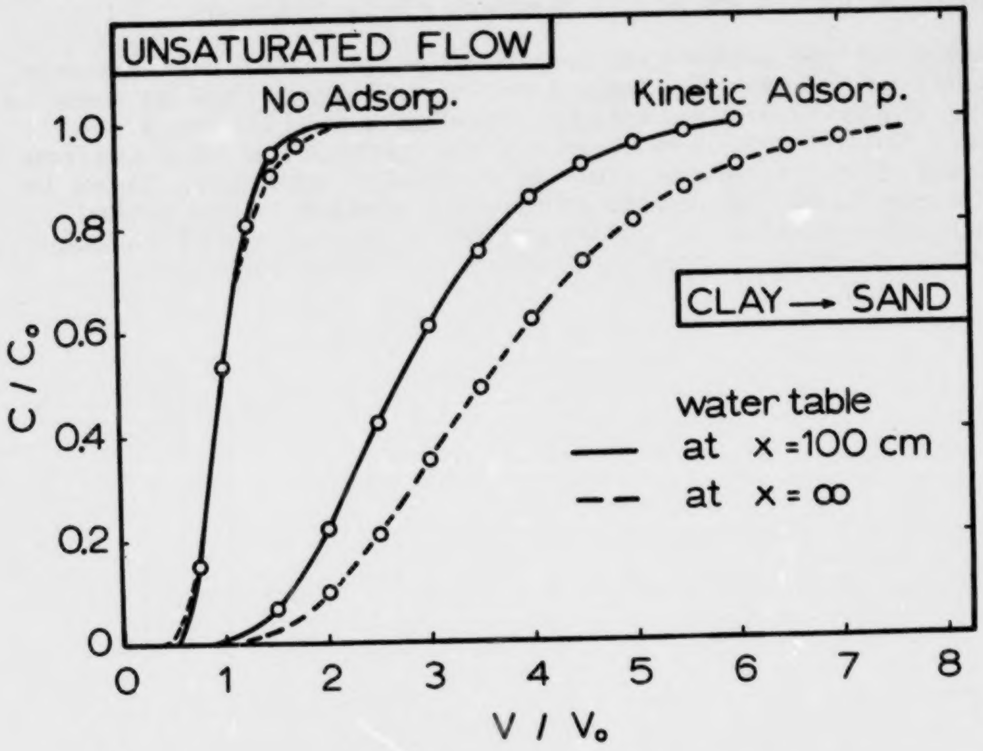

Figure 3. Adsorbed and nonadsorbed solute relative effluent solute concentration (C/Co) distributions from unsaturated clay-sand soil profiles. Open circles were calculated based on average soil-water content within each soil layer, whereas the solid and dashed lines were calculated using the soil-water content shown in Figures 2A and 2B.

If the water content distributions (Figure 2A and B) were considered uniform, with an average water content within each individual layer, the problem of solute transport and adsorption through unsaturated multilayered soil profiles can be significantly simplified as discussed in the previous section. The open circles in Figure 3 are calculated concentration distributions for adsorbed and nonadsorbed solutes when an average soil-water content within each layer was assumed. These results show that for all unsaturated profiles considered, the use of average soil-water contents (open circles) provided identical concentration distributions to those obtained where the actual water content distributions were used (dashed and solid lines). Thus, when a steady water flux (q) is maintained through a layered soil profile, concentration distributions of adsorbed and nonadsorbed solutes at a given location in the soil profile can be predicted using average soil-water contents. Results from laboratory experiments using adsorbed and nonadsorbed solutes and layered soil columns (Selim et al.[32]) support these findings.

Based on the above results, it was concluded that average microhydrologic characteristics for a soil layer can be used to describe the movement of solutes leaving a multilayered soil profile. This conclusion supports the assumption that uniform soil-water content can be used to represent each soil layer in order to simplify the solute transport problem. The above findings were helpful in modifying the research model to consider multilayered or nonhomogeneous soil profiles.

SECTION 5

MODELS FOR PLANT UPTAKE

The inherent complexity of the crop root zone and the dynamic nature of water and nutrient uptake by roots defies an exact mathematical description at a "microscopic" level. However, there have been several attempts to accomplish this difficult task. On a simplified scale, the root system can be represented by a line sink of uniform strength (absorptivity). The water transport equation for this case, written in cylindrical coordinates, has been solved for a variety of initial and boundary conditions. Depending upon the restrictiveness of the conditions, analytical solutions[33] as well as numerical solutions[34,35] to the flow equations are available. However, due to a lack of experimental data that characterize many of the crop parameters at a microscopic level, these models generally have not been verified.

In other modeling efforts, the microscopic flow processes near a root are ignored and the entire root system is treated as a distributed sink of known density or strength[36-39]. These macroscopic models have been able to provide an integrated description of soil-water extraction by crops grown under field conditions[40] and to simulate the effects of irrigation water and soil salinity on crop production[41]. Microscopic models, on the other hand, have been useful in identifying soil and crop parameters that are significant in determining water uptake by plant roots[35].

PLANT UPTAKE OF WATER

After an extensive literature search, the models proposed by Molz and Remson[37,38] and Nimah and Hanks[39] for describing soil-water uptake by plant roots were selected for further evaluation.

The process of soil-water flow to roots is ignored in macroscopic modeling approaches, and water extraction by plant roots is treated as a sink in the one-dimensional transient water flow equation:

$$\frac{\partial\theta}{\partial t} = \frac{\partial}{\partial z}[D(\theta)\ \frac{\partial\theta}{\partial z}\ ] - \frac{\partial}{\partial z}[K(\theta)] - W(z,\theta,t) \qquad (23)$$

where,

θ = volumetric soil-water content (cm^3/cm^3),
$D(\theta)$ = soil-water diffusivity (cm^2/day),
$K(\theta)$ = soil hydraulic conductivity (cm/day),
t = time (days),
z = soil depth (cm),
$W(z,\theta,t)$ = a sink term (day^{-1}) to account for uptake of soil water by plants.

Several functions have been postulated for $W(z,\theta,t)$. The form proposed by Molz and Remson[37] is:

$$W(z,\theta,t) = (ET) \frac{D(\theta)\ R(z,t)}{\int_o^L D(\theta)\ R(z,t)\ dz} \tag{24}$$

where,

ET = volumetric evapotranspiration rate per unit soil surface area (cm^3/cm^2/day),
L = depth of bottom of root zone (cm), and
$R(z,t)$ = "effective" plant root distribution function which is proportional to the root density distribution.

It should be recognized that equation (24) is an empirical model that distributes the evapotranspiration demand (ET) over the entire root zone according to the product $[D(\theta)\ R(z,t)]$. The transpiration demand (ET) could be made to vary with time.

The form of the plant water uptake sink term $[W(z,t)]$ used by Nimah and Hanks[39] is:

$$-W(z,t) = \frac{[H_r + (RRES \cdot z) - h(z,t) - s(z,t)]\ R(z) \cdot K(\theta)}{\Delta x \cdot \Delta z} \tag{25}$$

where, H_r is an effective root water potential; RRES is a root resistance term and the product (RRES·z) accounts for gravity term and friction loss in H_r; $h(z,t)$ is soil-water pressure head; $s(z,t)$ is the osmotic potential; Δx is assumed to be unity and is the distance from plant roots to where $h(z,t)$ is measured; Δz is soil depth increment; $R(z)$ is proportion of the total root activity in the depth increment Δz; and $K(\theta)$ is the hydraulic conductivity.

Major drawbacks of the Molz-Remson[37] approach are that they assume (i) all soil water to be available for plant root extraction, and (ii) that the evapotranspiration demand will be satisfied by the plant roots, regardless of the soil water status in the soil profile. The Molz-Remson model was modified during this project to overcome these two drawbacks. First, the total available water (TAW) to plant roots was defined as that water contained in the soil profile between "field capacity" (θ_{FC}) and 15-bar water contents (θ_{15}),

$$TAW = \int_0^L (\theta_{FC} - \theta_{15})\, dz \qquad (26)$$

Second, the evapotranspiration demand (ET) was set equal to potential evapotranspiration rate (PET) calculated from a Penman type model when available water (AW) in the profile was greater than or equal to 20% TAW. The value of ET was decreased linearly to zero when AW was less than 20% of TAW.

$$\begin{array}{ll} ET = PET & AW \geq 0.2\ TAW \\ ET < PET & AW < 0.2\ TAW \end{array} \qquad (27)$$

The modification used in equation (27) was based upon the experimental data of Ritchie[42]. The potential evapotranspiration demand (PET) on any given day of the growing season was calculated by a Penman-type model[43]. The value of PET was further adjusted by multiplying it by a "crop factor" to account for changes in crop water uptake demand during the season (Blaney and Criddle[44]).

The simple case of soil-water uptake by plant roots from a "static" soil profile (i.e., no vertical flow of water) was simulated using the Molz-Remson model as well as the Nimah-Hanks model. The soil profile was assumed to be at a "field capacity" soil-water content (θ_{FC}) of 0.08 cm^3/cm^3 throughout the root zone, while θ_{15} was set equal to 0.03 cm^3/cm^3. Thus, the total plant available water, as defined in equation (26), in the root zone (L=100 cm) was equal to 5 cm of water. The K(θ) function used was:

$$K(\theta) = Exp[-3.3470^{-0.62} + 10.1753] \qquad (28)$$

The root length distribution in the soil profile was described by:

$$R(z) = [3.384][Exp(-0.035z)][Sin(0.031415z)] \qquad (29)$$

and was assumed not to change during the 8-day simulation period. Note that the value of R(z) is equal to zero at z=0 and 100 cm with a maximum root density at z=23 cm. The potential evapotranspiration demand (PET) during the simulation period was assumed constant at 0.6 cm/day.

For the case described above, equation (23) reduces to:

$$\frac{\partial\theta}{\partial t} = -W(z,\theta,t) \qquad (30)$$

where, the changes in soil-water content (θ) are only due to plant uptake. The functional forms proposed by Molz-Remson (equation 24) and Nimah-Hanks (equation 25) were used to describe the sink term $W(z,\theta,t)$. In the evaluations presented in this report, the $D(\theta)$ function in equation (24) was replaced by $K(\theta)$ function due to a greater sensitivity of the latter to changes in θ.

The value of effective root water potential (H_r) in equation (25) is an unknown. Nimah and Hanks estimated its value at every time step by successive iterations to make the plant root uptake of water over the entire root zone equal to the transpiration demand. This process continued as long as H_r was higher than the potential below which the plant would wilt. Thus, in the Nimah-Hanks model, $0 \leq H_r \leq H_{wilt} = 15$ bars. The necessity of having to "search" for an appropriate H_r value can be avoided by solving equation (25) explicitly for H_r in the following manner and noting that:

$$PET\ (t) = \int_o^L W(z,\theta,t)dz \qquad (31)$$

Substitution of equation (25) for $W(z,\theta,t)$ in equation (31) and assuming $\Delta x=\Delta z=1.0$, yields:

$$PET(t) = \int_o^L [H_r+(RRES \cdot z)-h(z,t)-s(z,t)]\ R(z)\ K(\theta)\ dz \qquad (32)$$

Equation (32) may be expanded to:

$$PET(t) = H_r \int_o^L R(z)\ K(\theta)\ dz + RRES \int_o^L z\ R(z)\ K(\theta)\ dz - \int_o^L h(z,t)\ R(z)\ K(\theta)\ dz - \int_o^L s(z,t)\ R(z)\ K(\theta)\ dz \qquad (33)$$

Rearranging equation (33) to solve for H_r results in:

$$H_r = [PET(t) - RRES \int_o^L z\ R(z)\ K(\theta)\ dz + \int_o^L h(z,t)\ R(z)\ K(\theta)\ dz + \int_o^L s(z,t)\ R(z)\ K(\theta)\ dz] / \int_o^L R(z)\ K(\theta)\ dz \qquad (34)$$

Equation (34), therefore, allows for the calculation of H_r at every time step from known values of $PET(t)$, z, $R(z)$, and $K(\theta)$. It was assumed that $RRES = 1.0$ and $s(z,t) = 0.0$ for the evaluations presented in this report.

The soil-water content distributions at selected times resulting from root uptake, as described by the two models, are summarized in Table 1. It is apparent that both models predicted identical uptake patterns up to 4 days, but deviated for larger times. As illustrated in Figure 4, the potential evapotranspiration was met only up to 4 days in the Molz-Remson model, while in the Nimah-Hanks model "water stress" does not commence until the 6th day. Recall that the definition of water stress is different in the two models. In Nimah-Hanks model water stress is indicated by the approach of H_r to 15-bar value, while in the Molz-Remson model potential ET cannot be satisfied when $AW/TAW \leq 0.2$ as defined in equation (27). Therefore, the differences in the soil-water content profiles as predicted by the two models are due to the manner in which the physiological response of plants to water stress was conceptualized. The important conclusion, however, is that both Molz-Remson and Nimah-Hanks models predict identical water uptake patterns as long as there is no soil water stress. For this reason, the simpler Molz-Remson model (equation 24 with modifications described) will be used in our modeling efforts to simulate water uptake by plant roots.

PLANT UPTAKE OF NITROGEN

Nitrogen uptake by plants involves the movement of water soluble nitrogen species (NH_4 and NO_3) to roots followed by their absorption across the root surfaces. Mass flow and diffusion are the two major processes by which NH_4 and NO_3 are transported to the roots[45-49]. Convective flow of water towards roots in response to transpiration results in the mass transport of NH_4 and NO_3 to the roots along with the soil water. The concentration of these ions at the root surface decreases when the rate of root uptake exceeds the rate of supply of these ions by mass flow. Diffusion of NH_4 and NO_3 towards the roots occurs due to the concentration gradient.

Arguments abound in the literature as to the relative importance of mass-flow or diffusion as the major process by which nutrients are supplied to plant roots[45,47,49,52]. However, when supply by mass-flow is restricted (such as due to moisture stress), diffusion becomes a major mechanism of nutrient supply[53-56]. Mass-flow may be a dominant process for nonadsorbed nutrients with high solubilities (e.g. NO_3), while diffusion appears to be significant for adsorbed species (e.g. P,K,Zn,Fe, etc.). The relative importance of these two processes will also depend upon the geometry of the root system. Higher root densities result in shorter distances over which ions must be transported; hence, diffusion may be responsible for the transport of a considerable amount of a given nutrient[57] to the root surface.

TABLE 1. COMPARISON BETWEEN SOIL-WATER CONTENT (θ) PROFILES DURING AN 8-DAY PERIOD IN A SANDY SOIL AS SIMULATED USING THE MOLZ-REMSON (M-R) AND THE NIMAH-HANKS (N-H) MODELS FOR PLANT UPTAKE OF SOIL WATER.

Soil Depth (cm)	2 Days		4 Days		6 Days		8 Days	
	M-R	N-H	M-R	N-H	M-R	N-H	M-R	N-H
10	0.0638	0.0638	0.0513	0.0513	0.0405	0.0448	0.0319	0.0427
20	0.0621	0.0622	0.0500	0.0501	0.0396	0.0438	0.0314	0.0418
30	0.0623	0.0624	0.0502	0.0502	0.0397	0.0439	0.0314	0.0419
40	0.0633	0.0634	0.0510	0.0510	0.0402	0.0445	0.0318	0.0425
50	0.0651	0.0651	0.0523	0.0524	0.0412	0.0456	0.0324	0.0435
60	0.0674	0.0673	0.0542	0.0542	0.0424	0.0471	0.0333	0.0448
70	0.0702	0.0701	0.0568	0.0568	0.0442	0.0491	0.0344	0.0467
80	0.0734	0.0733	0.0604	0.0603	0.0466	0.0521	0.0360	0.0494
90	0.0769	0.0768	0.0660	0.0660	0.0506	0.0569	0.0386	0.0539

Due to the uncertainties in the mechanisms of nutrient transfer across root surfaces, several models have been proposed. These models may be classified into two groups. In the first group, the rate of solute uptake is assumed to proceed at such a rate as to maintain either a constant or zero solute concentration at the root surface[48,58]. In the second group of models, the solute flux into the roots is assumed constant or varies linearly or nonlinearly with solute concentration at the root surface[45,47,49,58,61-63]. The nitrogen species taken up by plant roots are NH_4 and NO_3. However, due to the relatively rapid transformation of NH_4 to NO_3 and the greater mobility of the latter ion, most researchers have considered only the uptake of NO_3 by plants.

From a sensitivity analysis of a nutrient uptake model that accounted for diffusive-convective flow to roots, van Keulen et

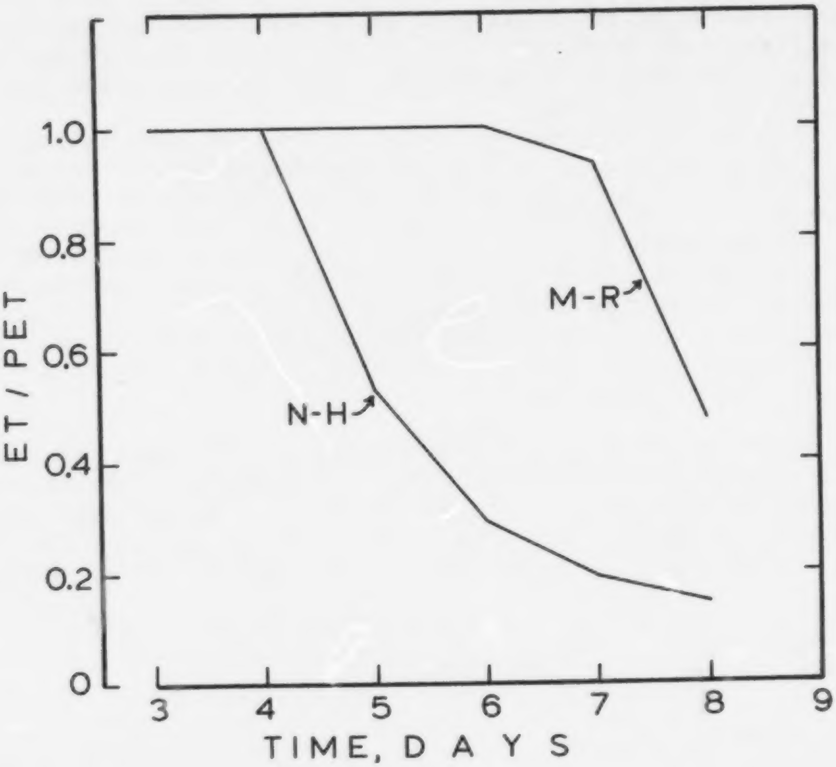

Figure 4. Evapotranspiration (ET) as a fraction of potential evapotranspiration (PET) with time as simulated by the Molz-Remson (M-R) and the Nimah-Hanks (N-H) models.

al.[64] concluded that virtually the whole nutrient supply in the root zone may be available in a short time to an actively growing root system. They suggested that root density played a significant role in determining plant nutrient uptake. Russell and Shone[65] demonstrated that when part of the intact root system of barley was exposed to more favorable conditions (higher nitrogen concentrations) than the remainder, root proliferation was limited exclusively to that zone with favorable conditions. Thus, higher root densities should result in a greater nutrient uptake by the root segments in the favorable environment. Similar conclusions were arrived at by Jungk and Barber[62,66] from a series of experiments where root trimming and/or split-root techniques were utilized to investigate nutrient uptake by plant roots. Brower and de Wit[67], however, have also observed root density increases when nutrients were limited. Our understanding of the physiology of the plant root systems regarding compensatory growth and uptake under conditions of nutrient and/or water stress is inadequate. The concentration of nutrients and root density (number, length, area, etc.) in a given soil volume appear to be important to plant root uptake. The transport of nutrients to root surfaces is not likely to be a limiting process as long as the root density is high.

It must be recognized that in all of the nitrogen uptake models discussed in the preceeding paragraphs, transport of water and solutes only in the radial direction towards the roots is considered; losses or gains of water and solutes within a unit volume soil element due to vertically upward or downward flow are ignored. Thus, the nutrient uptake models currently available treat the soil profile as being "static" with regard to vertical flow. A comprehensive three-dimensional treatment of water and solute flow to describe plant uptake is not available at the present time.

In light of the above discussion, the microscopic processes (diffusion and mass flow) responsible for transporting nitrogen to the root surfaces were ignored in this study and the uptake of nitrogen was modeled as a sink term in the flow equations. The rate of nitrogen uptake (q_N^{max}) was calculated as follows:

$$q_N^{max} = Q_N^{max} \Big/ \int_0^L R(z,t)\,dz \qquad (35)$$

where, Q_N^{max} represents the nitrogen uptake demand (μgN/day/cm^2 soil surface) of the crop under non-limiting nitrogen supply; the integral of the root length distribution, $R(z,t)$, over the rooting depth L yields the total root length (cm root/cm^2 soil surface); and q_N^{max} has the dimensions of μg N/day/cm root. The values of Q_N^{max} were determined by analyzing experimental data for cumulative nitrogen uptake during the season for a specific crop (in our case corn) grown under nonlimiting water and nitrogen conditions. This approach is similar to that used by Watts[63]. Empirical models were also developed (to be discussed later) using experimental data to simulate the root length distributions, R(z,t), in the soil profile at various times during the growing season.

In deriving equation (35), it was assumed that the root capacity for nitrogen absorption was uniform over the entire root system. Thus, root length distributions represented the "sink strength" for nitrogen uptake. However, the root absorption capacity is known to be neither constant nor uniform, but influenced by several factors[62,66,69-71] (e.g. root diameter, age, and distance from stem base). Based upon the work of Dibb and Welch[72], the uptake of both NO_3 and NH_4 species was considered. Data are presently unavailable to determine the fractional uptake of NH_4 and NO_3 when both species are present. The actual rate of nitrogen uptake (q_N) was determined by a Michaelis-Menton type relationship based on the total concentration of NH_4 and NO_3 species in the soil solution:

$$q_N = q_N^{max} \left[\frac{A(z,t) + B(z,t)}{K_m + A(z,t) + B(z,t)}\right] \tag{36}$$

where, A and B are solution concentrations of NH_4 and NO_3; K_m is the value of (A+B) when $q_N = 0.5q_N^{max}$. Total nitrogen uptake demand (q_N) was satisfied by uptake of both NH_4 and NO_3 as follows:

$$q_N = q_A + q_B \tag{37}$$

$$q_A = q_N^{max} \left[\frac{A(z,t)}{K_m + A(z,t) + B(z,t)}\right] \tag{38}$$

$$q_B = q_N^{max} \left[\frac{B(z,t)}{K_m + A(z,t) + B(z,t)}\right] \tag{39}$$

where, q_A and q_B are rate of uptake of NH_4 and NO_3, respectively, and other parameters are as defined previously. The value of q_A and q_B when multiplied by the R(z,t) in a given volume element of the soil profile yields the value for the corresponding uptake sink term in equations (12) and (13). Thus the total amount of nitrogen extracted from the root zone within a time increment Δt may be calculated as:

$$U_N = \int_o^L \int_{t_1}^{t_2} q_A \, R(z,t) \, dtdz + \int_o^L \int_{t_1}^{t_2} q_B R(z,t) \, dtdz \tag{40}$$

where U_N is cumulative amount (μgN) of nitrogen (NH_4+NO_3) taken up from the root zone during the time increment $\Delta t=t_2-t_1$; other parameters were defined previously.

In summary, in our uptake model the amount of nitrogen taken up by the plants is dependent upon (i) the nitrogen requirements of the plant (Q_N^{max}), (ii) the root length distributions [R(z,t)], and (iii) the concentration distributions of NH_4 and NO_3 within the root zone. Transport of nitrogen species to the root surfaces is implicitly ignored in our model.

ROOT GROWTH MODELS

Utilization of the models for water and nitrogen uptake, described in earlier sections, requires a knowledge of the exact nature of the root distribution in the soil profile at all times during the growing season. Reliable experimental techniques to measure root distribution are currently being evaluated[73]. However, measuring root lengths and numbers by the "line intersect" method[74] appears to be the most popular procedure.

Our understanding of the dynamics of root growth is sparse. Limited quantitative data do not permit formulation and/or verification of conceptual root growth models. Several researchers have investigated the influence of various soil and crop factors on root development. Some of the more important soil physical-chemical properties regulating root growth are: soil bulk density[75], porosity[75], soil-water suction[75], pH[76] and aluminum content[76]. Rooting habits (such as shallow or deep rooted) as well as sensitivity to the above listed soil parameters are not only different for individual crops but also vary from variety to variety for the same crop.

Root growth may be considered to consist of concurrent processes of proliferation, extension, senescence and death[77]. Localized increase in root density due to branching without an increase in the total volume of root zone is refered to as proliferation. Extension is the process by which the root system penetrates to deeper depths. Suberization and gradual reduction in root permeability is termed senescence. Further aging leads to eventual death of the roots. Following Hillel and Talpaz[77] the length of active roots, R_i^j, at depth i and time j may be expressed as:

$$R_i^j = R_i^{j-1} + R_i^{j-1}\, P\, \Delta t - R_i^{j-1}\, D\, \Delta t + R_i^{j-1}\, E\, \Delta t \qquad (41)$$

where, R_i^{j-1} is root density (cm root/cm^3 x soil) at the same depth at a previous time j-1 (Δt time units earlier); P is proliferation rate, D is death rate and E is rate of extension,

R_{i-1}^{j-1} is root length in the previous (j-1) time step in the overlaying depth increment (i-1). Note that P, D, and E are rates per unit time expressed as a fraction of the existing root length. The process of senescence is disregarded in equation (41). Thus, the use of Hillel-Talpaz[77] model would require a knowledge of at least three growth parameters (P, D, and E). Lambert et al.[78] presented a conceptual model to describe the development of two-dimensional root systems. Their model accounted for (i) the effect of soil-water suction (or water content) on rate of root growth at any position in the soil profile, and (ii) the concept of geotropism of roots, i.e. preference for downward rather than horizontal growth. Whisler[79] modified this model to include impedence of root growth resulting from soil layering.

The general problems in development and testing of models for root growth were summarized by Hillel and Talpaz[77] as follows:

> ".......... the very ease with which theoretical models can be developed into increasingly complex hypothetical constructions without any apparent logical limits presents a problem in itself. The imagination of modelers and the capability of computers already exceed the bounds of our experimental information on the behavior of the real system which we may pretend to simulate. However much we believe our own model to be based on essentially sound concepts of soil moisture and root system dynamics, it still requires rigorous testing, which is indeed a very arduous and painstaking task."

Because of these problems, empirical models were devised to simulate root length distributions on the basis of experimental data of NaNagara et al.[63] for corn (Zea mays L.) grown under field conditions on Maury soil. Empirical equations were obtained by "curve fitting" to measured distributions at selected times during the season. These equations are as follows:

$$R^*(z,t) = [R^*_{max}][\exp(-\beta z^2)][\cos(\frac{\pi z}{2L})] \tag{42}$$

where, $R^*(z,t)$ = root length density (cm root/plant/cm depth)

R^*_{max} = maximum root length density (at soil surface, z=0),

z = soil depth (cm)
L = depth to the bottom of root zone (cm)

The values of the parameters R^*_{max}, L, and β in equation (42) varied during the growing season as follows:

$$R^*_{max} = \begin{cases} 0 & ; N \leq 5 \\ (-0.05253N^2 + 24.26667N - 120); & N > 5 \end{cases} \tag{43}$$

$$L = \begin{cases} (0.06N^2 - 0.1N) & ; N \leq 29 \\ (-0.0112N^2 + 2.53N - 15.0); & N > 29 \end{cases} \tag{44}$$

$$\beta = \frac{\ln[2 \cos (\pi z_{1/2}/2L)]}{(z_{1/2})^2} \tag{45}$$

where,

$$z_{1/2} = \begin{cases} L[-0.0001854N^2 + 0.022N - 0.102] \\ (0.4)(L); \quad z_{1/2} < 0.4L \end{cases} \tag{46}$$

and represents the soil depth at which root length density is one-half the value of R^*_{max} and N is the number of days since planting. Note that the values of $R^*(z,t)$ are expressed as cm root/plant/depth. The effect of crop planting density (PD, plants/cm^2 surface) must be known prior to using the uptake models. For the case of 48,000 plants/ha, PD = 4.8×10^{-4} plants/cm^2 soil surface and the adjusted root density (cm root/cm^2 soil surface/cm depth) is:

$$R(z,t) = R^*(z,t) \times 4.8 \times 10^{-4} \tag{47}$$

Root length distributions calculated at selected times using these empirical equations are presented in Figure 5. Increases in root length density at all depths and deeper penetration of the soil profile by the root system with time is evident.

In adapting these root distributions for inclusion in the uptake models, it was assumed that root absorption capacity for water and nitrogen was uniform and remained constant during the growing season over the entire root system. We recognize that the empirical model presented here is not adequate for a general model. However, in the absence of a better understanding of root growth dynamics and the unavailability of input parameters for the conceptual models, the empirical models may satisfy our present needs.

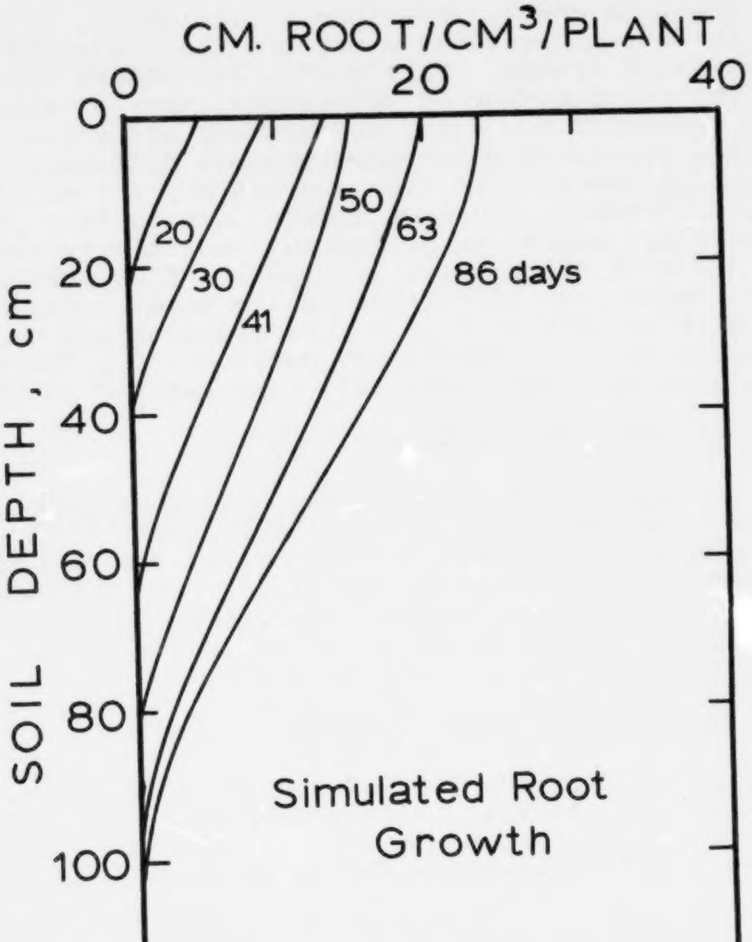

Figure 5. Root length density distributions for corn (Zea mays L.) at selected times during the growth season as calculated by the empirical model.

SECTION 6

MANAGEMENT MODEL

The research model, described in Section 4, is conceptually pleasing in that it provides a mechanistic description of the soil-water-plant system. This model, and others like it, require an extensive number of parameters, many of which are generally unavailable. Also, application and verification of these models for large watersheds becomes difficult owing to the spatial variability of input parameters for soil/plant properties. However, research models such as that presented in Section 4 are useful in performing sensitivity analyses to identify the most significant processes and/or parameters, thereby allowing simplifications in the model. Simpler models become desirable when only gross descriptions are required. A simple conceptual management-type model for describing the fate of nitrogen in the plant root zone is presented in this section.

TRANSPORT OF WATER AND NITROGEN

Several simplified forms of the transient, one-dimensional water flow model (equation 1) have been used[14,28,80]. Perhaps the most simplified concept is that of "piston displacement" used by Frere et al.[81] and Rao et al.[82]. The conceptual methods proposed by these latter authors are discussed in detail here. The technique is based on two principal assumptions: (i) all soil pore sequences participate in solute and water transport, and (ii) the soil water initially present in the profile is displaced ahead of the water entering at the soil surface.

Consider the infiltration of an amount of water, I, into a homogeneous soil profile, with a uniform initial soil-water content fraction of θ_i (cm³/cm³). The depth to which the wetting front will advance can be calculated from:

$$d_{wf} = \frac{I}{(\theta_f - \theta_i)}, \quad \theta_f > \theta_i \tag{48}$$

where, d_{wf} is the distance (cm) from the soil surface to the wetting front, and θ_f is soil water content in the wetted zone behind the wetting front. For infiltration of 5 and 10 cm of water into an initially dry ($\theta_i = 0$) soil, the wetting front depth (d_{wf}) would be 14.3 and 28.6 cm, respectively, when $\theta_f = 0.35$ cm³/

cm^3 (Figure 6). However, if θ_i was 0.10 cm^3/cm^3 and θ_f was 0.35 cm^3/cm^3, the wetting front would be at 20 and 40 cm, respectively, for the 5 and 10 cm water applications (Figure 7). Therefore, for a given water application and θ_f, the wetting front depth increases as θ_i increases.

If assumptions (i) and (ii) given above are valid, then the water at the observed wetting front for $\theta_i>0$ is the water initially contained in the soil profile and not that added at the soil surface. Hence, complete displacement of the initial water ($\theta_i>0$) results in a nonadsorbed solute front being located at:

$$d_{sf} = \frac{I}{\theta_f} \tag{49}$$

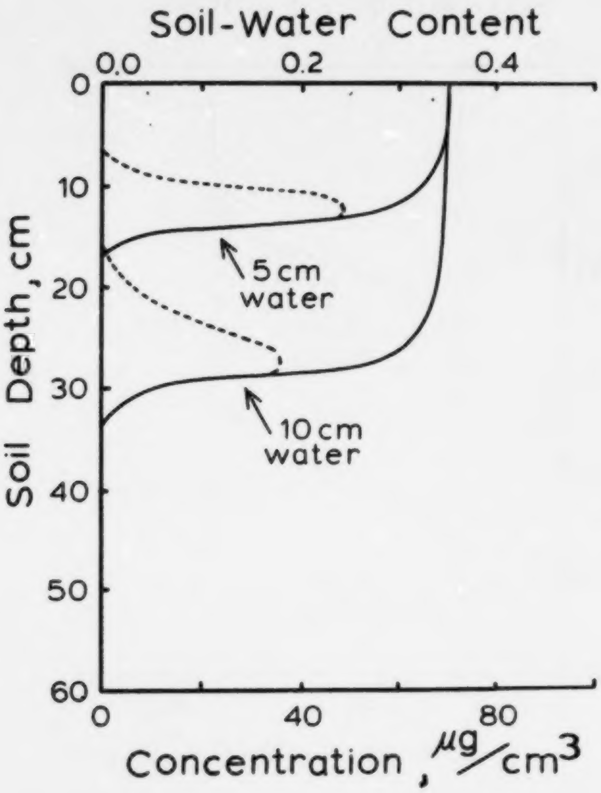

Figure 6. Distribution of soil-water (solid line) and nonadsorbed solute (dashed line) after 5 and 10 cm of water had infiltrated into an initially dry (θ_i=0) soil profile.

where d_{sf} is the solute front position (cm). Dividing equation (49) by equation (48) and rearranging terms yields:

$$\frac{d_{sf}}{d_{wf}} = [1 - \frac{\theta_i}{\theta_f}] ; \qquad \theta_f > \theta_i \tag{50}$$

Note that the value of the ratio (d_{sf}/d_{wf}) is equal to 1.0 when $\theta_i=0$ (i.e., infiltration into oven-dry soil); thus the nonadsorbed solute front rides on the wetting front. However, when $\theta_i>0$ (i.e., infiltration into moist soil), the nonadsorbed solute front would lag behind the observed wetting front $[(d_{sf}/d_{wf})<1]$. Equation (50) is not valid for the case of $\theta_i=\theta_f$, as the ratio (d_{sf}/d_{wf}) is equal to zero. Note that the nonadsorbed solute front position depends on the amount of water added and the average soil-water content in the wetted zone behind the wetting front, but not on the initial water content (Figures 6 and 7).

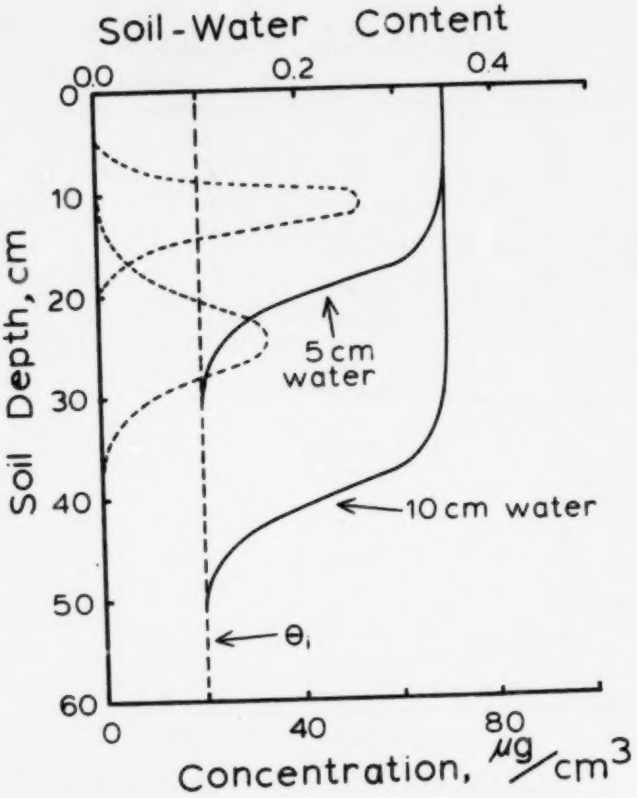

Figure 7. Distribution of soil-water (solid line) and nonadsorbed solute (dashed line) after 5 and 10 cm of water had infiltrated into a soil profile at a uniform initial water content (θ_i, shown as vertical dashed line) of 0.1 cm^3/cm^3.

This conclusion is in agreement with experimental observations of previous workers[82-85].

Published data for NO_3^- and Cl^- movement in several soils were used to test the validity of assumptions (i) and (ii). These data are presented in Figure 8 and are compared to equation (50). Considering the wide range in experimental conditions and that both laboratory and field data were included, the agreement between the 1:1 line and the data is excellent. Apparently, in all the cases considered, the initial soil water in the profile was displaced ahead of the applied water; thus, supporting our principal assumptions.

At the termination of infiltration, the soil water content in the wetted zone decreases due to drainage or redistribution until the profile attains a "field capacity" water content (θ_{FC}). The movement of the solute front due to this process is determined by the amount of "drainable" water above the depth d_{sf}.

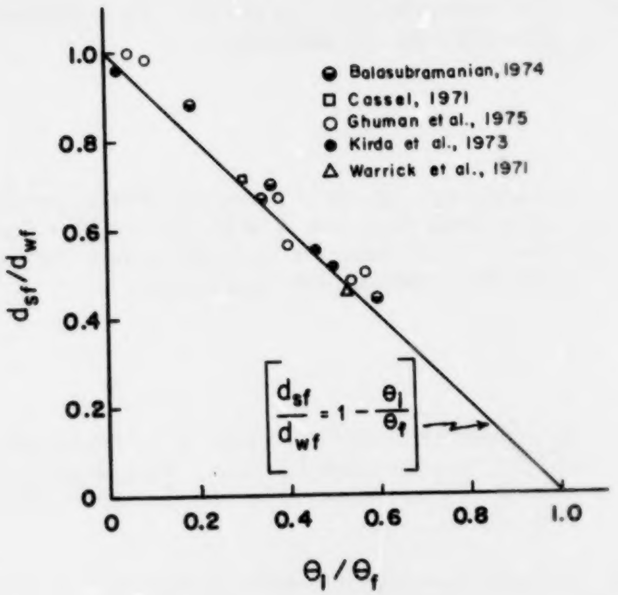

Figure 8. Agreement between d_{sf}/d_{wf} and θ_i/θ_f as calculated by Equation (50) and experimental data from various sources.

It can be shown that:

$$d'_{sf} = d_{sf} + \frac{(d_{sf})\ (\Delta\theta)}{\theta_{FC}} \tag{51}$$

where d'_{sf} is solute front location after redistribution, $\Delta\theta = (\theta_f - \theta_{FC})$, and the product $(d_{sf})(\Delta\theta)$ represents the amount of "drainable" water above d_{sf}. Substitution of equation (49) for d_{sf} in equation (51) yields:

$$d'_{sf} = \frac{I}{\theta_{FC}} \tag{52}$$

The validity of equation (52) is limited to the case where the solute front is initially located at the soil surface (z=0) prior to infiltration. For a case when the solute front is located at some depth d_i $(d_i>0)$ before infiltration, equation (52) must be modified to:

$$d'_{sf} = d_i + \frac{I}{\theta_{FC}} \tag{53}$$

The mobility or depth to which an adsorbed solute front penetrates is reduced due to adsorption-desorption processes. By assuming a linear and reversible equilibrium adsorption model, a retardation factor (R) can be calculated,

$$R = 1 + \frac{\rho K_D}{\theta_{FC}} \tag{54}$$

where, ρ is soil bulk density (g/cm^3), K_D is adsorption partition coefficient (cm^3/g), and θ_{FC} is field capacity water content (cm^3/cm^3). Equation (53) can be generalized to predict reactive front locations for adsorbed solutes:

$$d'_{sf} = d_i + \frac{1}{R}\,\frac{1}{\theta_{FC}} \tag{55}$$

where, R is defined by equation (54). For a nonadsorbed solute $(K_D=0)$ the retardation factor R equals one, and equation (55) reduces to equation (53). Note that d'_{sf} for a previous event becomes d_i for the next event.

Many practical solute transport problems occur in the presence of a growing crop. Extraction of water from the root zone results in a nonuniform soil-water content profile. Thus modifications must be made in the equations derived so far to account for this case. By assuming a "static" soil profile (i.e., the vertical flow of water stops after θ_{FC} is attained), equation (23) may be reduced to equation (30), which is repeated here:

$$\frac{\partial\theta}{\partial t} = -W(\theta,z,t)$$

where, the Molz-Remson[37] model (equation 24) was used to describe the uptake of soil water by roots.

Depletion of water by plant roots creates a soil-water deficit in the profile. The deficit (I_d) above the solute front, is:

$$I_d = \int_o^{d'_{sf}} [\theta_{FC} - \theta(z)]\ dz \qquad (56)$$

where, the water content profile $\theta(z)$ is predicted by equation (30) at any time, and d'_{sf} is defined by equation (55). The deficit (I_d) must be satisfied by an input (I) from an irrigation/ rainfall event before movement of the solute front can occur. Thus, the effective amount of water (I_e) for moving the solute front is:

$$I_e = I - I_d \qquad (57)$$

For the case when the deficit is overcome by an event (i.e., $I_e > 0$), the new location of the solute front may be calculated from:

$$d_{sf} = d_i + \frac{I_e}{\theta_{FC}} \cdot \frac{1}{R}, \qquad I_e > 0 \qquad (58)$$

However, for the case when the event is not large enough to overcome the deficit (i.e., $I_e<0$), there is no movement of the solute front:

$$d_{sf} = d_i, \qquad I_e \leq 0 \qquad (59)$$

The input water, after adjusting for the evapotranspiration loss, during the redistribution period (assumed to be two days), was distributed in the soil profile to a depth d_x by successive iterations to satisfy the following conditions:

$$(I - 2ET) = \int_o^{d_x} [\theta_{FC} - \theta(z)]dz, \qquad d_x \leq d_{sf} \qquad (60)$$

where, ET is the evapotranspiration demand (cm/day). All calculations involving root extraction were performed on an IBM 360/370 digital computer (FORTRAN IV program).

Leaching of a chloride pulse through a Eustis (Typic Quartzipsamment) fine sand field profile, with a fully established crop of millet [Pennisetum americanum (L.) K. Schum], was measured[89] during a 60-day period between August 1-September 24, 1973, at Gainesville, Florida. Chloride data was used to verify the present model. Experimentally measured[90] soil hydraulic conductivity versus soil-water content for the same field plot was fitted to the following relationship:

$$K(\theta) = \text{Exp}\ [B\theta^{\alpha} + D] \tag{61}$$

with $B = -3.3471$, $\alpha = -0.62$, and $D = 10.1753$. The effective root absorption function, $R(z)$ was assumed to be:

$$R(z) = \text{Exp}\ [-0.005z] - 0.471 \tag{62}$$

where, z is soil profile depth. Equation (62) describes an exponential decay root absorption function, where 39, 28, 19, 11, and 3% of the total root activity was present in each successive 30-cm segment of the soil profile to 150 cm. This empirical equation was developed to describe a fully established root system and was based on observed root density distributions for this crop. The potential evapotranspiration demand (PET) was assumed to remain constant at 0.3 cm/day during the 60-day simulation period. The rainfall distribution at the experimental site was also recorded[89] and used as input for the present model. The Eustis soil profile drains to a field capacity (θ_{FC}) of 0.08 cm^3/cm^3 two days after any input event. Plant available water was defined to be that held in the profile between field capacity (θ_{FC}) and 15-bar (θ_{15}=0.03) soil-water contents.

Experimentally measured[89] field data for chloride front location and that estimated by the present model are compared in Figure 9. Considering all the simplifying assumptions in the model, the agreement between measured and predicted values is good; thus, verifying the model for predicting solute front position in a field soil profile in the presence of a crop. The success of this simple model led to further improvements to incorporate microbial transformations and plant uptake of nitrogen. These modifications are discussed in the following sections.

NITROGEN TRANSFORMATIONS

The partial differential equation describing the simultaneous transport and transformation of nitrogen species is:

$$\frac{\partial}{\partial t}(\theta C_i) = -\frac{\partial q}{\partial z} \pm \phi_i \qquad (63)$$

where, $\partial(\theta C_i)/\partial t$ is change in the mass of the i^{th} nitrogen species with time, $(-\partial q/\partial z)$ is the net change mass due to transport processes (diffusion + mass flow), ϕ_i represents production or loss of mass due to transformations of the i^{th} species. Expanded versions of equation (63) for transformations during transient one-dimensional flow are given in Section 4 (see Equations 12-15). Because analytical solutions to these non-linear partial differential equations were unavailable, numerical solution techniques were employed to solve them.

The more complex model can be simplified, however, to a set of simple first-order kinetic equations if the total amounts $[T_i(t)]$ of a given nitrogen species in the profile are considered

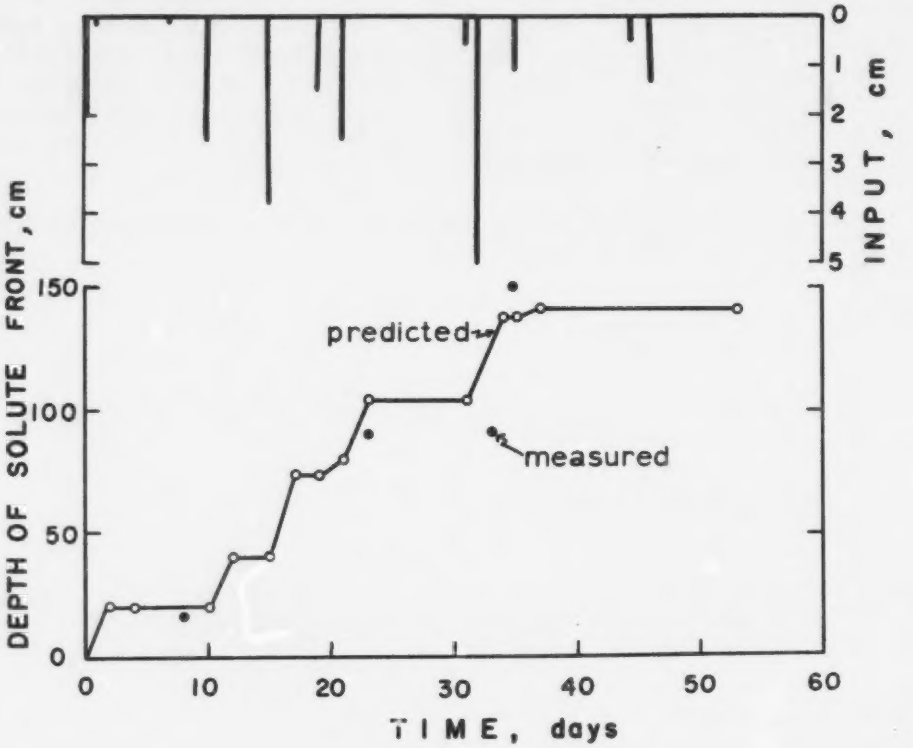

Figure 9. Comparison between measured (solid circles) and predicted (solid lines) position of a nonadsorbed solute front in a sandy soil at various times. The soil was planted to millet. [Pennisetum americanum (L.) K. Schum]

rather than actual concentration distributions $C_i(z,t)$. The total amounts in the root zone are defined as follows:

$$T_1 = \int_0^\infty \rho C_1 \, dz \tag{64}$$

$$T_2 = \int_0^\infty \theta C_2 \, dz \tag{65}$$

$$T_3 = \int_0^\infty \theta C_3 \, dz \tag{66}$$

$$T_4 = \int_0^\infty \rho C_4 \, dz \tag{67}$$

where, C_i represents the concentration distribution of the i^{th} species in the soil profile, ρ is the bulk density, θ is the volumetric soil water content, and the subscripts 1, 2, 3, 4 refer to exchangeable NH_4, solution-phase NH_4, solution-phase NO_3, and organic-N, respectively. First-order kinetic transformations considered in the present case were (i) equilibrium, reversible ion-exchange of NH_4, (ii) immobilization and nitrification of NH_4, and (iii) mineralization of organic-N. Immobilization of NO_3 is relatively less important than that of NH_4 in most situations; hence, this process was not considered in the management model. Furthermore, by assuming deep well-drained soil profiles, the process of denitrification was not included in the analysis presented in this section.

Expansion of equation (63) to include the transformations described above for NO_3 gives:

$$\frac{\partial(\theta C_3)}{\partial t} = -\frac{\partial q}{\partial z} + k_1 \theta C_2 \tag{68}$$

Integration of equation (68) over the soil depth (z) yields:

$$\frac{\partial}{\partial t} \int_0^L \theta C_3 \, dz = \int_0^L - \frac{\partial q}{\partial z} \, dz + \int_0^L k_1 \theta C_2 \, dz \tag{69}$$

By assuming the transformation rate coefficient k_1 to be independent of soil depth, recalling the definitions of equations (65) and (66), and integration of equation (69) gives:

$$\frac{dT_3}{dt} = \Delta q + k_1 T_2 \tag{70}$$

where, (dT_3/dt) is the change in the total mass of NO_3 in the profile with time, Δq is net solute flux, k_1 is kinetic rate for nitrification, and T_2 is total amount of solution-phase NH_4 in the profile. Equation (70) can be simplified further by assuming the net flux to be zero (i.e. $\Delta q=0$). This assumption can be satisfied in two ways: (i) if influx is equal to outflux, or (ii) when both influx and outflux are zero. We chose the latter condition, such that no solute was added to or left the profile for a specific time period. Thus, equation (70) reduces to a simple first-order rate equation as follows:

$$\frac{dT_3}{dt} = k_1T_2 \tag{71}$$

The simplification techniques described above were applied to the equations for other nitrogen species:

$$\frac{dT_1}{dt} = \overline{K}\frac{dT_2}{dt} \tag{72}$$

$$(1+\overline{K})\ \frac{dT_2}{dt} = -(k_1+k_4)\ T_2 + k_3T_4 \tag{73}$$

$$\frac{dT_4}{dt} = k_4T_2 - k_3T_4 \tag{74}$$

where, T_i and k_i are as defined previously, $\overline{K}$ is partition coefficient relating total mass of NH_4 in the solution-phase to that in the adsorbed-phase.

Two major assumptions involved in the derivation of equations (65) through (68) are: (i) the soil profile is homogeneous in that kinetic rate coefficients (k_i) and adsorption partition coefficient ($\overline{K}$) are constant with depth, and (ii) the net solute flux (Δq) is zero and/or inflow and outflow of solute are zero within the region of interest. Subject to these assumption and when the initial total amounts ($T_i°$) of each nitrogen species in the profile are known, the analytical solutions to equations (71) through (74) are as follows (Rao et al.[84]):

$$T_1 = \overline{K}T_2 \tag{75}$$

$$T_2 = A \exp(\beta_1 t) + B \exp(\beta_2 t) \tag{76}$$

$$T_3 = T_3^0 - \frac{k_1A}{\beta_1}\ [1-\exp(\beta_1 t)] - \frac{k_1B}{\beta_2}\ [1-\exp(\beta_2 t)] \tag{77}$$

$$T_4 = C \exp(\beta_1 t) + D \exp(\beta_2 t) \tag{78}$$

where,

$$2\beta_1 = -(k'_{14} + k_3) + [(k'_{14} - k_3)^2 + 4k_4k'_3]^{1/2} \tag{79}$$

$$2\beta_2 = -(k'_{14} + k_3) - [(k'_{14} - k_3)^2 + 4k_4k'_3]^{1/2} \tag{80}$$

$$k'_{14} = (k_1 + k_4)/(1 + \bar{K}) \tag{81}$$

$$k'_3 = k_3/(1 + K) \tag{82}$$

$$A = \frac{k'_3 T^0_4 - T^0_2 (k'_{14} + \beta_2)}{(\beta_1 - \beta_2)} \tag{83}$$

$$B = T^0_2 - A \tag{84}$$

$$C = \frac{k_4 T_2 - T^0_4 \ (k_3 + \beta_2)}{(\beta_1 - \beta_2)} \tag{85}$$

$$D = T^0_4 - C \tag{86}$$

also, T° and k_i are as defined previously.

The total amounts of each nitrogen species calculated using equations (75) through (86) were in agreement with those obtained with numerical solutions to the model for transport-transformations[4] under steady-state water flow. Results from these analytical solutions, when reduced for limited transformations (adsorption and nitrification of NH_4 only), agreed well with results obtained from the model presented by Cho[92]. A sensitivity analysis of the transformation submodel has been performed by Rao et al.[91] using these analytical solutions.

Since the management model was devised to evaluate the gross behavior of nitrogen in the root zone, the analytical solutions described here were utilized to describe microbiological transformations.

NITROGEN UPTAKE

Empirical Michaelis-Menton type equations were used to calculate nitrogen uptake by a growing root system. These equations related the nitrogen uptake rate (Q_N) to total amount (T_N) of mineral-N (NH_4 + NO_3) in the soil solution within the root zone:

$$Q_N = Q_N^{max} \left(\frac{T_N}{K_M + T_N}\right) \tag{87}$$

where, K_M is the value of T_N when $Q_N = 0.5Q_N^{max}$. Recall that Q_N^{max} represents the N-uptake demand (μg N/day/cm² soil surface) under "ideal" growth conditions. The actual uptake demand (Q_N) was assumed to be satisfied by absorption of both NO_3 and NH_4 in proportion to their respective total quantity in the soil solution in the root zone as follows:

$$Q_N = Q_2 + Q_3 \tag{88}$$

$$Q_2 = Q_N^{max} \left(\frac{T_2}{K_M + T_N}\right) \tag{89}$$

$$Q_3 = Q_N^{max} \left(\frac{T_3}{K_M + T_N}\right) \tag{90}$$

where Q_2 and Q_3 are uptake demand for NH_4 and NO_3, respectively, while T_2 and T_3 are total amounts of NH_4 and NO_3 in the soil solution-phase in the root zone.

The values of Q_N^{max} were obtained in a manner similar to that described in Section 5. The empirical root growth model, also described in Section 5, was used to calculate the root length density distribution in the soil profile, and to estimate the soil depth (L) to which roots had penetrated. The value of L was then used as the upper limit of integration in equations (64) through (67) in calculating the values of T_2 and T_3 in equations (88) and (89).

Application of the management model is limited to homogeneous soil profiles. Furthermore, the model is applicable only to deep, well-drained soil profiles due to assumptions made in the nitrogen transformation submodel. Finally, the management model presented here allows for estimation of the solute front position and the total amount of solute in the root zone, but does not permit calculation of solute concentration distributions within the soil profile.

SECTION 7

RESEARCH MODEL SIMULATIONS

In this section, the research model was used to provide simulated results for selected cases in order to describe the fate of applied nitrogen in the plant root zone. The values for the model parameters were chosen to represent some real systems and were based on published data.

TRANSPORT AND TRANSFORMATIONS

Simultaneous microbiological nitrogen transformations during transient unsaturated flow were described using equations (1) and (12) through (15). The root extraction of soil water in response to transpiration and plant uptake of nitrogen (Section 5) were not considered. In order to illustrate the importance of the transformation mechanisms and their dependence on soil water conditions, two cases were simulated. The first case was for transport and transformation of an applied NH_4NO_3 pulse in a uniform well-drained soil profile. The second case represents a soil profile with an impermeable barrier.

For both cases presented here, the soil parameters used represent a loamy soil profile. The initial soil water content (θ_i) was uniform at 0.1 cm^3/cm^3 throughout the profile. The soil profile was assumed void of initial mineral (NH_4+NO_3) nitrogen, while the "mineralizable" organic-N distribution at t=0 was described by:

$$OM(z) = 50.0\ [\exp(-0.025z)] \tag{91}$$

where, the maximum "mineralizable" organic-N content of 50μg N/gm was at the soil surface (z=0) and decreased exponentially with depth. It was assumed that NH_4NO_3 fertilizer was applied at the soil surface followed by infiltration of water for a period of 12 hours. It was further assumed that the applied NH_4NO_3 fertilizer was dissolved by the infiltrating water and entered the soil within 2 hours, resulting in an input solution concentration of 100μg N/ml for both NH_4 and NO_3. The soil surface was assumed to be maintained saturated ($\theta_{z=0} = \theta_{sat} = 0.36\ cm^3/cm^3$) during infiltration. The total amounts of nitrogen and water applied in this manner were 348 μgN/cm^2 soil surface and 9.1 cm of water, respectively. Evaporation at the soil surface was assumed constant at 0.3 cm/day during the redistribution period (t>12 hours).

The soil water content distribution in a deep uniform soil profile at selected times during water infiltration and redistribution is shown in Figure 10. At the termination of infiltration (12 hours), the wetting front had advanced to a depth of 36 cm. Given the nearly uniform soil water content of 0.36 cm^3/cm^3 in the wetted zone, the depth of wetting front (d_{wf}) can be calculated by equation (48) as 9.1/(0.36-0.1) = 35 cm.

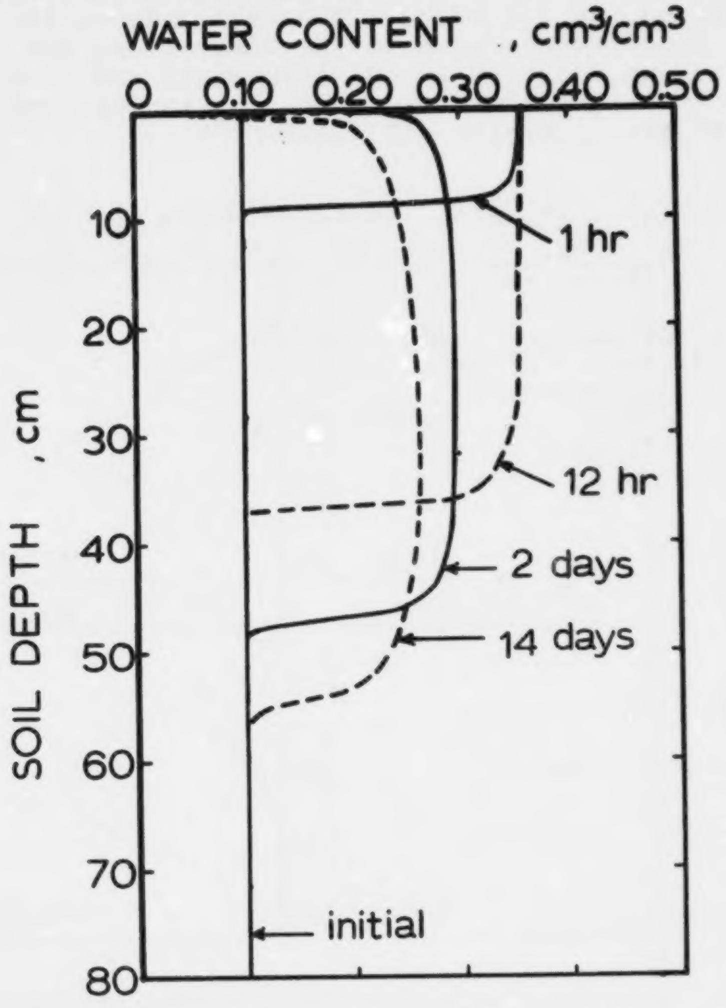

Figure 10. Simulated soil-water content distributions in a deep uniform loam soil profile during infiltration and redistribution of soil-water

During water redistribution, the wetting front advanced to lower depths as a result of drainage from the wetted zone. After 14 days, the wetting front was located at about the 56 cm depth, and the soil-water content in the wetted zone was approximately 0.21 cm^3/cm^3. Depletion of water due to evaporation resulted in decreased water contents close to the soil surface (Figure 10).

The solution-phase concentration distributions of NH_4 and NO_3 during infiltration and redistribution of water in a uniform soil profile are presented in Figure 11. The transformation rate coefficients chosen were $\bar{k}_1 = 0.01$, $\bar{k}_2 = 0.00001$, $\bar{k}_3 = \bar{k}_4 = \bar{k}_5 = 0.0001\ hr^{-1}$, and the adsorption coefficient (K_D) for NH_4 adsorption was 0.1 cm^3/g. The magnitude of the transformation rate coefficients used in the simulations are within the range of values reported in the literature and given in Table 3 in Appendix D (Stanford and Smith[16]; Stanford and Epstein[25]; Stanford et al.[87]; Miller and Johnson[24]).

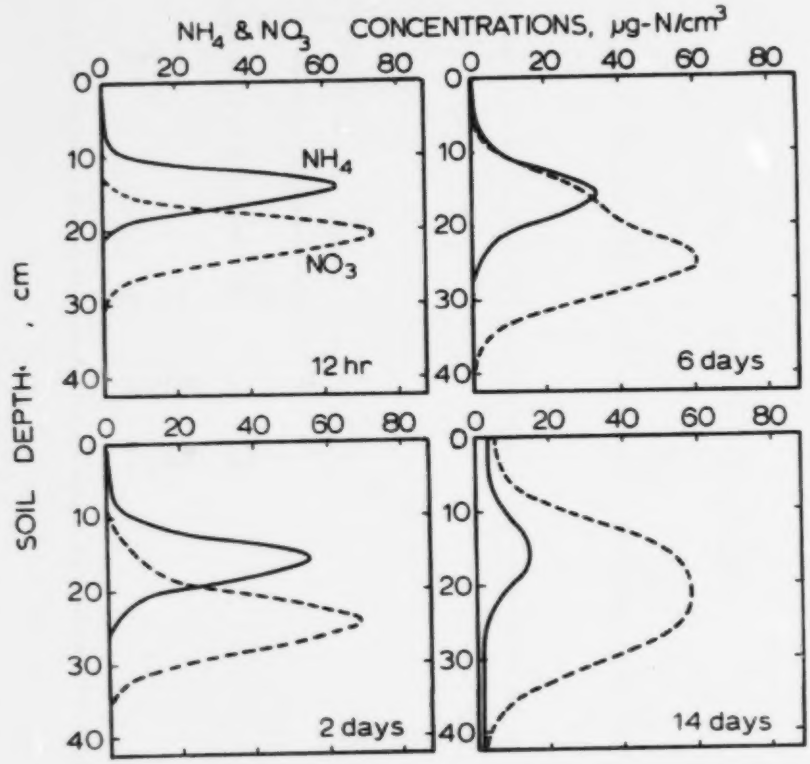

Figure 11. Simulated solution-phase concentration distributions of NO_3-N and NH_4-N in a deep uniform loam soil profile during infiltration and redistribution of soil-water. The rate coefficient for nitrification (k_1) was 0.01 hr^{-1}.

The position of the NO_3-N front at the termination of water infiltration (t=12 hrs) is at 25 cm and can be calculated by equation (37) with I = 9.1 and $\theta_f = 0.36$. The NH_4 pulse front is at about 17 cm and lags behind the NO_3 pulse due to adsorption. Additional movement of the NH_4 and NO_3 pulses during redistribution is small (Figure 11). However, the NO_3 concentration profiles show double peaks for times between 2 and 6 days. The position of the smaller peak coincides with the location of the NH_4 peak. The presence of the second peak on the NO_3 pulse is thus attributed to NO_3 generated by nitrification of NH_4 during redistribution. For greater times (t>6 days), the second peak disappears and the NO_3 concentration profile becomes broad and asymmetrical. A gradual decrease in the area under the NH_4 pulse is associated with a simultaneous increase in area under the NO_3 pulse due to nitrification. The effect of the nitrification rate coefficient (k_1) is clearly illustrated in Figure 12, where $\overline{k}_1$ was 0.1 hr^{-1}. Note that within 6 days more than 90% of NH_4 disappeared from the soil solution.

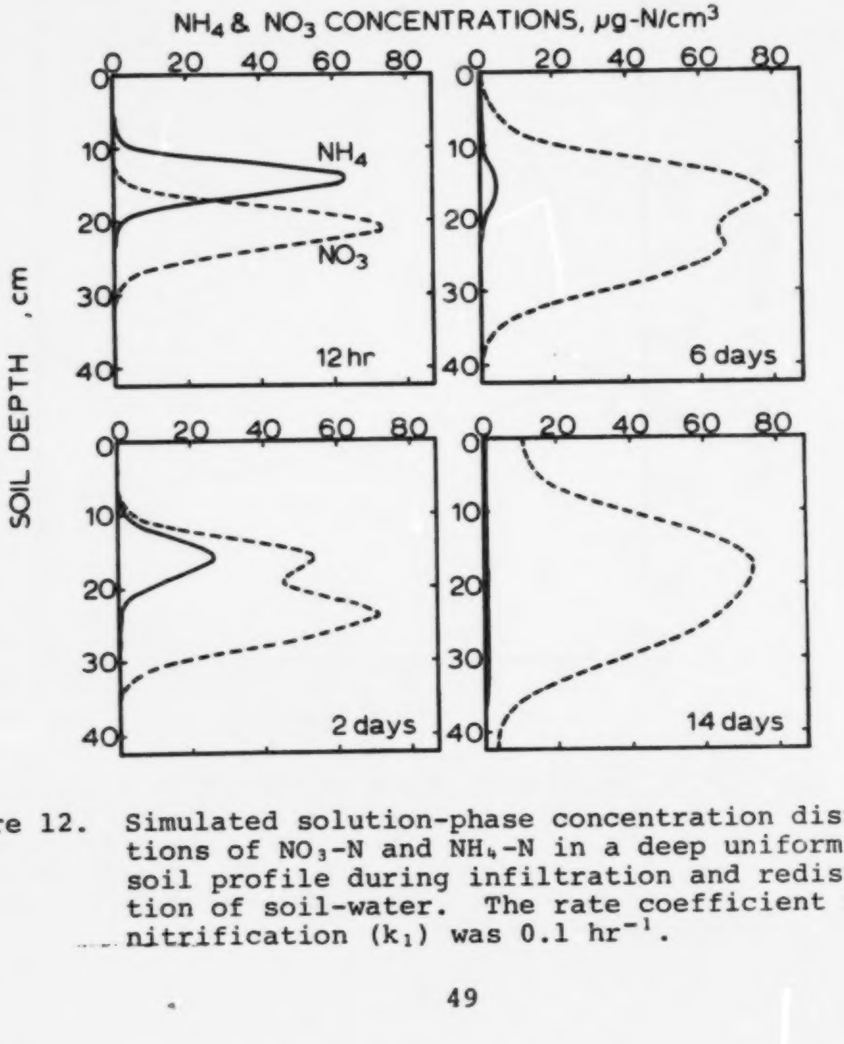

Figure 12. Simulated solution-phase concentration distributions of NO_3-N and NH_4-N in a deep uniform loam soil profile during infiltration and redistribution of soil-water. The rate coefficient for nitrification (k_1) was 0.1 hr^{-1}.

The total amounts of NO_3 and NH_4 (adsorbed + solution) present in the soil profile versus time for the cases where $\overline{k}_1 = 0.01$ or $0.1\ hr^{-1}$ are shown in Figure 13. Nearly all NH_4 was transformed within 4 days after application when $\overline{k}_1 = 0.1\ hr^{-1}$, while significant amounts of NH_4 remained in the profile when $\overline{k}_1 = 0.01\ hr^{-1}$. The decreases in amount of NH_4 are nearly equal to the increases in NO_3. The total amount of organic-N mineralized within the soil profile during the 14-day period was 75 μg N/cm^2 for $\overline{k}_1 = 0.01\ hr^{-1}$ and 76 μg N for $\overline{k}_1 = 0.1\ hr^{-1}$. For both cases, however, the amount of nitrate lost due to denitrification was negligible (0.35 μg N) because the soil-water contents were not favorable for denitrification (see equations 10a and 10b) during the simulated period.

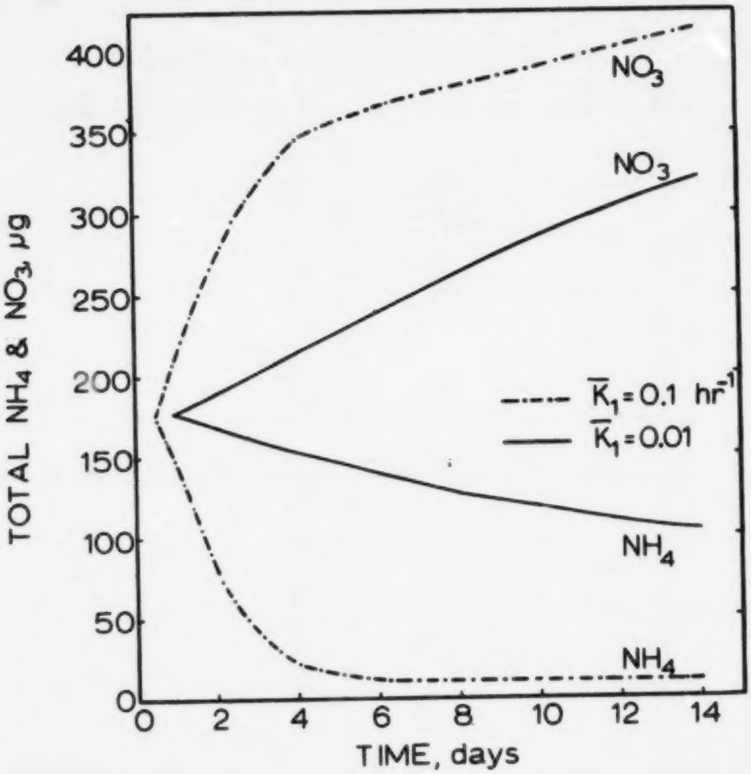

Figure 13. Total amounts of NH_4-N and NO_3-N in a deep uniform loam soil profile during infiltration and redistribution of soil-water. The nitrification rate ($\overline{k}_1$) was 0.01 or 0.1 hr^{-1}. These plots were derived from the simulated data presented in Figures 11 and 12.

The influence of an impermeable barrier at a depth of 40 cm in the soil profile is illustrated in Figure 14. The presence of a barrier resulted in higher soil-water contents at all depths during redistribution in comparison to a uniform well drained profile. Higher soil-water contents favor the denitrification of NO_3 as evidenced by the data presented in Figures 15 and 16. The transformation rate coefficients chosen were: $\overline{k}_1 = 0.01$, $\overline{k}_2 = 0.00001$, $\overline{k}_3 = \overline{k}_4 = 0.0001$, and $\overline{k}_5 = 0.01$ hr^{-1}. Losses of NO_3 due to denitrification during the early periods of redistribution (12 hrs<t<2 days) caused the maximum NO_3 concentration to decrease from 65 to 40 μg N/cm³. The total amount of NO_3 in the profile (i.e., area under the nitrate

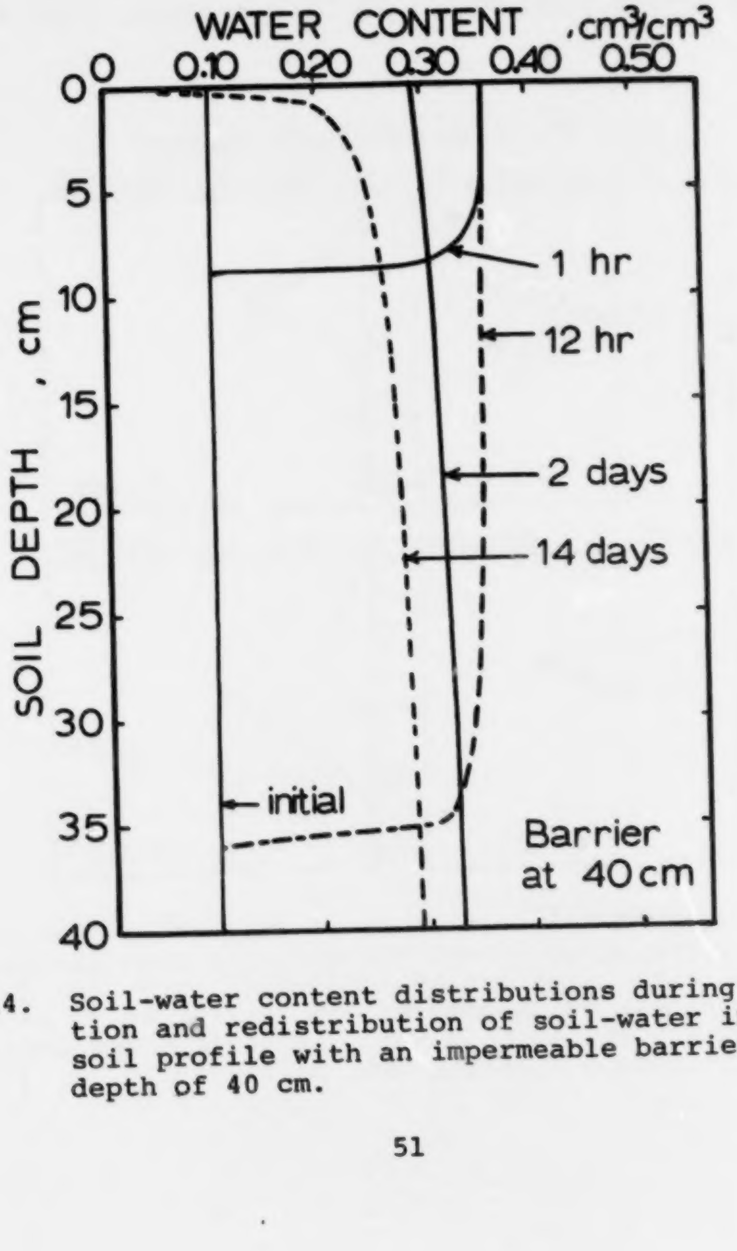

Figure 14. Soil-water content distributions during infiltration and redistribution of soil-water in a loam soil profile with an impermeable barrier at a depth of 40 cm.

pulse) had also decreased. However, for longer times (6 and 14 days), lower soil water contents were more favorable for nitrification than for denitrification. Thus, NO_3 began to accumulate in the soil profile (Figure 15). The effect of the magnitude of the denitrification rate coefficient are summarized in Figure 16. For $k_5 = 0.001\ hr^{-1}$ and $0.01\ hr^{-1}$, the total amount of NO_3 decreased and N-released increased up to 4 days. After this time, there was only a small amount of N released, while the total amount of NO_3 increased rapidly due to nitrification.

TRANSPORT, TRANSFORMATIONS, AND UPTAKE

The simulations presented in the previous section did not include plant uptake processes. In this section, simulations of

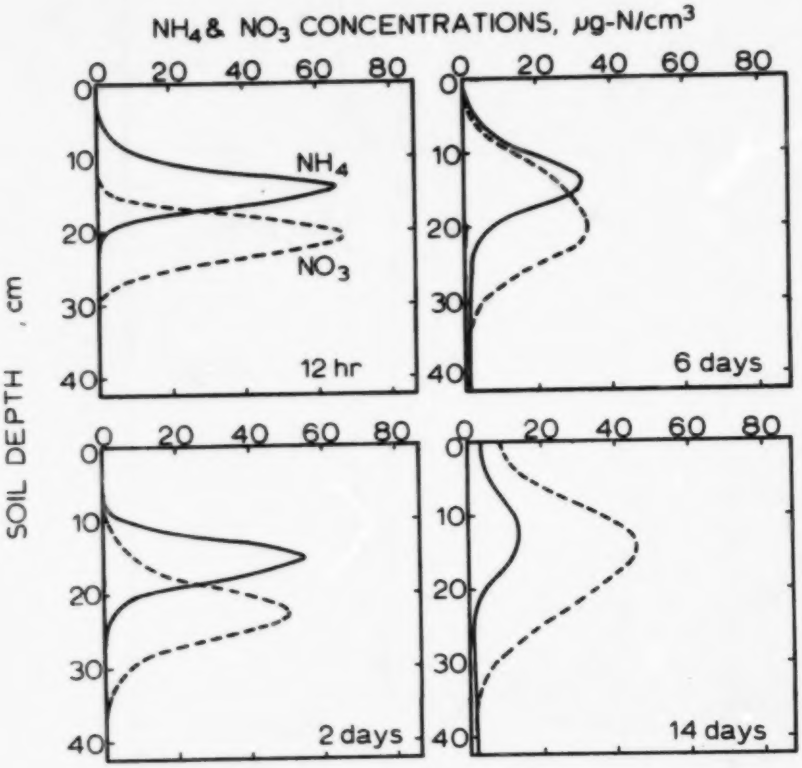

Figure 15. Simulated solution-phase concentration distributions of NH_4-N and NO_3-N during infiltration and redistribution of soil-water in a loam soil profile with an impermeable barrier at 40 cm depth. The kinetic rate coefficient for denitrification (k_1) was $0.01\ hr^{-1}$.

nitrogen behavior in the plant root zone are described using the complete research model. Thus, the major processes of simultaneous transport, transformations and plant uptake were considered. The soil parameters used in these simulations are similar to those used in the previous section. The plant parameters are for a corn crop and are based on experimental data of NaNagara et al.[63]. The simulations presented here commenced 34 days after planting and proceeded 83 days into the crop growing season. This 7-week period was chosen since it was the most active in terms of crop demand for nitrogen and water.

The initial soil-water content (θ_i) on the 34th day was assumed uniform at 0.1 cm^3/cm^3 over the entire crop root zone (0-90 cm), and the soil profile was assumed initially devoid of

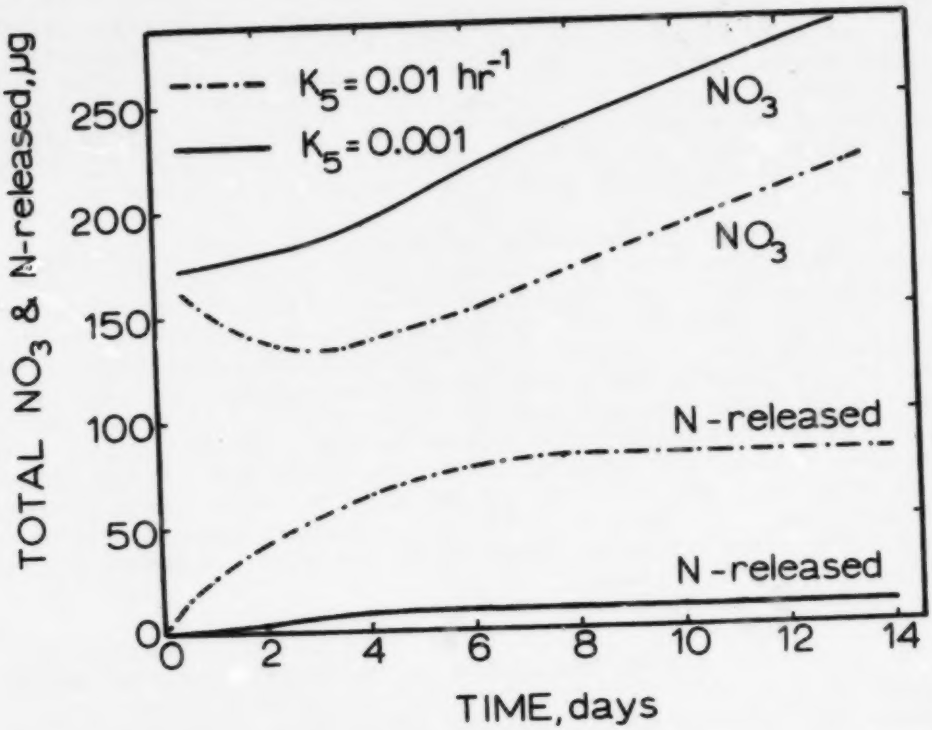

Figure 16. Total amounts of NO_3-N remaining and total amount of N released by denitrification during infiltration and redistribution of soil-water in a loam soil profile with an impermeable barrier at a depth of 40 cm. The denitrification rate coefficient (k_1) was 0.001 or 0.01 hr^{-1}.

any mineral nitrogen. The mineralizable organic-N distribution was described by equation (91) with a total of 2863 μg of organic-N/cm^2 in the root zone. The kinetic rate coefficients were $\bar{k}_1 = 0.01$, $\bar{k}_2 = 0.00001$, $\bar{k}_3 = \bar{k}_4 = 0.0001$ hr^{-1}, while losses due to denitrification were ignored ($\bar{k}_5 = 0.0$). The adsorption coefficient for NH_4 was 0.1 cm^3/g.

At day 34 of the growing season, NH_4NO_3 fertilizer was applied at the surface and was followed by two 9.1 cm water application which requires 12 hours. The soil surface was maintained saturated (h=0) during infiltration. In addition, it was assumed that the applied NH_4NO_3 fertilizer was dissolved and entered the soil in 4 hours. The total amounts of nitrogen applied in this manner was equivalent to 83 kg N/ha. Two additional irrigations of 3.2 and 3.3 cm of water were applied on the 48th and 62nd day of the growing season. Water losses due to evaporation at the soil surface were included in the evapotranspiration. A crop transpiration demand of 0.3 cm/day was assumed throughout the simulation period. The root uptake of water was described using the Molz-Remson model (equation 24), while plant uptake of NH_4 and NO_3 was simulated using the Michaelis-Menton type model (equations 38 and 39). The cumulative amount of nitrogen absorbed by the plant was calculated by equation (40), where the root density distributions, $R(z,t)$ were estimated by the empirical model described in Section 5.

The soil-water content distributions at selected times following the three irrigations are shown in Figure 17. The water content profile at the cessation of infiltration, t=0.5 day, of the first irrigation (Figure 17) was similar to that shown in Figure 10. However, for larger times, the soil water contents in the former case are lower than those for the latter as a result of water uptake by the plant roots. A total of 4.2 cm of soil water would be transpired by the plants during a two-week period if no water stress occurred. The second and third irrigations of 3.2 and 3.3 cm, respectively, were smaller than this amount, and resulted in multiple wetting fronts (Figure 17). However, more or less uniform soil-water contents existed in the surface at all times.

Solution concentrations of NO_3-N and NH_4-N in the soil profile at selected times following each irrigation are shown in Figures 18 and 19. The position of the NO_3-N front immediately at the end of the first irrigation (curve labeled 0.5 days in Figure 18) is at the 25 cm depth and can be calculated by equation (49) given I = 9.1 cm and a soil water content (θ_f) of 0.36 cm^3/cm^3 behind the wetting front. The NH_4-N front was calculated to be at the 17 cm depth; this retardation is due to ion-exchange. During the two-day period following the first irrigation, redistribution of soil water had caused the NO_3 and NH_4 pulses (Figures 18 and 19) to move to a depth

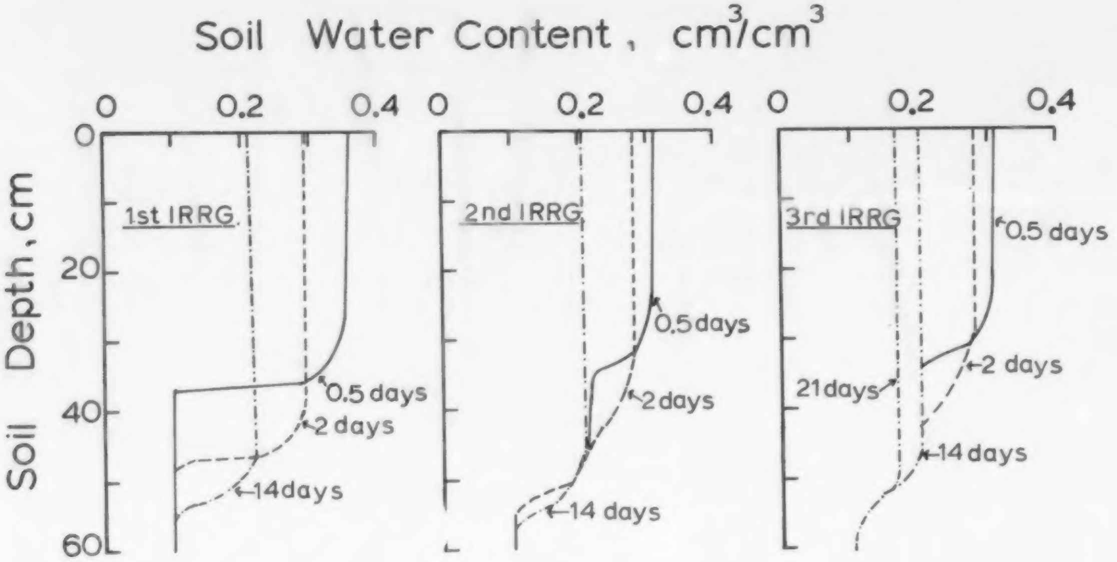

Figure 17. Simulated soil-water content distributions in a deep uniform loam soil profile during infiltration and redistribution following three irrigation events.

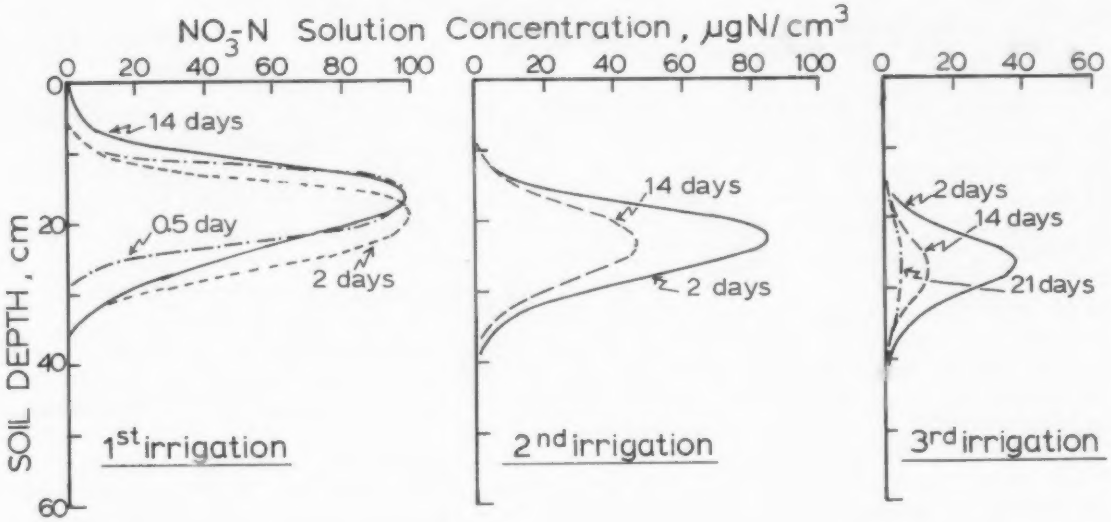

Figure 18. Simulated NO_3-N solution concentrations in the soil profile at selected times following three irrigation events (Figure 17).

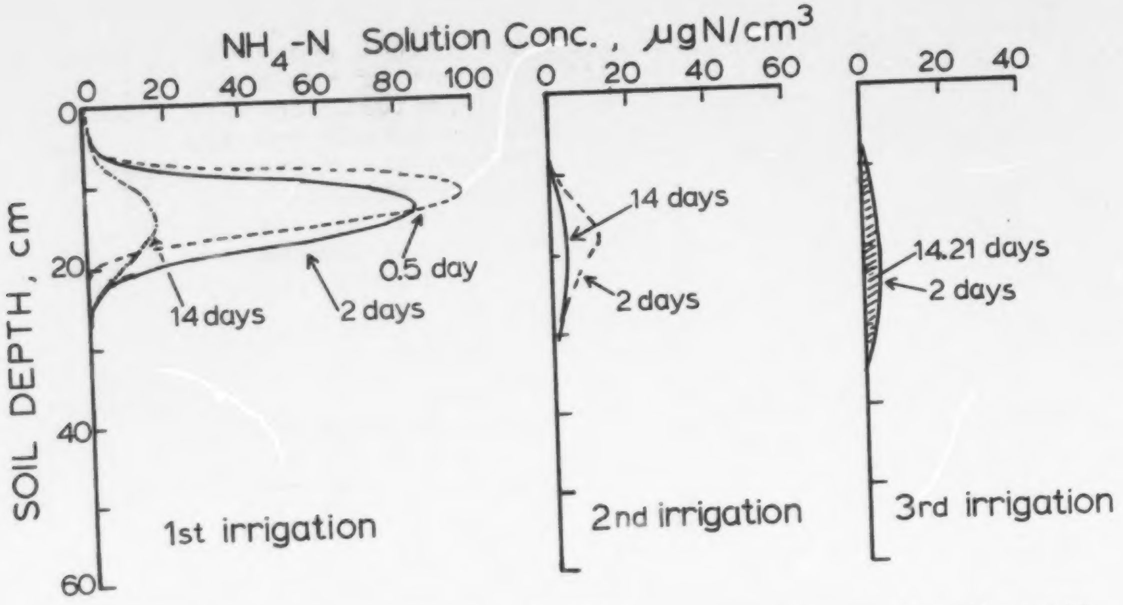

Figure 19. Simulated NH_4-N solution concentrations in the soil profile at selected times following three irrigation events (Figure 17).

of 29 and 19 cm. The total amount of NH_4-N in the soil solution had decreased during the 14-day period (Figure 19) principally due to nitrification and plant uptake.

Water redistribution and extraction by plant roots resulted in a fairly uniform soil-water content above the wetting front in the soil profile at all times during water redistribution. Such a uniform water content with soil depth is primarily due to the root density distribution [$F(z,t)$] used in this study (Figure 5) as well as the absence of direct evaporation from the soil surface. Selim et al.[95] found that the presence of soil surface evaporative conditions at the soil surface and a root extraction pattern which sharply decreased with depth resulted in a nonuniform soil-water content distribution pattern (Figure 20). Unlike the root distribution pattern of Figure 5, Selim et al.[95] used a root distribution in which 40, 30, 20, and 10% of the total water extraction was supplied, respectively, from each quarter (15 cm) of the root zone (60 cm depth). Figure 20 clearly shows that water uptake by plant roots resulted in a continued decrease in the water content in the root zone (60 cm depth). During this period, the wetting front associated with the applied irrigation water (4 cm) advanced with time to depths beyond the root zone.

From Figures 18 and 19, it is clear that the first irrigation of 9.1 cm caused significant movement of NH_4 and NO_3 in comparison to the second and the third irrigations of 3.2 cm and 3.3 cm, respectively. The total amounts of NH_4 and NO_3 present in the root zone continued to decrease as a result of transformations and plant uptake. NH_4 concentrations in soil solution (Figure 19) had diminished to less than 4 μg N/ml and that of NO_3 were less than 10 μg N/ml (Figure 18) by the 83rd day of the growing season (i.e., 21 days after third irrigation).

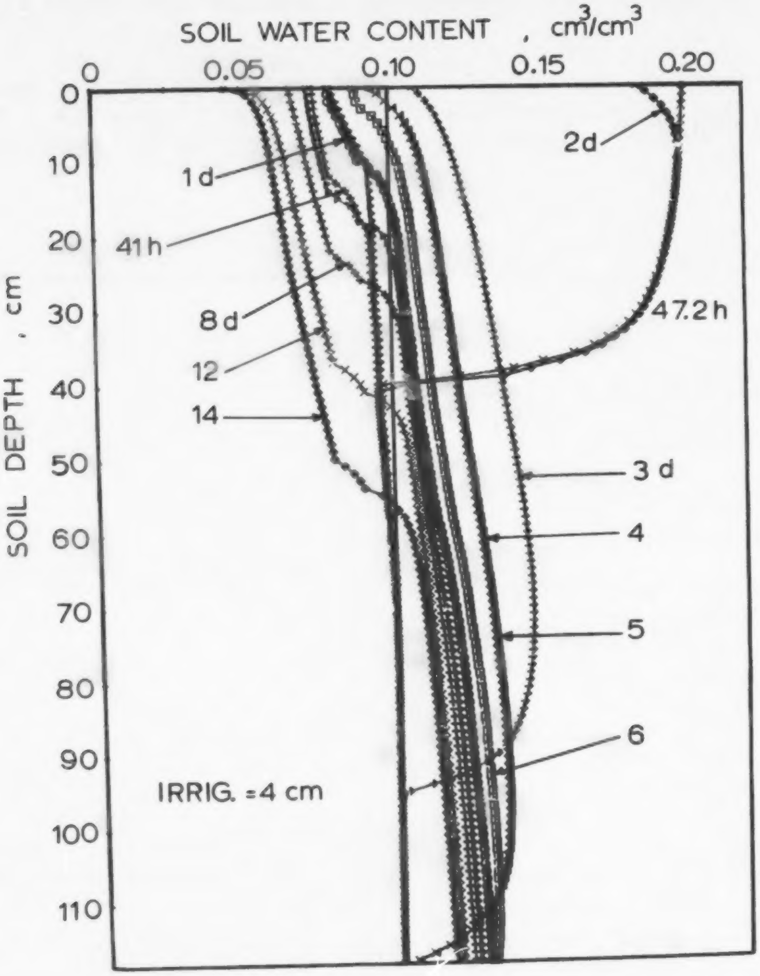

Figure 20. Soil-water content (θ) distributions with time during plant-water uptake and evaporation in a uniform soil profile of Lakeland soil (from Selim et al.[89]).

The total amounts of NO_3, NH_4 (sum of solution and exchangeable phases), and organic-N remaining in the root zone, as a percentage of that at the initiation of the simulations on the 34th day, are presented in Figure 21. The losses of nitrogen shown here are due only to transformations and plant uptake as there was no movement of soil water beyond the root zone. The rapid transformation of NH_4 is evident in Figure 21. The production of NO_3 due to nitrification was greater than that absorbed by the roots during the first week, giving rise to the plateau in the early portion of the NO_3 curve in Figure 21. The amount of NO_3 decreased rapidly after this time as NO_3 became the major source of N for plant uptake. The amount of N mineralized exceeded that immobilized during the 7-week simulation period.

The cumulative amount of nitrogen removed by the crop during 34-83 day growing period is shown in Figure 22. The curve marked "demand" represents the amount of N required by the

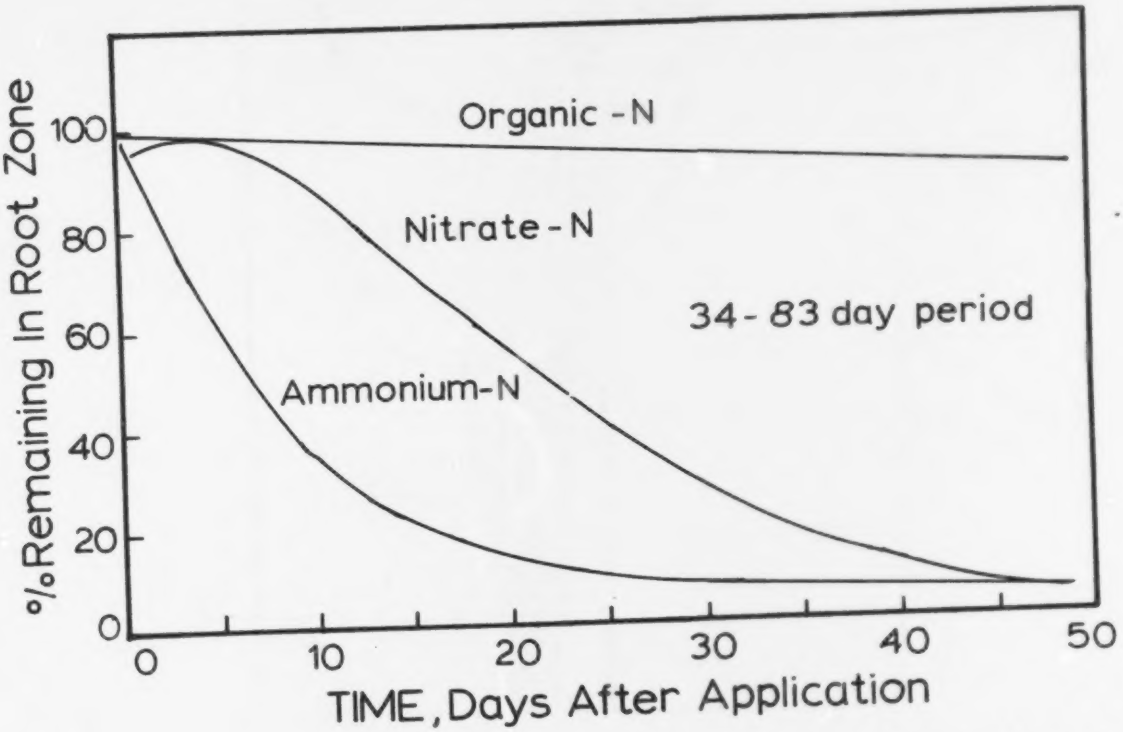

Figure 21. Percentage of applied nitrogen remaining within the plant root zone during the simulated growing season. The curves were based on data presented in Figures 18 and 19.

plants if maximum N-demand (Q_N^{max}) was satisfied at all times (i.e., ideal growth). The amount of nitrogen present in the crop root zone was insufficient during the latter part of the simulation period (times greater than 8 days in Figure 22) to meet the maximum demand. This resulted in a significant deviation of the simulated curve from the "ideal" curve. Such a nitrogen deficit, when it occurs under real conditions, would lead to decreased dry matter accumulation and reduced yields.

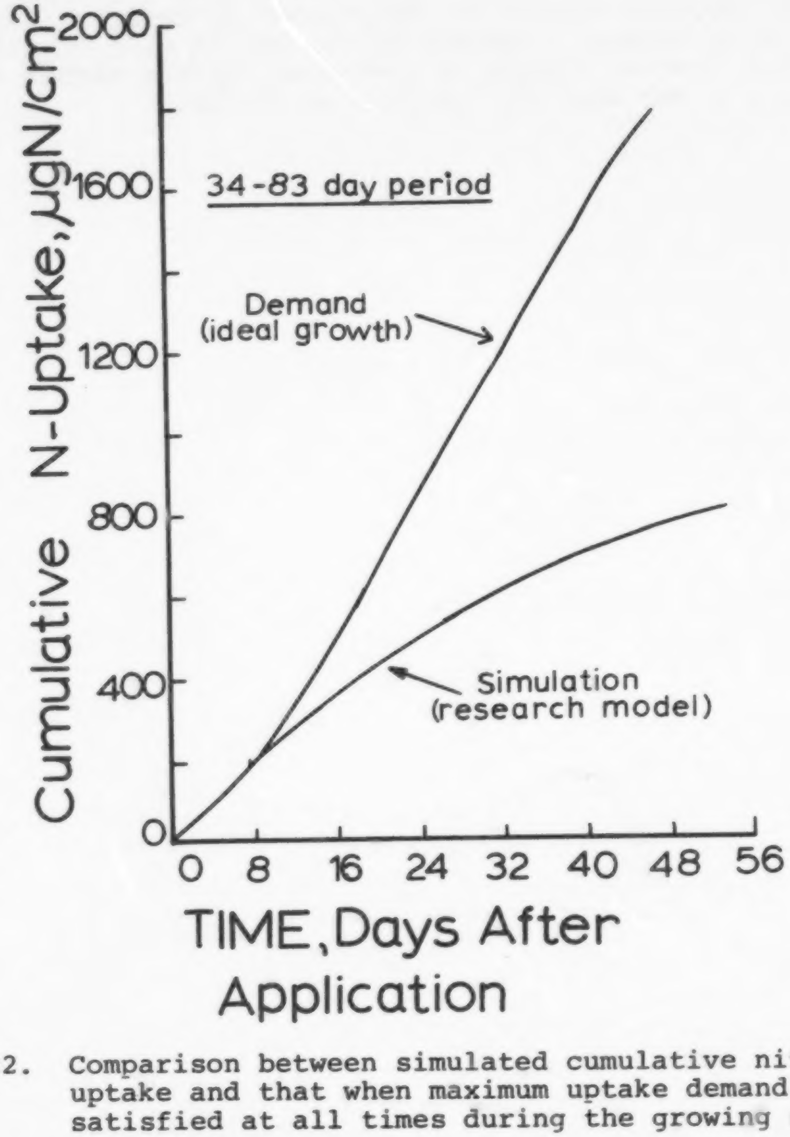

Figure 22. Comparison between simulated cumulative nitrogen uptake and that when maximum uptake demand is satisfied at all times during the growing season.

SUMMARY

The research model simulations presented here provide a detailed description of the fate of the various nitrogen species in the crop root zone during the growing season. However, limitations on available input parameters and the lack of a reliable data base do not permit verification of the research model. Experiments involving water and nitrogen movement and microbiological nitrogen transformations are needed for model verification. The soils on which these experiments are conducted must be well characterized in terms of soil-water properties. The nitrogen concentration and water content distributions in the soil profile should be documented at various times during the growing season. Consideration should also be given to the transient dynamic nature of the total system rather than initial and final plant and soil profile conditions.

SECTION 8

MANAGEMENT MODEL-SIMULATIONS

MODEL VERIFICATION

NaNagara et al.[59] have performed field experiments to measure nitrogen uptake by corn during an entire crop growing season. In addition to measuring nitrogen accumulation in the plant, these authors also obtained data on root length and nitrate concentration distributions as well as water losses by evapotranspiration throughout the season. These experimental data will be utilized to verify the management model described earlier. NaNagara et al.[59] have compared their data with predictions from two conceptual mechanistic models of nitrogen uptake by plants (Phillips et al.[49]). Model I considers the mass flow of nitrate into roots with water (i.e., passive uptake) as a result of water uptake by roots in response to the transpiration demand. By knowing the amount of water transpired in a given time period and the average nitrate-N concentration in the soil solution in a given region of the soil profile, the cumulative N-uptake was estimated. Model II considers the microscopic processes of nitrate transport to root surfaces by diffusion and mass flow. Furthermore, the rate of N-uptake by roots was assumed to be directly proportional to the nitrate concentration. Note that neither model I and model II considers uptake of the NH_4 species.

Additional input parameters used to simulate the data of NaNagara et al.[59] were provided by Phillips[89] and were: $\theta_{FC} = 0.4$, $\theta_{15}=0.15$, $R=2.0$, $k_1=0.1$ day^{-1}, $k_3=k_4=0.0003$ day^{-1}, $T^0_{NH_4} = 840$, $T^0_{NO_3}=2290$, and $T^0_{org-N}=3000$. The values of the transformation rate coefficients were not measured, but were selected to represent those of Maury soil (Kentucky) on which the field experiments were performed. A total of 18.7 cm of water was received as rainfall during the 112-day growth season, whereas accumulated water loss due to evapotranspiration was 23.79 cm.

The total amounts of NH_4- (solution + adsorbed), NO_3 and organic-N remaining in the root zone, as a fraction of that present initially, during the growing season are shown in Figure 23. These curves were plotted from the simulations obtained with the management model. It is apparent from Figure 23 that, although very little net mineralization of organic-N (74 μg) occurred, most of NH_4 was rapidly transformed during the first 40 days of the season. The total amount of NO_3 within the root zone increased up to 20 days in spite of plant uptake, suggesting that the rate of nitrification exceeded that of plant uptake. Beyond 20 days, however, the amount of NO_3-N decreased rapidly as NO_3 was the major source for plant uptake. As there was no loss of any nitrogen beyond the root zone, the changes in total amounts described above were due only to transformations and uptake.

The calculated cumulative amounts of nitrogen removed by corn using the management model (Model III) are compared in Table 2 with those experimentally measured by NaNagara et al.[59]. Nitrogen uptake values were also predicted by the two microscopic conceptual models of Phillips et al.[49] (Models I and II) and presented in Table 2. Reasonable agreement between measured data and all three predictive models (with widely different

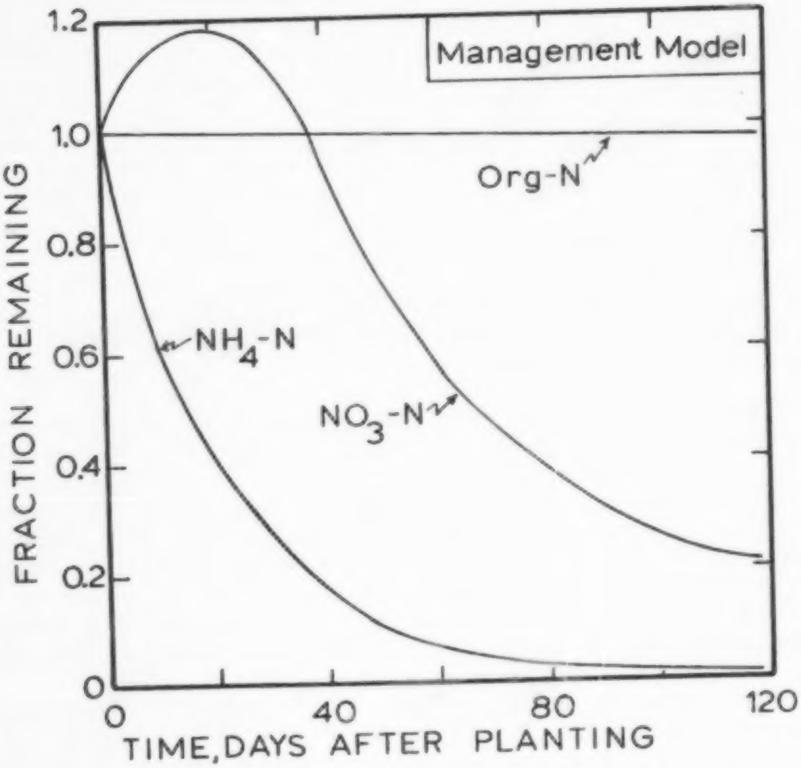

Figure 23. Fraction of applied nitrogen remaining in the plant root zone of Maury soil, simulated by the management model, during the corn growing season.

TABLE 2. COMPARISON BETWEEN MEASURED NITROGEN UPTAKE BY CORN (Zea mays L.) GROWN UNDER FIELD CONDITIONS AND THAT PREDICTED BY THREE SIMULATION MODELS.

Growth Period (days)	Measured N-uptake mg N/plant	Calculated N-uptake (mg N/plant)		
		Model I	Model II	Model III
34-49	1435	1097	1254	1928
49-76	1593	1101	2000	1948
76-97	974	1496	1278	683
Total 34-97	4002	3693	4533	4559
% Error		-7.7	+13.3	+13.9

conceptualization of uptake processes) makes acceptance or rejection of any of these models difficult. Close agreement between simple model predictions and measured data is encouraging considering all the approximations and simplifying assumptions involved in development of the management model; however, additional testing of the management model is needed. Finally, the input data requirements for this model are minimal in comparison to other models. Thus, the conceptual management model seems to hold promise.

MODEL SIMULATIONS

The management model was used to simulate selected irrigation application schemes in order to examine their relative efficiency in maximizing plant uptake of nitrogen and thereby minimizing nitrogen loss beyond the root zone. The soil parameters chosen represent a deep, well-drained, homogeneous sandy soil profile, while the crop parameters are for corn (similar to those used earlier in Section 7). The soil hydraulic conductivity function and the values of θ_{FC} and θ_{15} were those used in Section 5 for the sand (see Equation 28).

The two water management schemes simulated were: (i) natural rainfall with no supplemental irrigation, and (ii) controlled amounts of irrigation under no rainfall conditions. The amount of irrigation water applied was equal to or 1.5 times greater than the amount of soil water used by the plant. Irrigation was allowed only when the plant available water (AW) within the root zone was less than 60% of the total plant available water (TAW). Thus, the corn crop simulated here was never under "water stress" (as defined by Eq. 27) during the simulated 120-day crop growing season. The rainfall data used as input were obtained from weather records (for May-August, 1974) maintained at the Agronomy Research Farm of the University of Florida at Gainesville. A single application of NH_4NO_3 fertilizer at the rate of 300 kg N/ha at planting (time=0) was assumed. The initial amount of "mineralizable" organic-N in the 100 cm profile was set equal to 2863 μg N/cm^3. The first-order transformation rate coefficients for nitrification, mineralization, and immobilization were 0.12, 0.0024, and 0.0024 day^{-1}, respectively. The retardation factor (R) for NH_4 adsorption was set at 1.57. The entire soil profile was assumed to be initially at "field capacity" soil-water content (θ_{FC}=0.08 cm^3/cm^3).

The position of the nitrate pulse in the soil profile during the growing season, simulated for three water application schemes, is presented in Figure 24. Also shown is the progression of maximum depth (L) in the soil profile to which plant roots had grown. The nitrate pulse resides well within the crop root zone during the entire season for the case in which the amount of irrigation water was equal to that depleted by the crop (curve labeled 1.0 ET in Figure 24). For the case in which the amount

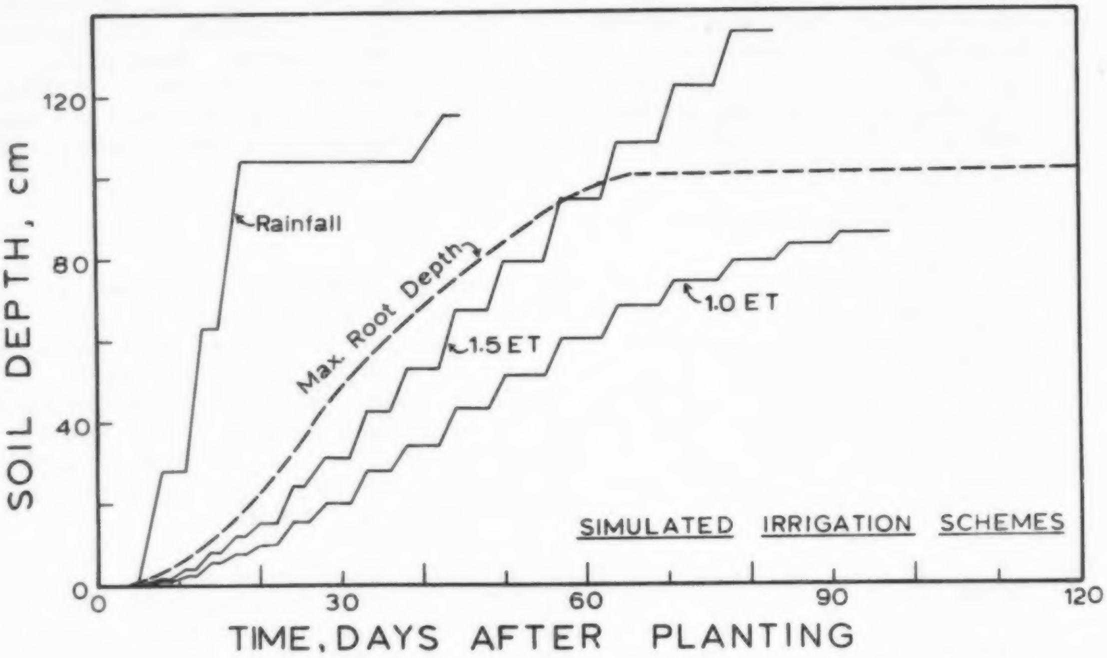

Figure 24. The predicted depth of nitrate front under three water application schemes during the growing season in a sandy soil profile. Increase in the maximum root zone depth (L) with time is also shown.

of irrigation water applied was 1.5 times that required by the crop (curve labeled 1.5 ET in Figure 24), the nitrate pulse was leached beyond the root zone after about 65 days. The intensity and the frequency of the rainfall events chosen here was such that the nitrate pulse was leached rapidly out of the root zone very early in the season (only five days after planting) as indicated by the curve labeled "rainfall" in Figure 24. Such observations are not uncommon in field studies involving sandy soils in Florida. A few major rainfall events of approximately 5 cm each can essentially move the fertilizer nitrogen out of plant root zone.

The effect of simulated water application management schemes on the cumulative nitrogen uptake by corn is illustrated in Figure 25. The "ideal" uptake demand for nitrogen was met under the 1.0 ET treatments at all times. This was possible since the nitrate pulse resided within the root zone and was available to roots for absorption in sufficient quantities. The "ideal" demand, however, was not satisfied for the 1.5 ET treatment; the time at which this curve deviated from the "ideal" (Figure 25) corresponds to the time when the nitrate pulse was leached out of the root zone (Figure 24). The cumulative nitrogen uptake curve for the rainfall treatment deviates significantly from the "ideal" curve at all times as could be surmized from Figure 24.

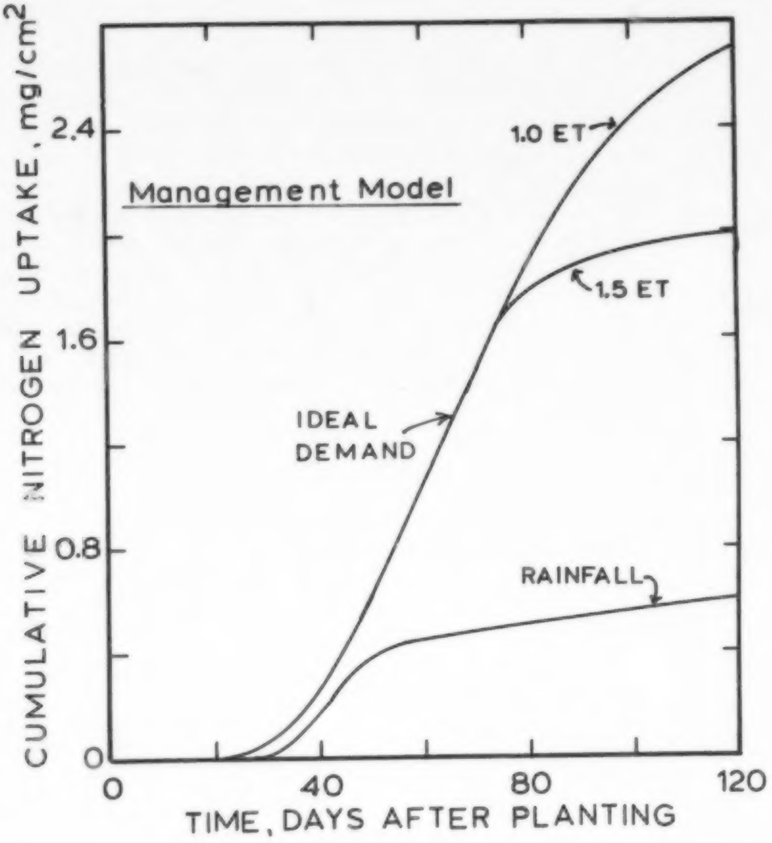

Figure 25. Cumulative nitrogen uptake by corn grown in a sandy soil under three water application schemes, as simulated by the management model.

REFERENCES

1. Bartholomew, V. W. and F. E. Clark, eds. 1965. Soil Nitrogen. Agronomy Monograph No. 10, Am. Soc. Agron., Inc. Madison, Wisconsin, 615 p.

2. Karplus, W. J. 1976. The future of mathematical models of water resources systems. in System Simulation in Water Resources. G. C. Vansteenkiste, ed. North-Holland Publishing Co., Amsterdam, The Netherlands, p. 11-18.

3. Tanji, K. K. and S. K. Gupta. 1977. Computer simulation modeling for nitrogen in irrigated crop lands. in Nitrogen and the Environment. D. R. Nielsen and J. McDonald, eds. Academic Press, N.Y.

4. Rao, P. S. C., H. M. Selim, J. M. Davidson, and D. A. Graetz. 1976. Simulation of transformations, ion-exchange, and transport of selected nitrogen species in soils. Soil Crop Sci. Soc. of Florida Proc. 35:161-164.

5. Quisenberry, V. L. and R. E. Phillips. 1976. Percolation of surface-applied water in the field. Soil Sci. Soc. Amer. Jour. 40:484-489.

6. van Genuchten, M. Th., and P. J. Wierenga. 1976. Mass transfer studies in sorbing porous media: I. Analytical solutions. Soil Sci. Soc. Amer. Jour. 40:473-480.

7. Kirkham, D. and W. L. Powers. 1972. Advanced Soil Physics Wiley-Interscience, New York.

8. Selim, H. M., R. S. Mansell, and A. Elzeftawy. 1976. Distributions of 2,4-D and water in soil during infiltration and redistribution. Soil Sci. 121:176-183.

9. Carnahan, P., H. Luther, and J. O. Wilkes. 1969. Applied Numerical Methods. Wiley, New York.

10. Salvadori, M. G., and M. L. Baron. 1961. Numerical Analysis in Engineering. Prentice-Hall, Englewood, New Jersey.

11. Davidson, J. M., G. H. Brusewitz, D. R. Baker, and A. L. Wood. 1975. Use of soil parameters for describing

pesticide movement through soils. Environmental Protection Technology Series, EPA-660/2-75-009.

12. Mehran, J. and K. K. Tanji. 1974. Computer modeling of nitrogen transformations in soils. Jour. Environ. Qual. 3:391-395.

13. Hagin, J. and A. Amberger. 1974. Contribution of fertilizers and manures to the N- and P- load of waters: A computer simulation. Final Report to the Deutsche Forschungs Gemeinschaft from Technion., Israel. 123 pp.

14. Beek, J. and M. J. Frissell. 1973. Simulation of nitrogen behavior in soils. Pudoc. Wageningen, The Netherlands. p. 67.

15. Misra, C., D. R. Nielsen, and J. W. Biggar. 1974. Nitrogen transformation in soil during leaching; I, II, III. Soil Sci. Soc. Amer. Proc. 38:289-304.

16. Stanford, G. and S. J. Smith. 1972. Nitrogen mineralization potentials of soils. Soil Sci. Soc. Amer. Proc. 36:465-472.

17. Stanford, G., M. H. Frere, and D. H. Schwaninger. 1973. Temperature coefficient of nitrogen mineralization. Soil Sci. 115:321-323.

18. Bremner, J. M. and K. Shaw. 1958. Denitrification in soils: I. Methods of investigations. J. Agric. Sci. 51:22-39.

19. Cooper, G. S. and R. L. Smith. 1963. Sequence of products formed during denitrification in some diverse western soils. Soil Sci. Soc. Amer. Proc. 27:659-662.

20. Stanford, G., J. O. Legg, S. Dzienzia, and E. C. Simpson, Jr. 1975. Denitrification and associated nitrogen transformations in soils. Soil Sci. 170:147-152.

21. Bowman, R. A. and D. D. Focht. 1974. The influence of glucose and nitrate concentrations upon denitrification rates in sandy soils. Soil Biol. & Biochem. 6:297-301.

22. McLaren, A. D. 1971. Kinetics of nitrification in soil: Growth of nitrifiers. Soil Sci. Soc. Amer. Proc. 35:91-95.

23. Selim, H. M., J. M. Davidson, P. S. C. Rao, and D. A. Graetz. 1977. Nitrogen transformations and transport during transient unsaturated water flow in soils. Manuscript submitted to Water Resour. Res.

24. Miller, R. D. and D. D. Johnson. 1964. The effect of soil moisture tension on carbon dioxide evolution, nitrification, and nitrogen mineralization. Soil Sci. Soc. Amer. Proc. 28:644-647.

25. Stanford, G. and E. Epstein. 1974. Nitrogen mineralization water relations in soils. Soil Sci. Soc. Amer. Proc. 38:103-107.

26. Myers, R. J. K. 1974. Soil processes affecting nitrogenous fertilizers. in Proc. Symp. Ecological Aspects of Fertilizer Technology and Use. D. R. Leece, ed. Sydney, Australia. Sponsored by Austr. Inst. Agrl. Sci., Syndey, New South Wales. Australia.

27. Davidson, J. M., L. T. Ou, and P. S. C. Rao. 1976. Behavior of high pesticide concentrations in soil water systems. in Residual Management by Land Disposal. Proc. of the Hazardous Waste Research Symp. Tucson, Arizona. EPA-600/9-76-015. p. 235-242.

28. Dutt, G. R., M. J. Shaffer, and W. J. Moore. 1972. Computer simulation model of dynamic bio-physiochemical processes in soils. Univ. of Arizona Tech. Bull. No. 196, 101 pp.

29. Remson, I., G. M. Hornberger, and F. J. Molz. 1971. Numerical Methods in Subsurface Hydrology with an Introduction to the Finite Element Method. Wiley-Interscience, N.Y. 448 p.

30. Selim, H. M., and D. Kirkham. 1973. Unsteady two-dimensional flow of water in unsaturated soils above an impervious barrier. Soil Sci. Soc. Amer. Proc. 37:489-495.

31. Varga, R. S. 1962. Matrix Iterative Analysis. Prentice Hall, New Jersey.

32. Selim, H. M., J. M. Davidson, and P. S. C. Rao. 1977. Transport of reactive solutes in multilayered soils. Soil Sci. Soc. Amer. Jour. 41:3-10.

33. Gardner, W. R. 1960. Dynamic aspects of water availability to plants. Soil Sci. 89:63-67.

34. Molz, F. J., I. Remson, A. A. Fungaroli, and R. L. Drake. 1968. Soil moisture availability for transpiration. Water Resour. Res. 4:1161-1169.

35. Hillel, D., C. G. E. M. van Beek, and H. Talpaz. 1975. A microscopic-scale model of soil water uptake and salt movement to plant roots. Soil Sci. 120:385-399.

36. Gardner, W. R. 1964. Relation of root distribution to water uptake and availability. Agron. J. 56:41-45.

37. Molz, F. J. and I. Remson. 1970. Extraction-term models of soil moisture use by transpiring plants. Water Resour. Res. 6:1346-1356.

38. Molz, R. J. and I. Remson. 1971. Application of an extraction-term model to the study of moisture flow to plant roots. Agron. J. 63:72-77.

39. Nimah, M. and R. J. Hanks. 1973. Model for estimating soil-water-plant-atmospheric interrelation: I. Description and sensitivity. Soil Sci. Soc. Amer. Proc. 37:522-527.

40. Nimah, M. and R. J. Hanks. 1973. Model for estimating soil-water-plant-atmospheric interrelations. II. Field test of model. Soil Sci. Soc. Amer. Proc. 37:528-532.

41. Childs, S. W. and R. J. Hanks. 1976. Model of soil salinity effects on crop growth. Soil Sci. Soc. Amer. Proc.

42. Ritchie, J. T. 1973. Influence of soil water status and meteorological conditions on evaporation from a corn canopy. Agron. J. 65:893-897.

43. Penman, H. I., D. E. Angus, C. H. M. van Bavel. 1967. Micro-climatic factors affecting evaporation and transpiration. in Irrigation of Agricultural Lands. R. M. Hagan, H. R. Haise, and J. W. Edminster, eds. Amer. Soc. of Agronomy. Madison, Wisconsin. p. 483-505.

44. Soil Conservation Service, USDA. 1970. Irrigation Water Requirements. Technical Release No. 21. Engineering Division, USDA-SCS. 88 p.

45. Nye, P. H. and J. A. Spiers. 1964. Simultaneous diffusion and mass flow to plant roots. Trans. 8th Int. Cong. Soil Sci., Bucharest, Rumania, 3:535-542.

46. Passioura, J. B. and M. H. Frere. 1967. Numerical analysis of the convection and diffusion of solutes to roots. Aust. J. Soil Res. 5:149-159.

47. Marriott, F. H. C. and P. H. Nye. 1968. The importance of mass flow in uptake of ions by roots from soil. Trans. 9th Cong. Soil Sci., Adelaide, Australia. 1:127-134.

48. Olsen, S. R. and W. D. Kemper. 1968. Movement of nutrients to plant roots. Adv. In Agron. 20:91-151.

49. Phillips, R. E., T. NaNagara; R. E. Zartman, and J. E. Leggett. 1976. Diffusion and mass flow of nitrate-nitrogen to plant roots. Agron. J. 6:63-66.

50. Olsen, S. R., W. D. Kemper, and R. D. Jackson. 1962. Phosphorous diffusion to plant roots. Soil Sci. Soc. Amer. Proc. 26:222-

51. Fried, M. and R. E. Shapiro. 1961. Soil-plant relationships in ion uptake. Ann. Rev. Plant. Physiol. 12:91-112.

52. Passioura, J. B. 1963. A mathematical model for uptake of ions from the soil solution. Plant and Soil. 18:225-238.

53. Halsted, E. H., S. A. Barber, D. O. Warncke, and J. B. Bole. 1968. Supply of Ca, Sr, Mn, and Zn to plant roots growing in soils. Soil Sci. Soc. Amer. Proc. 32:69-72.

54. Brewster, J. L. and P. B. Tinker. 1970. Nutrient cation flows in soil around plant roots. Soil. Sci. Soc. Amer. Proc. 34:421-426.

55. Bole, J. B. and S. A. Barber. 1971. Differentiation of Sr-Ca supply mechanisms to roots growing in soil, clay and exchange resin cultures. Soil Sci. Soc. Amer. Proc. 35: 768-772.

56. Elgawhary, S. M., G. L. Malzer, and S. A. Barber. 1972. Calcium and strontium transport to plant roots. Soil Sci. Soc. Amer. Proc. 36:794-799.

57. Barley, K. P. 1970. The configuration of the root system in relation to nutrient uptake. Adv. in Agron. 32:159-201.

58. Zartman, R. E., R. E. Phillips, and J. E. Leggett. 1976. Comparison of simulated and measured nitrogen accumulation in Burley tobacco. Agron. J. 68:406-410.

59. Lewis, D. G. and J. P. Quirk. 1967. Phosphate diffusion in soil and uptake by plants. IV. Computed uptake by model roots as a result of diffusive flow. Plant and Soil. 26:454-468.

60. Nye, P. H. and F. H. C. Marriott. 1969. A theoretical study of the distribution and substances around roots resulting from simultaneous diffusion and mass flow. Plant and Soil. 30:459-472.

61. Nielson, N. E. 1972. A transport kinetic concept of ion uptake from soils by plants. II. The concept and some theoretical considerations. Plant and Soil. 37:561-576.

62. Jungk, A. and S. A. Barber. 1975. Plant age and the phosphorus uptake characteristics of trimmed and untrimmed corn root systems. Plant and Soil. 42:227-239.

63. NaNagara, T., R. E. Phillips, and J. E. Leggett. 1976. Diffusion and mass flow of nitrate-nitrogen into corn roots grown under field conditions. Agron. J. 68:67-72.

64. van Keulen, H., N. G. Seligman, and J. Goudriaan. 1975. Availability of anions in the growth medium to roots of an actively growing plant. Neth. Jour. Agric. Sci. 23:131-138.

65. Russell, R. S., and M. G. T. Shone. 1972. Root function and the soil. Proc. 11th British Weed Control Conf. pp. 1183-1191.

66. Jungk, A. and S. A. Barber. 1974. Phosphate uptake rate of corn roots as related to the portion of roots exposed to phosphate. Agron. J. 66:554-557.

67. Brower, R. and C. T. deWit. 1969. A simulation model of plant growth with special attention to root growth and its consequences. in Root Growth. W. J. Whittington, ed. p. 224-242.

68. Watts, D. G. 1975. A soil-water-nitrogen-plant model for irrigated corn on coarse textured soils. Ph.D. Dissertation, Utah State Univ. 187 p.

69. Newman, E. I. 1974. Root and soil water relations. in The Plant Root and Its Environment. E. W. Carson, ed. Univ. Press of Virginia, Charlottesville, Virginia, p. 363-440.

70. Mengel, D. B. and S. A. Barber. 1974. Rate of nutrient uptake per unit of corn root under field conditions. Agron. J. 66:399-402.

71. Warncke, D. D. and S. A. Barber. 1974. Root development and nutrient uptake by corn grown in solution culture. Agron. J. 66:514-516.

72. Dibb, D. W. and L. F. Welch. 1976. Corn growth as affected by ammonium vs. nitrate absorbed from soil. Agron. J. 68:89-94.

73. Bohm, W., H. Maduakor, and H. M. Taylor. 1976. Comparison of five methods for characterizing soybean rooting density and development. Agron. Abstracts. 1976. p. 171.

74. Newman, E. I. 1965. A method for estimating the total length of root in a sample. J. Appl. Ecol. 2:139-145.

75. Taylor, H. M. 1974. Root behavior as affected by soil structure and soil strength. in The Plant Root and Its Environment, E. W. Carson, ed. Univ. Press of Virginia, Charlottesville, Virginia. p. 271-289.

76. Moore, D. P. 1974. Physiological effects of pH on roots. in The Plant Root and Its Environment, E. W. Carson, ed. Univ. Press of Virginia, Charlottesville, Virginia. p. 135-151.

77. Hillel, D. and H. Talpaz. 1976. Simulation of root growth and its effects of pattern of soil water uptake by non-uniform root system. Soil Sci. 121:307-312.

78. Lambert, J. R., D. N. Baker, and C. J. Phene. 1975. Simulation of soil processes under growing row crops. Paper presented at 1975 Winter Meeting of the Am. Soc. Agr. Engg., Chicago.

79. Whisler, F. D. 1977. Modifications to RHIZOS: A comparison of soil models on rooting development models (Unpublished manuscript).

80. Duffy, J., C. Chung, C. Boast, and M. Franklin. 1976. A simulation model of biophysiochemical transformations of nitrogen in tile-drained corn belt soils. J. Environ. Qual. 4:477-486.

81. Frere, M. H., C. A. Onstad, and H. N. Holtan. 1975. ACTMO, an agricultural chemical transport model. U.S. Dept. Agri., ARS-H-3, 54 pp.

82. Rao, P. S. C., J. M. Davidson, and L. C. Hammond. 1976. Estimation of nonreactive and reactive solute front locations in soils. Residual Management by Land Disposal. Proc. Hazardous Waste Research Symp. Tucson, Arizona. EPA-600/9-76-015. p. 235-242.

83. Balasubramanian, V. 1974. Adsorption, denitrification, and movement of applied ammonium and nitrate in Hawaiian soils. Ph.D. Dissertation, University of Hawaii. Diss. Abstr. Internl.

84. Kirda, D., D. R. Nielsen, and J. W. Biggar. 1973. Simultaneous transport of chloride and water during infiltration. Soil Sci. Soc. Amer. Proc. 37:339-345.

85. Kirda, C., D. R. Nielsen, and J. W. Biggar. 1974. The combined effects of infiltration and redistribution on leaching. Soil Sci. 117:323-330.

86. Warrick, A. W., J. W. Biggar, and D. R. Nielsen. 1971. Simultaneous solute and water transfer for an unsaturated soil. Water Resour. Res. 7:1216-1225.

87. Cassel, D. K. 1971. Water and solute movement in Svea loam for two water management regimes. Soil Sci. Soc. Amer. Proc. 35:859-866.

88. Ghuman, B. S., S. M. Verma, and S. S. Prihar. 1975. Effect of application rate, initial soil wetness, and redistribution time on salt displacement by water. Soil Sci. Soc. Amer. Proc. 39:7-10.

89. Graetz, D. A., L. C. Hammond, and J. M. Davidson. 1973. Nitrate movement in a Eustis sand planted to millet. Soil Crop Sci. Soc. Florida Proc. 33:157-160.

90. Hammond, L. C., J. M. Davidson, and D. A. Graetz. 1973. Unpublished data. Florida Agr. Exp. Sta.

91. Rao, P. S. C., R. E. Jessup, and J. M. Davidson. 1976. A model for kinetics of nitrogen transformations during leaching in soils: Analytical Solutions. Unpublished manuscript.

92. Cho, C. M. 1971. Convective transport of ammonium with nitrification in soil. Can. J. Soil Sci. 51:339-350.

93. Rao, P. S. C., J. M. Davidson, and R. E. Jessup. 1977. A simple model for description of the fate of nitrogen in crop root zone. Manuscript prepared for Agronomy Journal.

94. Stanford, G., J. N. Carter, and S. J. Smith. 1974. Estimates of potentially mineralizable soil nitrogen based on short-term incubations. Soil Sci. Soc. Amer. Proc. 38:99-102.

95. Selim, H. M., L. C. Hammond, and R. S. Mansell. 1977. Soil water movement and uptake by plants during water infiltration and redistribution. Soil Crop Sci. Soc. Florida Proc. (in press).

96. Phillips, R. E. 1976. Personal communication of unpublished data.

97. Broadbent, F. E., K. B. Tyler, and G. N. Hill. 1957. Nitrification of ammonical fertilizers in some California soils. Hilgardia 27:247-267.

98. Cooper, G. S. and R. L. Smith. 1963. Sequence of products formed during denitrification in some diverse western soils. Soil Sci. Soc. Amer. Proc. 27:659-662.

99. Justice, J. K. and R. L. Smith. 1962. Nitrification of ammonium sulfate in a calcareous soil as influenced by combinations of moisture, temperature, and levels of added nitrogen. Soil Sci. Soc. Amer. Proc. 26:246-250.

100. Stojanovic, B. J. and F. E. Broadbent. 1956. Immobilization and mineralization rates of nitrogen during decomposition of plant residues. Soil Sci. Soc. Amer. Proc. 20:213-218.

101. Chichester, F. W., J. O. Legg, and G. Stanford. 1975. Relative mineralization rates of indegenous and recently neosporated ^{15}N-labeled nitrogen. Soil Sci. 120:455-460.

102. Kirda, C., J. L. Starr, C. Misra, J. W. Biggar and D. R. Nielsen. 1974. Nitrification and denitrification during miscible displacement in unsaturated soil. Soil Sci. Soc. Amer. Proc. 38:772-776.

103. Starr, J. L., F. E. Broadbent, and D. R. Nielsen. 1974. Nitrogen transformations during continuous leaching. Soil Sci. Soc. Amer. Proc. 38:283-289.

104. Rolston, D. E. and A. M. Marino. 1976. Simultaneous transport of nitrate and gaseous denitrification products in soil. Soil Sci. Soc. Amer. Jour. 40:860-865.

105. Jansson, S. L. 1958. Tracer studies on nitrogen transformations in soil with special attention to mineralization-immobilization relationships. K. Lantbrules-Hoegskol. Ann. 25:101-361.

106. Jansson, S. L. 1963. Balance sheet and residual effects of fertilizer nitrogen in a 6-year study with ^{15}N. Soil Sci. 95:31-37.

107. Jansson, S. L. 1971. Use of ^{15}N in studies of soil nitrogen. in Soil Biochemistry (Volume 2), A. D. McLaren and J. Skujs, eds. Marcel Decker Inc., N.Y. p. 129-166.

108. Legg, J. O., F. W. Chichester, G. Stanford and W. H. DeMar. 1971. Incorporation of ^{15}N-tagged mineral nitrogen into stable forms of soil organic nitrogen. Soil Sci. Soc. Amer. Proc. 35:273-276.

109. Stanford, G., J. O. Legg, and F. W. Chichester. 1970. Transformation of fertilizer nitrogen in soil: I. Interpretations based on chemical extractions of labeled and unlabeled nitrogen. Plant Soil. 33:425-436.

110. Chichester, F. W. 1970. Transformation of fertilizer nitrogen in soil: II. Total and ^{15}N labelled nitrogen

of soil organomineral sedimentation fractions. Plant Soil. 33:437-457.

111. Van Veen, J. A. 1977. The behavior of nitrogen in soil: A computer simulation model. Doctoral Dissertation. The Free University of Amsterdam, Amsterdam, The Netherlands.

112. Browder, J. A. and B. G. Volk. 1977. Systems model of carbon transformations in soil subsidence. Ecological Modelling. (in press)

113. Reddy, K. R., R. Khaleel, M. R. Overcash, and P. W. Westerman. 1977. Conceptual modeling of nonpoint source pollution from land areas receiving animal wastes: I. Nitrogen transformations. A paper presented at the 1977 summer meetings of the American Society of Agricultural Engineers at Raleigh, N.C. June 21-29, 1977.

114. Reddy, K. R., W. H. Patrick, and R. E. Phillips. 1977. The role of diffusion in determining the order and rate of denitrification in submerged soil. Soil Sci. Soc. Amer. Jour. (in press)

APPENDIX A

DESCRIPTION OF THE COMPUTER PROGRAM FOR THE RESEARCH MODEL

The Northeast Regional Data Center (NERDC) of the State University System (SUS) of Florida at Gainesville, FL is equipped with an AMDAHL 470 V/6-II computer. The Amdahl computer is software-compatible with IBM 370/165 computers. The numerical solutions comprising the research model (Section 4) required a total of 256K bytes of main storage for execution. Actual CPU (computer processing units) time required for a given simulation run will increase with increasing intensity and/or frequency of the water input events. As an example, CPU time for the three irrigation events discussed in Section 7 (page 50) was 25, 5, and 5 minutes, respectively. Recall that the first event included the infiltration of 9.1 cm of water over a 12-hour period, while 3.2 cm of water infiltrated in 4-hours in the latter two events.

The computer program consists of a source program and seventeen subprograms, and an input data section. The names of the subprograms are AXISPL, GRAPH, CHECKT, WATER, MOISD, INITWT, SBCW, INITST, DADJ, DADJD, CHECKN, AMONIA, NITRAT, GASORB, OUTPUT, TINT, and TRIDM. In addition, there are five subroutine functions namely; ZZ1, ZZ2, ZZ3, ZZ4, and ZZ5. The user of this program must provide parameters in the form of punched data cards in the data section, and as FORTRAN statements in the SBCW and WATER subprograms as well as subroutine functions ZZ1, ZZ2, ZZ3, ZZ4, and ZZ5. The remaining source program and subprograms need not be altered and remain valid for all situations.

The main function of the main program is prescribing the DIMENSION and COMMON statements, reading input parameters, and establishing the entire sequence of the program. Subprograms INITWT, INITST, and MOISD provide the initial distributions of all the variables and calculates Δz and Δt according to the stability criteria. Subprogram SBCW provides h at z=0 according to the boundary condition for the water flow equation, which may be altered by the user as desired. Subprograms WATER, AMONIA, and NITRAT provide the solution for water head (h), NH_4 concentration (A) and NO_3 concentration (B), respectively. Subprogram GASORG calculates the amount of organic-N and gaseous-N. Subprogram TRIDM provides the solution for a linear system of equations with a tridiagonal coefficient matrix. Subroutine functions ZZ1, ZZ2, ZZ3, ZZ4, ZZ5 are used in conjunction with subprograms AMONIA , NITRAT, and GASORG and provide the reaction rate coefficients, (k_1, k_2, k_3, k_4, and k_5) as a function of soil water suction, soil-water content and/or organic-N content at every time step and incremental soil depth.

The dispersion coefficient D and the hydraulic conductivity K are calculated at each time step in the WATER subprogram. Here, D and K are provided as a function of (q/θ) and θ, respectively. In addition, Cap(h) and conversion of h to θ at all incremental points in the soil profile were calculated in the WATER subprogram. This conversion is based on the θ versus h relationship (in a tabular form) for each soil.

An important feature of the program is that increments of Δz and Δt are adjusted automatically to satisfy stability and convergence criteria for the water and solute finite difference equations. These adjustments are carried out after every 20 time steps using subprograms DADJ and DADJD. Another program feature is that the number of nodal points (increments) are automatically calculated from the length of the flow region (soil profile). Only that portion of the flow region where water and solute are present is considered. The adjustments of the number of nodal points are made using subprogram CHECKN. This number is checked every 20 time steps, and no further changes of the number of increments will occur when the total column length is reached. This feature minimizes the unnecessary use of a large number of nodal points and saves considerable CPU time. A third feature of the program is that output data and plots are provided at specified times. This adjustment is carried out using subprogram CHECKT, where t's are continuously adjusted until the prescribed times are reached. For each prescribed time; h, θ, K, q, NH_4-N, NO_3-N, organic-N, gaseous-N throughout the soil column are printed using subprogram OUTPUT. Subprograms AXISPL and GRAPH plots (using GOULD plotter) for θ, NH_4, NO_3, and Org-N versus depth for various times can also be obtained. The scale and length of each plot is prescribed in these subprograms and may be changed by the user.

PROGRAM PARAMETERS

The following parameters are inputs to be provided in the DATA section of the computer program

NX = number of data points of the soil water characteristic relationship (θ versus h),

THC = water content θ from soil water characteristic relationship (dimension = NX), cm^3/cm^3,

HC = corresponding water suction h from soil water characteristic relationship (dimension = NX), cm,

DZ = initial approximation for Δz, cm,

DT = initial approximation for Δt, days,

DISP = initial approximations for dispersion coefficient D, cm^2/day,

THMIN = estimated minimum soil water content, cm^3/cm^3,

THMAX = maximum soil water content, cm^3/cm^3,

NT = number of prescribed times at which data are desired,

TIT = times at which output are desired (dimension = NT), days,

NTGR = number of prescribed times at which plots (using GOULD plotter) are desired,

TGRAPH = times at which plots are desired (dimension = NTGR), days,

RKD = K_D (see equation 13), cm^3/g,

RK1 = $\bar{k}_1$ (see equation 6a, 6b), day^{-1},

RK2 = $\bar{k}_2$ (see equation 7), day^{-1},

RK3 = $\bar{k}_3$ (see equation 8a, 8b), day^{-1},

RK4 = $\bar{k}_4$ (see equation 9), day^{-1},

RK5 = $\bar{k}_5$ (see equations 10a, 10b), day^{-1},

ZZ1 = k_1 (see equations 6a, 6b), day^{-1},

ZZ2 = k_2 (see equation 7), day^{-1},

ZZ3 = k_3 (see equations 8a, 8b), day^{-1},

ZZ4 = k_4 (see equation 9), day^{-1},

ZZ5 = k_5 (see equation 10a, 10b), day^{-1},

NTT = number of points for initial distributions of water and nitrogen species in the soil profile,

XXX = depths at which initial distributions are given (dimension = NTT), cm, C1 = initial distribution of water suction (h) in the soil profile (dimension = NTT), cm,

C2 = initial distribution of soil water content (θ) in the soil profile (dimension = NTT), cm^3/cm^3,

C3 = initial distribution of NH_4 in soil solution (dimension = NTT), $\mu g\ N/cm^3$,

C4 = initial distribution of NO_3 in soil solution (dimension = NTT), $\mu g\ N/cm^3$,

C5 = initial distribution of organic-N per gram soil (dimension = NTT), μg N/g soil,

C6 = initial distribution of gaseous-N per gram soil (dimension = NTT), μg N/g soil,

ROU = ρ, soil bulk density, g/cm^3,

COLUMN = length of soil profile, cm,

TSALT = length of time of solute application, days,

TWD = length of time of water infiltration, days,

CONST = hydraulic conductivity at saturation, cm/day,

AC = a coefficient for K versus relationship,

BC = a coefficient for K versus relationship,

CSNH4 = concentration of NH_4 in applied solution, $\mu g\ N/cm^3$,

CSNO3 = concentration of NO_3 in applied solution, $\mu g\ N/cm^3$,

DFLUX = evaporative flux during water redistribution (time> TWD), cm/day,

Input parameters to be provided in subprogram WATER are

CON = water hydraulic conductivity K, cm/day,

DISPC = dispersion coefficient D, cm^2/day,

Input parameters to be provided in subprogram SBCW is

H(1) = water head h at z=0 during infiltration and maximum h during redistribution, cm,

Other notations used in the program are:

TH = soil water content, cm^3/cm^3,

H = water suction, h, cm,

CNH4 = concentration of NH_4 in soil solution, A, μg N/cm ,

CNO3 = concentration of NO_3 in soil solution, B, μg N/cm ,

CORGN = amount of organic-N per gram soil, OM, μg N/g,

CNO2 = amount of gaseous-N per gram soil, G, μg N/g,

CAP = soil water capacity, Cap(h),

WFLUX = soil water flux, q, cm/day.

APPENDIX B

FLOW CHART OF THE COMPUTER PROGRAM

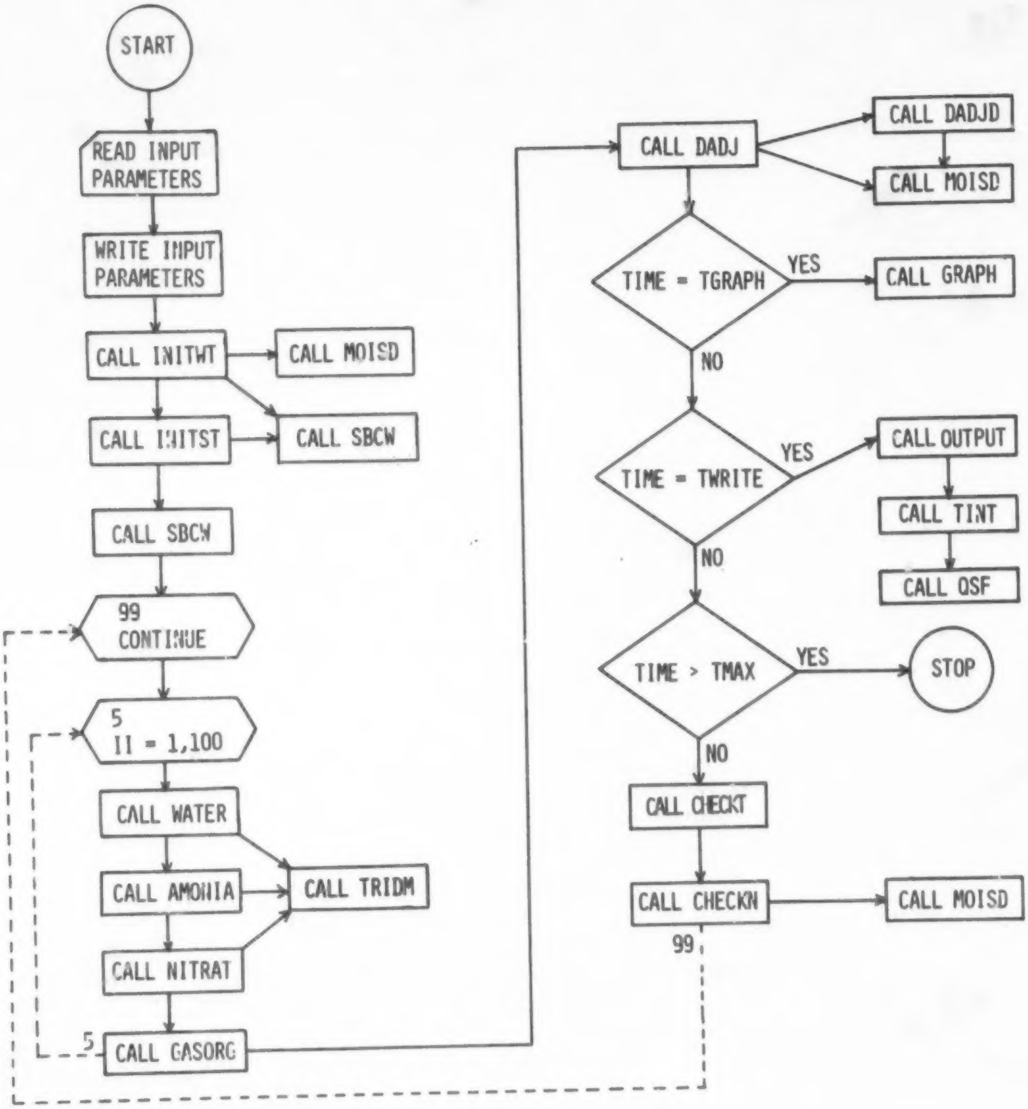
START
READ INPUT PARAMETERS
WRITE INPUT PARAMETERS
CALL INITWT
CALL MOISD
CALL INITST
CALL SBCW
CALL SBCW
99 CONTINUE
5 II = 1,100
CALL WATER
CALL AMONIA
CALL TRIDM
CALL NITRAT
5
CALL GASORG
CALL DADJ
CALL DADJD
CALL MOISD
TIME = TGRAPH
YES
CALL GRAPH
NO
TIME = TWRITE
YES
CALL OUTPUT
CALL TINT
CALL QSF
NO
TIME > TMAX
YES
STOP
NO
CALL CHECKT
CALL CHECKN
CALL MOISD
99

APPENDIX C

FORTRAN PROGRAM LISTING

```
C
      COMMON/L1/ TH(810),CNH4(810),CNO3(810),CORGN(810),CNO2(810),
     *VP(810),DISPC(810)
      COMMON/L2/ AA(610),EE(610),CC(610),R(610),X(610)
      COMMON/L3/ N,NM1,NM2,NP1,NP2
      COMMON/L4/ ALPHA,BETA,DT,DZ
      COMMON/L5/ RKD,RK1,RK2,RK3,RK4,RK5
      COMMON/L6/ SFLUX,CSNH4,CSNO3
      COMMON/L7/ROU,COLUMN,DFLUX
      COMMON/L8/ DISP,THMAX,THMIN,HMIN,CORGNI
      COMMON/L9/TIME,TPRINT,TWRITE
      COMMON/L10/ H(810),CON(810),CAP(810)
      COMMON/L11/ THC(40),HC(40),CAPC(40)
      COMMON/L12/ AC,BC,NX,NX1,CONST
      COMMON/L13/ WFLUX(810)
      COMMON/L14/ VO,TWD,TSALT
      COMMON/L15/ TIT(30),TC,DTDT,IT,IL,NT
      COMMON/L16/IC,IWT
      COMMON/L17/ XXX(30),C1(30),C2(30),C3(30),C4(30),C5(30),C6(30)
      COMMON/L19/ TGRAPH(15),NTGR,ITGR
  100 FORMAT(8F10.3)
  200 FORMAT(5E10.4)
  300 FORMAT(2I4)
      READ(5,300) NX
      NX1=NX-1
      READ(5,100)  (THC(I),I=1,NX)
      WRITE(6,100) (THC(I),I=1,NX)
      READ(5,100)  (HC(I),I=1,NX)
      WRITE(6,100) (HC(I),I=1,NX)
      READ(5,100)  DZ,DT
      WRITE(6,100) DZ,DT
      READ(5,100)   DISP,THMAX,THMIN,HMIN,CORGNI
      WRITE(6,100)  DISP,THMAX,THMIN,HMIN,CORGNI
      READ(5,100) COLUMN,ROU,CSNH4,CSNO3,DFLUX
      WRITE(6,100) COLUMN,ROU,CSNH4,CSNO3,DFLUX
      READ(5,200) AC,BC,CONST
      WRITE(6,200) AC,BC,CONST
      READ(5,300)  NT
      READ(5,100) (TIT(I),I=1,NT)
      WRITE(6,100) (TIT(I),I=1,NT)
      READ(5,300) NTT
      READ(5,100) (XXX(I),I=1,NTT)
      WRITE(6,100) (XXX(I),I=1,NTT)
      READ(5,100) (C1(I),I=1,NTT)
      WRITE(6,100) (C1(I),I=1,NTT)
      READ(5,100) (C2(I),I=1,NTT)
      WRITE(6,100) (C2(I),I=1,NTT)
      READ(5,100) (C3(I),I=1,NTT)
      WRITE(6,100) (C3(I),I=1,NTT)
      READ(5,100) (C4(I),I=1,NTT)
      WRITE(6,100) (C4(I),I=1,NTT)
      READ(5,100) (C5(I),I=1,NTT)
      WRITE(6,100) (C5(I),I=1,NTT)
      READ(5,100) (C6(I),I=1,NTT)
      WRITE(6,100) (C6(I),I=1,NTT)
      READ(5,300) NTGR
      READ(5,100)  (TGRAPH(I),I=1,NTGR)
      WRITE(6,100) (TGRAPH(I),I=1,NTGR)
      READ(5,100) RKD,RK1,RK2,RK3,RK4,RK5
      WRITE(6,100) RKD,RK1,RK2,RK3,RK4,RK5
      ITGR=1
      DO  2  I=1,NTT
      C1(I)=-4900.0
    2 C2(I)=0.100
      IT=1
      TC=TIT(IT)
      N=25
      N=40
      NM1=N-1
      NM2=N-2
      NP1=N+1
      NP2=N+2
      TSALT=1.00
      TWD=10.0
      TWD=12.0
      SFLUX=CONST
```

Reproduced from
best available copy.

```
C
      CALL INITWT
      CALL INITST
      IC=2
      IWT=-1
      CALL AXISPL
C
      H(1)=-100.0
      THMIN=0.10
      COLUMN=90.0
      COLUMN=45.0
      TIME=0.0
      CALL SBCW
      IL=250
      IL=20
      IL=40
      IL=100
   99 CONTINUE
      DO  5  II=1.IL
      CALL WATER
      CALL AMONIA
      CALL NITRAT
      CALL GASORG
    5 CONTINUE
      TIME=TIME+IL*DT
      WRITE(6.200)  DZ.DT.TIME.ALPHA.BETA
      CALL DADJ
      WRITE(6.200)  DZ.DT.TIME.ALPHA.BETA
      TWRITE=ABS(TIME-TGRAPH(ITGR))
      IF(TWRITE.LE.1.0E-3)  CALL GRAPH
      IF(TIME.GE.TIT(NT))  CALL PLOT(0.0.0.0.999)
      TWRITE=ABS(TIME-TC)
      IF(TWRITE.LE.1.0E-3)  CALL OUTPUT
      IF(TIME.GE.TIT(NT)) STOP
      CALL CHECKT
      CALL CHECKN
      GO TO 99
      END
```

```
C
      SUBROUTINE WATER
      COMMON/L1/ TH(810).CNH4(810).CNO3(810).CORGN(810).CNO2(810).
     *VP(810).DISPC(810)
      COMMON/L2/ AA(610).BB(610).CC(610).R(610).X(610)
      COMMON/L3/ N.NM1.NM2.NP1.NP2
      COMMON/L4/ ALPHA.BETA.DT.DZ
      COMMON/L5/ RKD.RK1.RK2.RK3.RK4.RK5
      COMMON/L6/ SFLUX.CSNH4.CSNO3
      COMMON/L7/ ROU
      COMMON/L8/ DISP.THMAX.THMIN.HMIN.CORGNI
      COMMON/L9/TIME.TPRINT.TWRITE
      COMMON/L10/ H(810).CON(810).CAP(810)
      COMMON/L11/ THC(40).HC(40).CAPC(40)
      COMMON/L12/ AC.BC.NX.NX1.CONST
      COMMON/L13/ WFLUX(810)
      COMMON/L14/ W0.TWD.TSALT
      CL1=40.0
      AD=AC/100.0
      NCL1=CL1/DZ+0.0010
      NCL2=NCL1+1
      NCL3=NCL1+2
      DO  90  I=1.NP1
   90 CON(I)=AC*EXP(BC*(TH(I)+TH(I+1))*0.50)
      IF(NCL3.GE.NP1) GO TO 92
      DO  91  I=NCL3.NP1
   91 CON(I)=AD*EXP(BC*(TH(I)+TH(I+1))*0.50)
      CON(NCL2)=(CON(NCL1)*CON(NCL3))*2/(CON(NCL1)+CON(NCL3))
   92 CONTINUE
      DO  1  I=1.NM2
      AA(I)=CAP(I+1)+ALPHA*(CON(I+1)+CON(I))
      BB(I)=-ALPHA*CON(I+1)
      CC(I)=-ALPHA*CON(I+1)
    1 CONTINUE
      AA(NM1)=CAP(N)+ALPHA*CON(N)
      DO 2 I=1.NM1
      X1=CAP(I+1)*H(I+1)
      X2=ALPHA*CON(I)*H(I)-ALPHA*H(I+1)*(CON(I+1)+CON(I))
      X3=ALPHA*CON(I+1)*H(I+2)
      X4=-BETA*(CON(I+1)-CON(I))
      R(I)=X1+X2+X3+X4
    2 CONTINUE
      R(1)=R(1)+ALPHA*CON(1)*H(1)
      CALL TRIDM(AA.BB.CC.R.X.NM1)
      DO 3 K=2.N
    3 H(K)=X(K-1)
      H(NP1)=H(N)
      H(NP2)=H(N)
      CALL SBCW
      DO  15  J=1.NP2
      IF(H(J).LT.HC(1)) GO TO 25
      TH(J)=THC(1)
   15 CAP(J)=CAPC(1)
   25 CONTINUE
      DO  60  I=1.NP2
      DO  80  K=1.NX1
      IF(H(I).GT.HC(K+1))  GO TO 70
   80 CONTINUE
   70 TH(I)=THC(K)+CAPC(K)*(H(I)-HC(K))
      IF(TH(I).GT.THC(1)) TH(I)=THC(1)
      CAP(I)=CAPC(K)
   60 CONTINUE
      DO  95  I=1.NP1
      WFLUX(I)=-CON(I)*(H(I+1)-H(I))/DZ+CON(I)
      DISPC(I)=0.02580+0.12740*ABS(WFLUX(I)/TH(I))**1.3550
   95 CONTINUE
      RETURN
      END
      SUBRCUTINE AMONIA
C     NH-4  PRGRAM
      CCMMON/L1/ TH(810).CNH4(810).CNO3(810).CORGN(810).CNO2(810).
     *VP(810).DISPC(810)
      CCMMCN/L2/ AA(610).EB(610).CC(610).R(610).X(610)
      COMMON/L3/ N.NM1.NM2.NF1.NP2
      COMMON/L4/ ALPHA.BETA.DT.DZ
      COMMON/L5/ RKD.RK1.RK2.RK3.RK4.RK5
      COMMON/L6/ SFLUX.CSNH4.CSNO3
      CCMMCN/L7/ FOU
      COMMCN/L8/ CISP.THMAX.THMIN.HMIN.CORGNI
      COMMON/L9/TIME.TPRINT.TWRITE
      COMMON/L10/ H(810).CDN(810).CAP(810)
      COMMON/L11/ THC(40).HC(40).CAPC(40)
      COMMON/L12/ AC.BC.NX.NX1.CONST
      COMMCN/L13/ WFLUX(810)
      COMMON/L14/ VO.TWD.TSALT
      COMMON/L15/ TIT(30).TC.DTDT.IT.IL.NT
      FF=2.0*DZ
      SSINF=WFLUX(1)
      CNH4(1)=(SSINF*FF*CSNH4+DISP*TH(1)*CNH4(3))/(SSINF*FF+DISP*TH(1))
      DO  1    I=1.NP1
      DISP=DISPC(I)
      VP(I)=WFLUX(I)-DISP*(TH(I+1)-TH(I))/DZ
    1 CONTINUE
      IF(SFLUX.LE.0.0)  GC TO 13
C
C
      DO  5  I=1.NM2
      DISP=DISPC(I+1)
      RKK=1.C+RKD*FOU/TH(I+1)
      AA(I)=RKK+2.C*ALPHA*DISP-BETA*VP(I+1)/TH(I+1)
      AA(I)=RKK+2.0*ALPHA*CISP
      BB(I)=BETA*VP(I+1)/TH(I+1)-ALPHA*DISP
      BB(I)=-ALFHA*DISP
      DISP=DISPC(I+2)
      CC(I)=-ALFHA*DISP
    5 CONTINUE
      DISP=DISPC(N)
      RKK=1.0+RKD*FOU/TH(N)
      AA(NM1)=RKK+ALFHA*DISP
      DO  10   M=1.NM1
      I=M+1
      DISP=DISPC(I)
      RKK=1.0+RKD*FOL/TH(I)
      R(M)=RKK*CNH4(I)+ALFHA*DISP*(CNH4(I+1)-2.0*CNH4(I)+CNH4(I-1))
      ZK1=ZZ1(RK1.TH(I).H(I).Z.TIME)
      ZK3=ZZ3(RK3.TH(I).H(I).Z.TIME)
      R(M)=R(M)-DT*(ZK1+PK4)*CNH4(I)+(ROU*DT/TH(I))*ZK3*CORGN(I)
      R(M)=R(M)-BETA*(VP(I)/TH(I))*(CNH4(I+1)-CNH4(I))
   10 CONTINUE
      DISP=DISPC(2)
      R(1)=R(1)+ALFHA*DISP*CNH4(1)
      GO TO 14
C
   13 CONTINUE
      CNH4(1)=CNH4(2)
      DO  11  I=1.NM2
      DISP=DISPC(I+1)
      RKK=1.0+RKD*FOU/TH(I+1)
      AA(I)=RKK+2.0*ALPHA*DISP-BETA*VP(I+1)/TH(I+1)
      BB(I)=BETA*VP(I+1)/TH(I+1)-ALPHA*DISP
      DISP=DISPC(I+2)
      CC(I)=-ALFHA*DISP
   11 CONTINUE
      DISP=DISPC(N)
      RKK=1.0+RKD*FOU/TH(N)
      AA(NM1)=RKK+ALPHA*DISP
      DISP=DISPC(2)
      RKK=1.0+RKD*FOL/TH(2)
      AA(1)=RKK+1.0*ALPHA*DISP-BETA*VP(2)/TH(2)
      DO  12   M=1.NM1
      I=M+1
      DISP=DISPC(I)
      RKK=1.0+RKD*FOL/TH(I)

      R(M)=RKK*CNH4(I)+ALPHA*DISP*(CNH4(I+1)-2.0*CNH4(I)+CNH4(I-1))
      ZK1=ZZ1(RK1.TH(I).H(I).Z.TIME)
      ZK3=ZZ3(RK3.TH(I).H(I).Z.TIME)
      R(M)=R(M)-DT*(ZK1+RK4)*CNH4(I)+(ROU*DT/TH(I))*ZK3*CORGN(I)
   12 CONTINUE
   14 CONTINUE
      CALL TRIDM(AA.BB.CC.R.X.NM1)
      DO  15   I=2.N
   15 CNH4(I)=X(I-1)
      CNH4(NP1)=CNH4(N)
      RETURN
      END
```

```
C
      SUBROUTINE NITRAT
C     NO-3  PRGRAM
      COMMON/L1/ TH(810),CNH4(810),CNO3(810),CORGN(810),CNO2(810),
     *VP(810),DISPC(810)
      COMMON/L2/ AA(610),BB(610),CC(610),R(610),X(610)
      COMMON/L3/ N,NM1,NM2,NP1,NP2
      COMMON/L4/ ALPHA,BETA,DT,DZ
      COMMON/L5/ RKD,RK1,RK2,RK3,RK4,RK5
      COMMON/L6/ SFLUX,CSNH4,CSNO3
      COMMON/L7/ ROU
      COMMON/L8/ DISP,THMAX,THMIN,HMIN,CORGNI
      COMMON/L9/TIME,TPRINT,TWRITE
      COMMON/L10/ H(810),CCN(810),CAP(810)
      COMMON/L11/ THC(40),HC(40),CAPC(40)
      COMMON/L12/ AC,BC,NX,NX1,CONST
      COMMON/L13/ WFLUX(810)
      COMMON/L14/ V0,TWD,TSALT
      FF=2.0*DZ
      SSINF=WFLUX(1)
      CNO3(1)=(SSINF*FF*CSNO3+DISP*TH(1)*CNO3(3))/(SSINF*FF+DISP*TH(1))
      IF(SFLUX.LE.0.0)  GO TO 13
      DO  5  I=1,NM2
      DISP=DISPC(I+1)
      AA(I)=1.0+2.0*ALPHA*DISP-BETA*VP(I+1)/TH(I+1)
      BB(I)=BETA*VP(I+1)/TH(I+1)-ALPHA*DISP
      DISP=DISPC(I+2)
      CC(I)=-ALPHA*DISP
    5 CONTINUE
      DISP=DISPC(N)
      AA(NM1)=1.0+ALPHA*DISP
      DO  10   M=1,NM1
      I=M+1
      DISP=DISPC(I)
      R(M)=CNO3(I)+ALPHA*DISP*(CNO3(I+1)-2.0*CNO3(I)+CNO3(I-1))
      Z=CORGN(I)/CORGN(1)
      ZK1=ZZ1(RK1,TH(I),H(I),Z,TIME)
      ZK5=ZZ5(RK5,TH(I),H(I),Z,TIME)
      R(M)=R(M)+ZK1*DT*CNH4(I)-DT*(RK2+ZK5)*CNO3(I)
   10 CONTINUE
      DISP=DISPC(2)
      R(1)=R(1)+ALPHA*DISP*CNO3(1)
      GO TO 14
C
   13 CONTINUE
      CNO3(1)=CNO3(2)
      DO  11 I=1,NM2
      DISP=DISPC(I+1)
      AA(I)=1.0+2.0*ALPHA*DISP-BETA*VP(I+1)/TH(I+1)
      BB(I)=BETA*VP(I+1)/TH(I+1)-ALPHA*DISP
      DISP=DISPC(I+2)
      CC(I)=-ALPHA*DISP
   11 CONTINUE
      DISP=DISPC(N)
      AA(NM1)=1.0+ALPHA*DISP
      DISP=DISPC(2)
      AA(1)=1.0+1.0*ALPHA*DISP-BETA*VP(2)/TH(2)
      DO  12   M=1,NM1
      I=M+1
      DISP=DISPC(I)
      R(M)=CNO3(I)+ALPHA*DISP*(CNO3(I+1)-2.0*CNO3(I)+CNO3(I-1))
      Z=CORGN(I)/CORGN(1)
      ZK1=ZZ1(RK1,TH(I),H(I),Z,TIME)
      ZK5=ZZ5(RK5,TH(I),H(I),Z,TIME)
      R(M)=R(M)+ZK1*DT*CNH4(I)-DT*(RK2+ZK5)*CNO3(I)
   12 CONTINUE
   14 CONTINUE
      CALL TRIDM(AA,BB,CC,R,X,NM1)
      DO  15   I=2,N
   15 CNO3(I)=X(I-1)
      CNO3(NP1)=CNO3(N)
      RETURN
      END
```

```
C
      FUNCTION ZZ1(RK1,WC,HH,Z,TIME)
      ZZ1=0.0
      WH=-HH
      IF(WH.GT.15000.0) RETURN
      IF(WH.GT.10.0) GO TO 1
      RETURN
    1 IF(WH.GT.50.0) GO TO 2
      ZZ1=RK1*(WH-10.0)*0.00500
      RETURN
    2 IF(WH.GT.100.0) GO TO 3
      ZZ1=RK1*(0.200+(WH-50.0)*0.0060)
      RETURN
    3 IF(WH.GT.433.0) GO TO 4
      ZZ1=RK1*(0.500+(WH-100.0)*0.00150)
      RETURN
    4 ZZ1=RK1*(1.000-(WH-433.0)*0.00020)
      IF(WH.GT.1000.0) ZZ1=RK1*(0.950-0.050*WH/1000.0)
      RETURN


LEVEL  21                    ZZ2                      DATE = 77097

      FUNCTION ZZ2(RK2,WC,WH,Z,TIME)
      ZZ2=RK2
      RETURN


LEVEL  21                    ZZ3                      DATE = 77097

      FUNCTION ZZ3(RK3,WC,HH,Z,TIME)
      ZZ3=0.0
      WH=-HH
      IF(WH.GT.20000.0) RETURN
      IF(WH.GT.50.0) GO TO 1
      ZZ3=RK3*(0.250+0.00640*(50.0-WH))
      RETURN
    1 IF(WH.GT.200.0) GO TO 2
      ZZ3=RK3*(0.250+0.00500*(WH-50.0))
      RETURN
    2 CONTINUE
      ZZ3=RK3
      IF(WH.GT.2000.0) ZZ3=RK3*(1.0-0.050*WH/1000.0)
      RETURN
      END


LEVEL  21                    ZZ4                      DATE = 77097

      FUNCTION ZZ4(RK4,WC,WH,Z,TIME)
      ZZ4=RK4
      RETURN
      END


LEVEL  21                    ZZ5                      DATE = 77097

      FUNCTION ZZ5(RK5,WC,WH,Z,TIME)
      WSAT=0.360
      ZZ5=0.0
      IF((WC/WSAT).LT.0.80) RETURN
      ZZ5=RK5*(WC-0.80*WSAT)/(0.10*WSAT)
      IF(WC.GE.(0.90*WSAT)) ZZ5=RK5
      ZZ5=ZZ5*Z
      RETURN
      END
```

```
C
      SUBROUTINE INITWT
      COMMON/L1/ TH(810),CNH4(810),CNO3(810),CORGN(810),CNO2(810),
     *VP(810),DISFC(810)
      COMMON/L2/ AA(610),EE(610),CC(610),R(610),X(610)
      COMMON/L3/ N,NM1,NM2,NP1,NP2
      COMMON/L4/ ALPHA,BETA,DT,DZ
      COMMON/L5/ RKD,RK1,RK2,RK3,RK4,RK5
      COMMON/L6/ SFLUX,CSNH4,CSNO3
      COMMON/L7/ ECU
      COMMON/L8/ DISP,THMAX,THMIN,HMIN,CORGNI
      COMMON/L9/TIME,TPRINT,TWRITE
      COMMON/L10/ H(810),CON(810),CAP(810)
      COMMON/L11/ THC(40),HC(40),CAPC(40)
      COMMON/L12/ AC,BC,NX,NX1,CONST
      COMMON/L13/ WFLUX(810)
      COMMON/L14/ V0,TWD,TSALT
      COMMON/L17/ XXX(30),C1(30),C2(30),C3(30),C4(30),C5(30),C6(30)
      DO  5  I=1,NX1
      CAPC(I)=(THC(I+1)-THC(I))/(HC(I+1)-HC(I))
    5 CONTINUE
      CAPC(NX)=CAPC(NX1)
C
C
    6 CONTINUE
      ALPHA=DT/(2.0*DZ*DZ)
      BETA=DT/DZ
      TTT=CONST/CAPC(1)
      TTT=TTT*ALPHA
      IF(TTT.LE.2.00)  GO TO 8
      IF(DZ.GE.0.099)  GO TO 7
      DZ=DZ*2.0
      GO TO 6
    7 DT=DT/2.0
      GO TO 6
    8 CONTINUE
      CALL MCISD(1,NP2)
      CALL SBCW
      DO  25  I=1,NP2
      DO  15  K=1,NX1
      IF(H(I).GT.HC(K+1)) GO TO 20
   15 CONTINUE
   20 CAP(I)=CAPC(K)
   25 CONTINUE
      RETURN
      END
```

```
C
      SUBROUTINE  INITST
      COMMON/L1/  TH(810),CNH4(810),CNO3(810),CORGN(810),CNO2(810),
     *VP(810),DISPC(810)
      COMMON/L2/  AA(610),EE(610),CC(610),R(610),X(610)
      COMMON/L3/  N,NM1,NM2,NP1,NP2
      COMMON/L4/  ALPHA,BETA,DT,DZ
      COMMON/L5/  RKD,RK1,RK2,RK3,RK4,RK5
      COMMON/L6/  SFLUX,CSNH4,CSNO3
      COMMON/L7/  FCU
      COMMON/L8/  DISP,THMAX,THMIN,HMIN,CORGNI
      COMMON/L9/TIME,TPRINT,TWRITE
      COMMON/L10/  H(810),CON(810),CAP(810)
      COMMON/L11/  THC(40),HC(40),CAPC(40)
      COMMON/L12/  AC,BC,NX,NX1,CONST
      COMMON/L13/  WFLUX(810)
      COMMON/L14/  V0,TWD,TSALT
      COMMON/L17/  XXX(30),C1(30),C2(30),C3(30),C4(30),C5(30),C6(30)
      THAVR=(THMAX+THMIN)/2
    1 CONTINUE
      APAR=SFLUX-DISP*(THMIN-THAVR)/DZ
      APAR=SFLUX-DISP*(THMIN-THMAX)/DZ
      V0=APAR/THAVR
      V0=SFLUX/THMAX
      V0=APAR/THMIN
      ALPHA=DT/(2.0*DZ*DZ)
      BETA=DT/DZ
      DV0=DISP/V0
      DZV0=0.50*DZ/V0
      IF(DZ.GT.DV0)  GO TO 2
      IF(DT.GT.DZV0)  GO TO 3
      GO TO 4
    2 DZ=DZ/2
      GO TO 1
    3 DT=DT/2
      GO TO 1
    4 CONTINUE
    6 CONTINUE
      ALPHA=DT/(2.0*DZ*DZ)
      BETA=DT/DZ
      TTT=CONST/CAPC(1)
      TTT=TTT*ALPHA
      IF(TTT.LE.2.00)  GO TO 8
      DT=DT/2.0
      GO TO 6
    8 CONTINUE
      CALL MOISC(1,NP2)
      RETURN
      END
```

```
C
      SUBROUTINE TINT
      COMMON/L1/ TH(810).CNH4(810).CNO3(810).CORGN(810).CNO2(810).
     *VP(810).DISPC(810)
      COMMON/L2/ AA(610).BB(610).CC(610).R(610).X(610)
      COMMON/L3/ N.NM1.NM2.NP1.NP2
      COMMON/L4/ ALPHA.BETA.CT.DZ
      COMMON/L5/ RKD.RK1.RK2.RK3.RK4.RK5
      COMMON/L6/ SFLUX.CSNH4.CSNO3
      COMMON/L7/ ROU
      COMMON/L8/ DISP.THMAX.THMIN
      COMMON/L9/TIME.TPRINT.TWRITE
      COMMON/L10/ H(810).CON(810).CAP(810)
      COMMON/L11/ THC(40).HC(40).CAPC(40)
      COMMON/L12/ AC.BC.NX.NX1.CONST
      COMMON/L13/ WFLUX(810)
      COMMON/L14/ V0.TWD.TSALT
  100 FORMAT(5X.'TIME .HOURS ='.F10.5/.
     *5X.'LENGTH OF SOIL PROFILE. CM='.F10.5/.
     *5X.'VOLUME OF WATER IN THE SOIL PROFILE . CM ='.F10.5/)
  200 FORMAT(5X.'TOTAL NH-4 IN EXCH. PHASE. MG ='.F10.5/.
     *5X.'TOTAL NH-4 IN SOIL SOLUTION PHASE. MG ='.F10.5/.
     *5X.'TOTAL NH-4 IN SOIL. MG ='.F10.5/)
  300 FORMAT(5X.'TOTAL NO-3 IN SOIL SOLUTION. MG='.F10.5/.
     *5X.'TOTAL ORGANIC N IN THE SOIL. MG ='.F10.5/.
     *5X.'TOTAL N    RELEASED FROM THE SOIL. MG ='.F10.5//)
C
      DO  5  I=1.NP1
      X(I)=TH(I)*CNH4(I)
    5 CONTINUE
      CALL QSF(DZ.X.AA.NP1)
      TNH4C=AA(NP1)
      CALL QSF(DZ.CNH4.AA.NP1)
      TNH4SS=AA(NP1)*ROU*RKD
      TNH4T=TNH4C+TNH4SS
C
      DO  10 I=1.NP1
      X(I)=TH(I)*CNO3(I)
   10 CONTINUE
      CALL QSF(DZ.X.AA.NP1)
      TNO3=AA(NP1)
C
      DO  15 I=1.NP1
      X(I)=ROU*CORGN(I)
   15 CONTINUE
      CALL QSF(DZ.X.AA.NP1)
      TORGN=AA(NP1)
C
      CALL QSF(DZ.TH.AA.NP1)
      TW=AA(NP1)
      DO  20  I=1.NP2
      X(I)=ROU*CNO2(I)
   20 CONTINUE
      CALL QSF(DZ.X.AA.NP1)
      TGASN=AA(NP1)
      CL=N*DZ
      WRITE(6.100)  TIME.CL.TW
      WRITE(6.200)  TNH4SS.TNH4C.TNH4T
      WRITE(6.300)  TNO3.TORGN.TGASN
C
C
      CALL SECW
      RETURN
      END
```

```
C
      SUBROUTINE CADJ
      COMMON/L1/ TH(810),CNH4(810),CNO3(810),CORGN(810),CNO2(810),
     *VP(810),DISPC(810)
      COMMON/L2/ AA(610),BB(610),CC(610),R(610),X(610)
      COMMON/L3/ N,NP1,NP2,NF1,NP2
      COMMON/L4/ ALPHA,BETA,DT,DZ
      COMMON/L5/ RKD,RK1,RK2,RK3,RK4,RK5
      COMMON/L6/ SFLUX,CSNH4,CSNO3
      COMMON/L7/RCU,COLUMN,DFLUX
      COMMON/L8/ DISP,THMAX,THMIN,HMIN,CORGNI
      COMMON/L9/TIME,TPRINT,TWRITE
      COMMON/L10/ H(810),CON(810),CAP(810)
      COMMON/L11/ THC(40),HC(40),CAPC(40)
      COMMON/L12/ AC,BC,NX,NX1,CONST
      COMMON/L13/ WFLUX(810)
      COMMON/L14/ V0,TWD,TSALT
      COMMON/L17/ XXX(30),C1(30),C2(30),C3(30),C4(30),C5(30),C6(30)
      IF(ABS(TIME-TSALT).GT.1.0E-3) GO TO 5
      CSNH4=0.0
      CSNO3=0.0
    5 CONTINUE
      IF(ABS(TIME-TWD).GT.1.0E-3) GO TO 10
      SFLUX=DFLUX
   10 CONTINUE
      IF(DZ.GT.0.590) RETURN
      IF(TIME.GT.TWD) CALL CADJD
      KK=2
      L=10
      V1=VP(L)/TH(L)
      IF(V1.LT.0.050) V1=0.050
      IF((KK*ALPHA).GT.0.20) RETURN
      IF((KK*ALPHA).GT.(0.011/CON(L))) GO TO 11
      DZV0=0.50*DZ/V1
      IF((DT*KK).LT.DZV0) DT=DT*KK
      ALPHA=DT/(2.0*DZ*DZ)
      BETA=DT/DZ
   11 CONTINUE
      IF(ABS(TH(L)-THMIN).LT.0.0550) RETURN
      DV0=0.50*DISPC(L)/V1
      IF((DZ*KK).GT.DV0) RETURN
      DZ=DZ*KK
      M=1
      DO  15 I=1,NF1,KK
      H(M)=H(I)
      TH(M)=TH(I)
      CAP(M)=CAP(I)
      CNO3(M)=CNO3(I)
      CNH4(M)=CNH4(I)
      CORGN(M)=CORGN(I)
      CNO2(M)=CNO2(I)
      DISPC(M)=DISPC(I)
      M=M+1
   15 CONTINUE
      CALL MOISD(M,NP2)
      DO  35  I=M,NP2
      DO  25  K=1,NX1
      IF(H(I).GT.HC(K+1)) GO TO 30
   25 CONTINUE
   30 CAP(I)=CAPC(K)
   35 CONTINUE
      ALPHA=DT/(2.0*DZ*DZ)
      BETA=DT/DZ
      RETURN
      END
```

```
C
      SUBROUTINE CADJD
      COMMON/L1/ TH(810),CNH4(810),CNO3(810),CORGN(810),CNO2(810),
     *VP(810),DISPC(810)
      COMMON/L2/ AA(610),BB(610),CC(610),R(610),X(610)
      COMMON/L3/ N,NM1,NM2,NP1,NP2
      COMMON/L4/ ALPHA,BETA,DT,DZ
      COMMON/L5/ RKD,RK1,RK2,RK3,RK4,RK5
      COMMON/L6/ SFLUX,CSNH4,CSNO3
      COMMON/L7/ FOU
      COMMON/L8/ DISP,THMAX,THMIN,HMIN,CORGNI
      COMMON/L9/TIME,TPRINT,TWRITE
      COMMON/L10/ H(810),CON(810),CAP(810)
      COMMON/L11/ THC(40),HC(40),CAPC(40)
      COMMON/L12/ AC,BC,NX,NX1,CONST
      COMMON/L13/ WFLUX(810)
      COMMON/L14/ V0,TWD,TSALT
      COMMON/L17/ XXX(30),C1(30),C2(30),C3(30),C4(30),C5(30),C6(30)
      DTT=DT
      DZZ=DZ
      KK=2
      L=10
      V1=VP(L)/TH(L)
      IF(V1.LT.0.0250) V1=0.0250
      DZV0=0.50*DZ/V1
      IF((DT*KK).LT.DZV0) DTT=DT*KK
      IF(TIME.GT.50.0) V1=0.012
      DV0=0.50*DISPC(L)/V1
      IF((DZ*KK).GT.DV0) KK=1
      DZZ=DZ*KK
      ALPHAN=DTT/(2.0*DZZ*DZZ)
      IF(ALPHAN.GT.0.20) RETURN
      DT=DTT
      DZ=DZZ
      ALPHA=DT/(2.0*DZ*DZ)
      BETA=DT/DZ
      IF(KK.GT.1) GO TO 5
      RETURN
    5 CONTINUE
      M=1
      DO  15 I=1,NP1,KK
      H(M)=H(I)
      TH(M)=TH(I)
      CAP(M)=CAP(I)
      CNO3(M)=CNO3(I)
      CNH4(M)=CNH4(I)
      CORGN(M)=CORGN(I)
      CNO2(M)=CNO2(I)
      DISPC(M)=DISPC(I)
      M=M+1
   15 CONTINUE
      CALL MCISD(M,NP2)
      DO  35  I=M,NP2
      DO  25  K=1,NX1
      IF(H(I).GT.HC(K+1)) GO TO 30
   25 CONTINUE
   30 CAP(I)=CAPC(K)
   35 CONTINUE
      RETURN
      END
```

```
C
      SUBROUTINE CHECKT
      COMMON/L4/ ALPHA,BETA,CT,DZ
      COMMON/L9/TIME,TPRINT,TWRITE
      COMMON/L15/ TIT(30),TC,DTDT,IT,IL,NT
      DTDT=DT
      TWRITE=ABS(TIME-TC)
      IF(TWRITE.LT.1.0E-3)  RETURN
      TIME10=TIME+IL*DT
      IF((TIME.LT.TC).AND.(TIME10.GE.TC)) GO TO 30
      RETURN
   30 DT=(TC-TIME)/IL
      ALPHA=DT/(2.0*DZ*DZ)
      BETA=DT/DZ
      RETURN
      END


C
      SUBROUTINE TRIDM(A,B,C,D,X,N)
      DIMENSION A(1),B(1),C(1),D(1),X(1)
      DO  1  I=2,N
      C(I-1)=C(I-1)/A(I-1)
      A(I)=A(I)-(C(I-1)*B(I-1))
    1 CONTINUE
      X(1)=D(1)
      DO  2  I=2,N
      X(I)=D(I)-(C(I-1)*X(I-1))
    2 CONTINUE
      X(N)=X(N)/A(N)
      DO  3  I=2,N
      X(N+1-I)=(X(N+1-I)-(B(N+1-I)*X(N+2-I)))/A(N+1-I)
    3 CONTINUE
      RETURN
      END


C
      SUBROUTINE CHECKN
      COMMON/L1/ TH(810),CNH4(810),CNO3(810),CORGN(810),CNO2(810),
     *VP(810),DISPC(810)
      COMMON/L3/ N,NM1,NM2,NP1,NP2
      COMMON/L4/ ALPHA,BETA,CT,DZ
      COMMON/L5/ RKD,RK1,RK2,RK3,RK4,RK5
      COMMON/L6/ SFLUX,CSNH4,CSNO3
      COMMON/L7/RCU,COLUMN,DFLUX
      COMMON/L8/ DISP,THMAX,THMIN,HMIN,CORGNI
      COMMON/L9/TIME,TPRINT,TWRITE
      COMMON/L10/ H(810),CON(810),CAP(810)
      COMMON/L11/ THC(40),HC(40),CAPC(40)
      COMMON/L12/ AC,BC,NX,NX1,CONST
      COMMON/L13/ WFLUX(810)
      COMMON/L14/ VO,TWC,TSALT
      COMMON/L15/ TIT(30),TC,DTDT,IT,IL,NT
      COMMON/L17/ XXX(30),C1(30),C2(30),C3(30),C4(30),C5(30),C6(30)
      MM=10
      MM=20
      NM1F=COLUMN/DZ
      IF(N-NM1F) 10,5,20
    5 RETURN
   10 IF(N.GT.580) RETURN
      IF(ABS(TH(N-20)-THMIN).LT.0.0020)  RETURN
      NM1F=N+MM
      NNNN=NM1F+2
      CALL MOISD(NP1,NNNN)
      DO  16  I=NP1,NNNN
      DO  17  K=1,NX
      IF(H(I).GT.HC(K+1)) GO TO 18
   17 CONTINUE
   18 CAP(I)=CAPC(K)
   16 CONTINUE
   20 N=NM1F
      NM1=N-1
      NM2=N-2
      NP1=N+1
      NP2=N+2
      RETURN
      END
```

```
C
      SUBROUTINE SECW
      COMMON/L1/ TH(810),CNH4(810),CNO3(810),CORGN(810),CNO2(810),
     *VP(810),DISFC(810)
      COMMON/L2/ AA(610),BB(610),CC(610),R(610),X(610)
      COMMON/L3/ N,NM1,NM2,NP1,NP2
      COMMON/L4/ ALPHA,BETA,DT,DZ
      COMMON/L5/ RKD,RK1,RK2,RK3,RK4,RK5
      COMMON/L6/ SFLUX,CSNH4,CSNO3
      COMMON/L7/ ROU
      COMMON/L8/ DISP,THMAX,THMIN
      COMMON/L9/TIME,TPRINT,TWRITE
      COMMON/L10/ H(810),CON(810),CAP(810)
      COMMON/L11/ THC(40),HC(40),CAPC(40)
      COMMON/L12/ AC,BC,NX,NX1,CONST
      COMMON/L13/ WFLUX(810)
      COMMON/L14/ VO,TWC,TSALT
      IF(SFLUX.GT.0.0) GO TO 5
      CONS=AC*EXP(BC*(TH(1)+TH(2))*0.50)
      ADJ=DZ*(1.0-SFLUX/CONS)
      H(1)=H(2)-ADJ
      IF(H(1).LT.(-30000.)) H(1)=-30000.0
      RETURN
C
    5 CONTINUE
      H(1)=H(1)+0.400
      IF(H(1).GT.0.0) H(1)=0.0
      RETURN
      END


C
      SUBROUTINE GASCRG
      COMMON/L1/ TH(810),CNH4(810),CNO3(810),CORGN(810),CNO2(810),
     *VP(810),DISFC(810)
      COMMON/L2/ AA(610),BB(610),CC(610),R(610),X(610)
      COMMON/L3/ N,NM1,NM2,NP1,NP2
      COMMON/L4/ ALPHA,BETA,DT,DZ
      COMMON/L5/ RKD,RK1,RK2,RK3,RK4,RK5
      COMMON/L6/ SFLUX,CSNH4,CSNO3
      COMMON/L7/ ROU
      COMMON/L8/ DISP,THMAX,THMIN
      COMMON/L9/TIME,TPRINT,TWRITE
      COMMON/L10/ H(810),CON(810),CAP(810)
      COMMON/L13/ WFLUX(810)
      COMMON/L14/ VO,TWC,TSALT
      DO  5  I=1,NP1
      ZK3=ZZ3(RK3,TH(I),H(I),Z,TIME)
      Z=CORGN(I)/CORGN(I)
      ZK5=ZZ5(RK5,TH(I),H(I),Z,TIME)
      CORGN(I)=CORGN(I)+(DT/ROU)*(TH(I)*RK2*CNO3(I)+TH(I)*RK4*CNH4(I)-
     $ROU*ZK3*CORGN(I))
      CNO2(I)=CNO2(I)+(DT/ROU)*ZK5*TH(I)*CNO3(I)
    5 CONTINUE
      RETURN
      END
```

```
C
      SUBROUTINE GRAPH
      COMMON/L1/ TH(810),CNH4(810),CNO3(810),CORGN(810),CNO2(810),
     *VP(810),DISFC(810)
      COMMON/L3/ N,NM1,NM2,NP1,NP2
      COMMON/L4/ ALPHA,BETA,DT,DZ
      COMMON/L16/IC,IWT
      COMMON/L18/ TGRAPH(15),NTGR,ITGR
      IF(ITGR.GT.NTGR) RETURN
      CALL LINEWT(IWT)
      XL=14.0
      YL=7.0
      KK=1.0/DZ+0.010
      KKK=N
      IF((DZ*N).GT.120.0)  KKK=120*KK-1
      SYMSZ=0.100
C
      X1=0.0
      DO  10  I=1,KKK,KK
      YS=TH(I)*10.0
      XS=X1/10.0
      CALL SYMBOL(XS,YS,SYMSZ,IC,0.0,-2)
      X1=X1+1.0
   10 CONTINUE
      CALL PLOT(0.0,YL,-3)
      X1=0.0
      DO  20  I=1,KKK,KK
      YS=CNH4(I)/20.0
      XS=X1/10.0
      CALL SYMBOL(XS,YS,SYMSZ,IC,0.0,-2)
      X1=X1+1.0
   20 CONTINUE
      CALL PLOT(XL,-YL,-3)
      X1=0.0
      DO  30  I=1,KKK,KK
      YS=CORGN(I)/10.0
      XS=X1/10.0
      CALL SYMBOL(XS,YS,SYMSZ,IC,0.0,-2)
      X1=X1+1.0
   30 CONTINUE
      CALL PLOT(0.0,YL,-3)
      X1=0.0
      DO  40  I=1,KKK,KK
      YS=CNO3(I)/20.0
      XS=X1/10.0
      CALL SYMBOL(XS,YS,SYMSZ,IC,0.0,-2)
      X1=X1+1.0
   40 CONTINUE
      CALL PLOT(-XL,-YL,-3)
      ITGR=ITGR+1
      IC=IC+1
      IF(IC.GT.7) IC=0
      IWT=IWT+1
      IF(IWT)  1,2,2
    2 IWT=-2
      RETURN
    1 IWT=-1
      RETURN
      END
```

```
C
      SUBROUTINE AXISPL
      COMMON/L16/IC,INT,
      XL=14.0
      YL=7.0
      XSIZE=12.010
      YSIZE1=6.010
      YSIZE2=8.010
      CALL PLOTS(-60.0,-20.0)
      CALL PLOT(1.0,1.0,-3)
      CALL LINEWT(INT)
      CALL AXIS(0.0,0.0,'DEPTH,CM',-8,XSIZE,0.0,0.0,10.0)
      CALL AXIS(0.0,0.0,'  THETA ',8,YSIZE1,90.0,0.0,0.10)
      CALL PLOT(0.0,YL,-3)
      CALL AXIS(0.0,0.0,'DEPTH,CM',-8,XSIZE,0.0,0.0,10.0)
      CALL AXIS(0.0,0.0,'NH4-N,MG',8,YSIZE2,90.0,0.0,20.0)
      CALL PLOT(XL,-YL,-3)
      CALL AXIS(0.0,0.0,'DEPTH,CM',-8,XSIZE,0.0,0.0,10.0)
      CALL AXIS(0.0,0.0,'ORG.N,MG',8,YSIZE1,90.0,0.0,10.0)
      CALL PLOT(0.0,YL,-3)
      CALL AXIS(0.0,0.0,'DEPTH,CM',-8,XSIZE,0.0,0.0,10.0)
      CALL AXIS(0.0,0.0,'NO3-N,MG',8,YSIZE2,90.0,0.0,20.0)
      CALL PLOT(-XL,-YL,-3)
      RETURN
      END


LEVEL  21                      MAIN                    DATE = 77097            19/33/46

C
      SUBROUTINE MOISD(I1,I2)
      COMMON/L1/ TH(810),CNH4(810),CNO3(810),CORGN(810),CNO2(810),
     *VP(810),DISFC(810)
      COMMON/L3/ N,NM1,NM2,NP1,NP2
      COMMON/L4/ ALPHA,BETA,DT,DZ
      COMMON/L10/ H(810),CON(810),CAP(810)
      COMMON/L17/ XXX(30),C1(30),C2(30),C3(30),C4(30),C5(30),C6(30)
      I=1
      DO  20  K=I1,I2
      A=DZ*(K-1)
    5 IF(A.LE.XXX(I+1)) GO TO 10
      I=I+1
      GO TO 5
   10 H(K)=C1(I)+(A-XXX(I))*((C1(I+1)-C1(I))/(XXX(I+1)-XXX(I)))
      TH(K)=C2(I)+(A-XXX(I))*((C2(I+1)-C2(I))/(XXX(I+1)-XXX(I)))
      CNH4(K)=C3(I)+(A-XXX(I))*((C3(I+1)-C3(I))/(XXX(I+1)-XXX(I)))
      CNO3(K)=C4(I)+(A-XXX(I))*((C4(I+1)-C4(I))/(XXX(I+1)-XXX(I)))
      CORGN(K)=C5(I)+(A-XXX(I))*((C5(I+1)-C5(I))/(XXX(I+1)-XXX(I)))
      CORGN(K)=50.00/EXP(0.0250*DZ*K)
      CNO2(K)=C6(I)+(A-XXX(I))*((C6(I+1)-C6(I))/(XXX(I+1)-XXX(I)))
   20 CONTINUE
      RETURN
      END
```

Reproduced from
best available copy.

```
C
      SUBROUTINE OUTPUT
      COMMON/L1/ TH(810).CNH4(810).CNO3(810).CORGN(810).CNO2(810).
     *VP(810).DISFC(810)
      COMMON/L2/ AA(610).EE(610).CC(610).R(610).X(610)
      COMMON/L3/ N.NM1.NM2.NP1.NP2
      COMMON/L4/ ALPHA.BETA.DT.DZ
      COMMON/L5/ RKD.RK1.RK2.RK3.RK4.RK5
      COMMON/L6/ SFLUX.CSNH4.CSNO3
      COMMON/L7/ ECU
      COMMON/L8/ CISF.THMAX.THMIN.HMIN.CORGNI
      COMMON/L9/TIME.TPRINT.TWRITE
      COMMON/L10/ H(810).CON(810).CAP(810)
      COMMON/L11/ THC(40).HC(40).CAPC(40)
      COMMON/L12/ AC.BC.NX.NX1.CONST
      COMMON/L13/ WFLUX(810)
      COMMON/L14/ V0.TWD.TSALT
      COMMON/L15/ TIT(30).TC.DTDT.IT.IL.NT
 100  FORMAT('1')
  200 FORMAT(///.50X.'TIME = '.E12.5//.4X.'DEPTH.CM'.4X.'SUCTION.CM'.
     *4X.'THETA'.7X.'HYDR.COND.'.T56.'WATER FLUX'.
     $T72.'NH4'.T85.'NO3'.T97.'CORGN'.5X.'   NO2')
  400 FORMAT(10E13.4)
      WRITE(6.100)
      TIME=TC
      WRITE(6.200) TIME
      DO 20 I=1.NP1
      ZZ=(I-1)*DZ
      WRITE(6,400) ZZ.H(I).TH(I).CON(I).WFLUX(I).CNH4(I).CNO3(I).
     *CORGN(I).CNO2(I)
   20 CONTINUE
      CALL TINT
      IT=IT+1
      IF(IT.GT.NT) STOP
      TC=TIT(IT)
      DT=DTDT
      ALPHA=DT/(2.0*DZ*DZ)
      BETA=DT/DZ
   25 CONTINUE
      KK=2
      TTT=CONST/CAPC(1)
      TTT=TTT*ALPHA
      IF(TTT.LE.2.00)  GO TO 30
      RETURN
   30 CONTINUE
      DZV0=0.50*DZ/(VP(10)/TH(10))
      IF((DT*KK).LT.DZV0) DT=DT*KK
      ALPHA=DT/(2.0*DZ*DZ)
      BETA=DT/DZ
      RETURN
      END
```

APPENDIX D

KINETIC RATE COEFFICIENTS FOR THE NITROGEN TRANSFORMATIONS

A literature search was conducted to determine the magnitude and differences in the first order transformation rate coefficients observed by various research groups. Transformation rate coefficients are used in the simulation models presented in this report (Sections 4 and 6). The values, listed in Table 3, are intended to serve as a guide in estimating the rate coefficients for a given soil type. The reader is also referred to the regression equations developed by Dutt et al.[28] which relate selected soil properties to the rate coefficients. The following comments should be taken into account in utilizing Table 3.

(1) The rate coefficients given in Table 3 were, in most cases, obtained from laboratory studies where "ideal" environmental conditions for the transformation being investigated were maintained (e.g., in the denitrification study of Cooper and Smith[90], the atmosphere in the incubation vessel was replaced by 100% He and a supplementary carbon source was added to the soil).

(2) In most experiments dealing with nitrogen transformations in soils, only the resulting or net effects of several simultaneous reactions can be measured. When two processes (such as mineralization and immobilization) are working in opposite directions, the difference between these reactions is measured by a net increase (if mineralization prevails) or net decrease (if immobilization prevails) in the NH_4 and NO_3 concentrations. It is possible that although the opposing processes are both vigorous and extensive, the net effects may be small. Thus, in a majority of the laboratory studies, the net result of several simultaneous reactions has been attributed to a single transformation process. Isotope tracer studies[105-110] using ^{15}N have been, however, helpful in overcoming these drawbacks.

(3) The mineralization-immobilization rate coefficients listed in Table 3 were based on soil organic matter data. The uniformity in the composition and degradation rate of this innate material appears to be fairly well-established (e.g., data of Stanford and Smith[16] and Stanford et al.[17]). Because of the complexity of the composition of plant residues and animal wastes, it may be necessary to simulate transformations of their

individual components (e.g. Hagin and Amberger[13], Beek and Frissell[14], van Veen[111], Browder and Volk[112]). The values of rate constants for mineralization of organic nitrogen to nitrate-N as well as rates of NH_3 volatilization in manure treated soils have been compiled by Reddy et al.[113].

(4) Several investigators[18-20] have reported that denitrification follows zero-order kinetics. Bowman and Focht[21] have pointed out that many of these studies were conducted at high nitrate concentrations, where zero-order kinetics may be expected (as the substrate is non-limiting). Reddy et al.[114] suggested that results from many laboratory incubation experiments dealing with denitrification follow psuedo-first-order kinetics when in fact the reaction kinetics were zero-order. They attributed this to a diffusion-controlled supply of NH_4 and/or NO_3 to the "active" denitrification zones in soils.

TABLE 3. KINETIC TRANSFORMATION RATE COEFFICIENTS FOR VARIOUS NITROGEN SPECIES IN SELECTED SOILS

PROCESS	SOIL TYPE	RATE COEFFICIENT (day^{-1})	EXPERIMENTAL CONDITIONS	REFERENCE
Mineralization:				
OM → NH_4	Chester silt loam	0.0073	Laboratory incubation at 20°C, carbon supplement added.	101
OM → NH_4	Hagerstown silt loam	0.0078		
OM → NH_4	Salinas clay	0.001	Laboratory incubation at 24°C, 100% relative humidity. Data of Broadbent et al.[97].	12
OM → NH_4	29 soils with a wide range in properties	0.0077	Laboratory incubation at 35°C.	16
OM → NH_4	11 soils with a wide range in properties	0.001 - 0.0078	Laboratory incubation at temperatures ranging from 5° - 35°C.	17
Immobilization:				
NH_4 → OM	Ontario loam	0.15	Laboratory incubation at 30°C. Carbon supplement, data of Stojanovic and Broadbent[100].	12
NO_3 → OM	Ontario loam	0.15		
Nitrification:				
NH_4 → NO_2	Salinas clay	0.22	Laboratory incubation at 24°C and 100% relative	

TABLE 3. Continued

PROCESS	SOIL TYPE	RATE COEFFICIENT (day^{-1})	EXPERIMENTAL CONDITIONS	REFERENCE
$NO_2 \rightarrow NO_3$	Salinas clay	9.0	humidity. Data of Broadbent et al.[97].	12
$NH_4 \rightarrow NO_2$	Milville loam	0.143	Laboratory incubation at 22°C, 1/3-bar and 1-bar water contents. Data of Justice and Smith[99].	12
$NO_2 \rightarrow NO_3$	Milville loam	9.0		
$NH_4 \rightarrow NO_3$	Tippera clay loam	0.0033 - 0.0543	Laboratory incubation at temperatures ranging from 20-60°C.	26
$NH_4 \rightarrow NO_3$	Columbia silt loam	0.24 - 0.72	Steady-state flow through soil column maintained at -85 cm suction.	15
$NH_4 \rightarrow NO_3$	Hanford sandy loam	0.76 - 1.11	Steady-state flow through soil column, used ^{15}N.	103
$NH_4 \rightarrow NO_3$	Columbia silt loam	0.24 - 0.62	Steady-state and transient concentration profiles in soil column, used ^{15}N.	102
Denitrification:				
$NO_3 \rightarrow NO_2$	Columbia silt loam	0.024 - 1.08	Steady-state flow through soil columns. O_2 level ranged from 0 to 25%.	15
$NO_3 \rightarrow (N_2 + N_2O)$	Yolo loam	0.004 - 0.032	Laboratory soil columns, used ^{15}N.	104

TABLE 3. Continued

PROCESS	SOIL TYPE	RATE COEFFICIENT (day^{-1})	EXPERIMENTAL CONDITIONS	REFERENCE
$NO_3 \rightarrow NO_2$	Hanford sandy loam	0.04 - 0.075	Steady-state flow through soil columns, ised N.	103
$NO_3 \rightarrow (N_2 + N_2O)$	Columbia silt loam	0.048 - 0.192	Transient and steady-state concentration profiles in soil columns.	102

APPENDIX E

LIST OF PUBLICATIONS RESULTING FROM THIS PROJECT

1. Rao, P. S. C., H. M. Selim, J. M. Davidson, and D. A. Graetz. 1976. Simulation of transformations, ion-exchange, and transport of selected nitrogen species in soils. Soil Crop Sci. Soc. Florida Proc. 35:161-164.

2. Rao, P.S.C., J. M. Davidson, and L. C. Hammond. 1976. Estimation of nonreactive and reactive solute front locations in soils. in Residual Management by Land Disposal. Proc. of Hazardous Waste Res. Symp. Tucson, Arizona. EPA-600/9-76-015, p. 235-242.

3. Selim, H. M., J. M. Davidson, and P. S. C. Rao. 1977. Transport of reactive solutes in multilayered soils. Soil Sci. Soc. Amer. J. 41:3-10.

4. Selim, H. M., J. M. Davidson, P. S. C. Rao, and D. A. Graetz. 1977. Nitrogen transformations and transport during transient unsaturated flow in soils. (submitted to Water Resour. Res.) Presented at the 68th annual meetings of Ann. Soc. Agron., Houston, TX.

5. Selim, H. M. and J. M. Davidson. 1977. Numerical solution of nitrogen transformations and transport equations during transient unsaturated flow in soils. SHARE Program Library.

6. Davidson, J. M., P. S. C. Rao, and R. E. Jessup. 1977. A critique of the paper "computer simulation modeling for nitrogen in irrigated cropland" by K. K. Tanji and S. K. Gupta. in Nitrogen and Soil Environment. D. R. Nielsen and Judy McDonald, eds. Academic Press, N.Y. (in press)

7. Davidson, J. M., P. S. C. Rao, and H. M. Selim. 1977. Simulation of nitrogen movement, transformations and plant uptake in the root zone. Proc. of National Conf. on Irrigation Return Flow Quality Management. Fort Collins, Colo. p. 9-18.

8. Rao, P. S. C., R. E. Jessup, and J. M. Davidson. 1977. A simple model for description of the fate of nitrogen in the crop root zone. Submitted to Agron. J.

9. Rao, P. S. C., P. V. Rao, and J. M. Davidson. 1977. Estimation of the spatial variability of the soil-water flux. Soil Sci. Soc. Amer. Jour. Vol. 41 (in press).